# Experimental Investigation of Aluminum Matrix Composite Reinforced by Aluminum Oxide and Graphite Micro Particles.

**Robale Dinsa Daba**

**PGR/18142/2011**

A thesis submitted to

The Department of Mechanical Design and Manufacturing Engineering

School of Mechanical Chemical and Materials Engineering

Presented in Partial Fulfillment of the Requirement for the Degree of

Master's in Manufacturing Engineering

Office of Graduate studies

Adama Science and Technology University

Adama

Nov,2020

# Experimental Investigation of Aluminum Matrix Composite Reinforced by Aluminum Oxide and Graphite Micro Particles

**Robale Dinsa Daba**

**PGR/18142/2011**

A thesis submitted in partial fulfillment of the requirements for the degree of Master's in Manufacturing Engineering

Thesis Adviser: Dr Devendra Kumar Sinha

Program of Mechanical Design and Manufacturing, Engineering, School of Mechanical, Chemical and Materials Engineering, (SoMCME), ASTU, ADAMA, Ethiopia.

Co-Adviser: Dr Habtamu Beri

Program of Mechanical Design and Manufacturing, Engineering, School of Mechanical, Chemical and Materials Engineering, (SoMCME), ASTU, ADAMA, Ethiopia.

Department of Mechanical Design and Manufacturing Engineering

School of Mechanical Chemical and Materials Engineering

Office of Graduate Studies

Adama Science and Technology University

Adama

Nov,2020

APPROVAL OF BOARD OF EXAMINERS

We the under signed members of the board of examiners of the final open defense by Robale Dinsa have read and evaluated his thesis entitled “Experimental Investigation of Aluminum Metal Matrix Composite Reinforced by Aluminum Oxide and Graphite Micro Particles “And examined the candidate .this is therefore, to clarify that the thesis has been accepted in partial fulfillment of the requirement of the masters on manufacturing engineering.

| | | |
|---|---|---|
| _____ | _____ | _____ |
| Name of student | Signature | Date |
| _____ | _____ | _____ |
| Advisor | Signature | Date |
| _____ | _____ | _____ |
| External examiner | Signature | Date |
| _____ | _____ | _____ |
| Internal examiner | Signature | Date |
| _____ | _____ | _____ |
| Chair person | Signature | Date |
| _____ | _____ | _____ |
| Head of department | Signature | Date |
| _____ | _____ | _____ |
| School dean | Signature | Date |
| _____ | _____ | _____ |
| Post graduate dean | Signature | Date |

ADVISOR'S APPROVAL SHEET

To: Design and Manufacturing Engineering Department

Subject: Thesis Submission

This is to certify that the thesis entitled "Experimental Investigation of Aluminum Metal Matrix Composite Reinforced by Aluminum Oxide and Graphite Micro Particles" submitted in partial fulfillment of the requirement for the degree of Master's in Manufacturing Engineering, the Graduate program of the department of Design And Manufacturing Engineering and has been carried out by Robale Dinsa Id PGR/18142/11, under my supervision. Therefore, i recommend that the student has fulfilled the requirement and hence here by he can submit the thesis to the department.

| _____ | _____ | _____ |
|---|---|---|
| Name of main advisor | Signature | Date |
| _____ | _____ | _____ |
| Name of co-advisor | Signature | Date |

## DECLARATION

I certify that research work titled “Experimental investigation of aluminum alloy metal matrix composite reinforced with Aluminum oxide and Graphite micro particles” is my own work. The work has not been presented elsewhere for assessment. Where material has been used from other sources it has been properly acknowledged / referred.

Name: _____signature:_____Date:_____

This MSc thesis has been submitted for examination with my approval as a thesis Adviser.

Name: _____Signature:_____Date:_____

This MSc thesis has been submitted for examination with my approval as a thesis Co-Adviser.

Name: _____Signature:_____Date:_____

**ACKNOWLEDGMENT**

Above all I would like to thank almighty God for his undying support, encouragement and endless love trough out completing this work. Secondly It is my gratitude to acknowledge Adama Science and Technology University top management and school deans for their unreserved cooperation in realizing the research thesis completion. Secondly, i do like to express his profound gratefulness to my thesis advisor **Dr. Devendra Kumar Sinha** Ass. Professor, Department of Design and Manufacturing Engineering of Adama Science and Technology, for his priceless help in completing this thesis and for his encouragement on publishing this research work on journal. Moreover my special thanks goes to **Dr. Habtamu Beri** my co-advisor for his support in facilitating this research work and for giving me marvelous suggestion in completing this work. I would furthermore like to express his gratitude to **Mr. Mengistu Gelaw**, Lecturer and Head Department of Design And Manufacturing Engineering for encouraging and cooperating me with what so ever he can through completing this thesis. I would also like to thank ASTU Lab Assistants Mr Bundi Lecturer And The Lab Assistant of Chemical Engineering Lab, Mr Andualem The Lab Assistant Of Ceramic Lab At Material Science Engineering Lab, Mr Henock The Lab Assistant Of Metal Lab At Material Science Engineering, Mr Yeshane Lab Assistant Of Biology Department, Dr Teshome Associate Dean Of School Of Computational Science, Mr Daniel Manufacturing shop Assistant, Mr Abbebe Manufacturing Shop chief , Mr Akililu Lab Assistant Of Design And Manufacturing Lab.

At last but not the least I would like to thank my mother Sr Abebu Gutema and my family for their support and priceless love throughout my life.

## Contents

## LIST OF TABLES

## LIST OF FIGURES

## LIST OF ACRONYMS AND ABREVIATION

| | |
|---|---|
| $Al_2O_3$ | Aluminum Oxide |
| Gr | Graphite |
| BN | Boron Nitride |
| SiC | Silicon Carbide |
| $B_4C$ | Boron Carbide |
| AMC | Aluminium Matrix Composite |
| MMC | Metal Matrix Composite |
| HAMC | Hybrid Aluminium Matrix Composite |
| Al | Aluminium |
| UTS | Universal Testing Machine |
| % Wt% | Weight Percentage |
| Mg | Magnesium |
| SEM | Scanning Electron Microscope |
| CoF | Coefficient of Friction |
| CYS | Compression Yield Strength |
| AA | Aluminium Alloy |
| ASTM | American Society of Testing And Materials |
| UTS | Ultimate Tensile Strength |
| Vol% | Volume Percentage |
| EDS | Electron Dispersive Spectrum |
| Ti | Titanium Alloy |
| DRX | Dynamic Re-crystallization |
| Nacl | Sodium Chloride |

| | |
|---|---|
| XPS | X-Ray Photo Spectroscope |
| XRD | X Ray Diffracto-meter |
| TEM | Transmission Electron Microscope |
| N | Newton |
| ANOVA | Analysis Of Variance |
| DOE | Design of Experiment |

## *ABSTRACT*

*In the present scenario, composite materials are replacing Aluminum and its alloys due to the requirement of lightweight high strength material. This thesis interrogates an experimental study of the mechanical properties and tribological property of Aluminum metal matrix composite reinforced by aluminum oxide and graphite micro-particle by using powder metallurgy production method with 20mm diameter and 6 mm length. Taguchi L16 orthogonal array has been utilized for the plan and design of experiments. This experiment is conducted by using a ball milling machine, hydraulic press, sintering furnace, Vicker hardness testing machine, scanning electron microscope, optical microscope, compression testing machine, tribometer. The sampling method was conducted according to the ASTM standard for each measurement. The mechanical properties investigated are Actual density, Theoretical density, Porosity, hardness, compressive strength, wear loss, and coefficient of friction. The optimizations of parameters have been done by using the Taguchi method and Hybrid Grey relational analyses and Taguchi method. The experimental investigations revealed that with an increase in Al2O3 weight percentage the actual density, hardness and compressive strength increased and decreased with an increase in weight presentation of graphite microparticles. Nevertheless the wear loss and coefficient of friction of the composite decreased with an increase in the weight percentage of graphite. The optimum condition for the grey relational analysis of hardness and compressive strength is 20% Al2O3, 1.5%Gr, compaction pressure of 60 Mpa and 60 minutes of compaction time, and 120 minutes of milling time. The condition corresponding to the optimum condition is 20% Al2O3, 1.5%Gr, compaction pressure of 60 Mpa, 45 minutes of compaction time, and 30 minutes of milling time. The Wear resistance has improved by 43.93% with an increase in weight percentage of graphite from 0% to 4.5% whereas wear resistance increased from 30% to 37% with an increase in reinforcement from 10wt% to 20 wt% of aluminum oxide, nevertheless, increment by 7% was observed for those samples with aluminum oxide reinforcement being permanent when the hybrid graphite reinforcement increased from 0 to 4.5wt%. The developed composite material is found to be of excellent mechanical and metallurgical properties besides high strength to weight ratio.*



***Keywords:*** *Aluminum Matrix Composite; Aluminum Oxide; Graphite; Taguchi;*

# CHAPTER ONE

# INTRODUCTION

## 1.1 Background of study

The introduction of ceramic whiskers as reinforcement and the development of 'in-situ' eutectics in the 1960s aided high-temperature applications in aircraft engines. In the late 1970s, the automobile industries started to take MMCs seriously. In the last 20 years, MMCs evolved from laboratories to a class of materials with numerous applications and commercial markets ( A. J. Cyria (2011))

In the present world, the necessity of advanced material is raising worldwide to achieve the desired mechanical and Tribological property. New-fangled engineering technology demand materials with a wide spectrum of properties, which are quite unmanageable to meet by single (monolithic) material (M. Rahimian et al. (2010), M. O. Bodunrin et al. (2015). Momentarily, wide ranges of industries demand a material with satisfying strength as well as lessened weight (A. A. Premnath et al. (2014). Aluminum matrix composites (AMC) with particles reinforcements have made multitudinous applications arising as a perpetual necessity in high performance and high accomplishment components of the military, automotive, aerospace, and electronics industry due to improved properties such as low density, low coefficient of thermal expansion, cost-effective, high corrosion and oxidation resistance, high stiffness, good wear resistance, energy-efficient and high toughness (S Dharmalingaml et al (2013), M.A Ibrahim et al. (2019), M. O. Bodunrin et al .(2015), M. Kumar and A. M. Murugan (2017). Aluminum Metal Matrix composites have been a very precious addition to the scope of modern materials for elevated performance tribological applications (A. Baradeswaran and A. Elayaperumal (2013))

Various studies (K. Kanthavel et al. (2016), M. O. Bodunrin et al. (2015), M. Rahimian et al. (2011)) revealed that acquiring a homogenous and uniform distribution of the reinforcement particles in a finely grained aluminum matrix pay off the improvement of tribological and mechanical properties of the composite. Exceptionally reinforcement aluminum matrix by ceramic is proved by (A. A. Premnath et al. (2014), M. A Ibrahim et al. (2019), G. Iacob et al. (2015), and M. O. Bodunrin et al. (2015)) to result in a distinctive increase on the hardness of the AMC. Numerous fabrication techniques of MMC are available, such as die-casting, stir casting,

spray deposition and powder metallurgy for fabricating a near net-shaped MMC component with better surface finish (A. A. Premnath et al. (2014)).

Fabrication of MMCs has various challenges such as poor wettability porosity formation, and inconsistent distribution of reinforcement particles. Attaining uniform or consistent distribution of reinforcement is a primitive requirement (N. Radhika and R. Subramaniam,2013). The powder metallurgy fabrication technique is the most appropriate method for the preparation of metal matrix composites. In relative to casting methods, its greatest advantage is its low processing temperature (S Dharmalingaml et al.(2013), X. Qu et al.(2018), M. Rahimian et al.(2010), and V. N. Gaitonde et al.(2012). Due to this unwelcomed phases between the reinforcement and the matrix phase are prevented. Additionally, reinforcement particles are in like manner uniformly distributed in the matrix (K. Kanthavel et al.(2016), N. Radhika and R. Subramaniam,(2013), and A. A. Premnath et al. (2014)). The major advantage of the powder metallurgy process is its applicability to mass production. Another extra important powder metallurgies feature is the fabrication by near-net-shape, which is cost-efficient (X. Qu, et al. (2018), M. Rahimian et al. (2011)]. Powder metallurgy is the technique with extraordinary development in late years due to its efficiency to give more uniform distribution. Components fabricated by this technology need minimal surface finishing and have economic/technical advantages which made them very preferable for several applications in industry (G. Iacob et al. (2015). The powder metallurgy production method is the most appropriate method for producing metal matrix composites. When it is compared with the melting method powder metallurgy is advantageous due to its low processing temperature. As a result of this undesired phases between the reinforcement and matrix phase are prevented. Consequently, reinforcement particles are uniformly distributed in the matrix. An additional important feature is the fabrication of near-net-shape parts, which is cost-efficient (M. Rahimian, et al. (2011).

From the recent archival literature survey, it is noticed that imperceptible researchers investigated aluminum matrix composite reinforced by Al2O3 and graphite particles. Al2O3 is selected as reinforcement owing to its high hardness and low coefficient of thermal expansion, highly wear-resistant, good mechanical properties, high-temperature strength, and thermal shock resistance. In this experimental investigation, an effort is made to advance composite utilizing reinforcement particles. Taguchi L16 orthogonal array design of an experiment is adopted to recognize the effect of the parameters on the mechanical property of the composite. Moreover,

mathematical modeling and parameters optimization is executed. Consequently, mechanical properties of the developed samples were examined to recognize Al2O3 and graphite reinforcement effect in aluminum alloy matrix (A. A. Premnath et al. (2014)). The effects of compaction pressure, compaction time, milling time, and reinforcement particles weight percentage on the properties such as theoretical density, micro-hardness, and microstructure have been studied in this experimental investigation.

## 1.2 Aluminium Alloys

Aluminum became economically competent in industrial engineering applications as recently as the end of 19 century. In the decades, the Wright brothers created an entirely novel industry which developed in partnership with the Aluminium and Aluminium alloy industry outgrowth of fracture-resistant, strong, and structurally reliable parts for ultimately for air missiles bodies' engines, and airframes, satellite components, and fuel cells. The aluminum industry development was not limited to these outgrowths. The first advertorial application of Aluminium was new-fangled items such as house numbers serving trays Cooking utensils and mirror frames were also a prior early commercialized. (ASM international 1993) In recent years stringent requirements of material quality in the automotive and aerospace industries have necessitated the development of low weight aluminum alloys. The application of aluminum and its alloy are more in an industry in comparison to other metal alloys (K. K. Alaneme and K. O. Sanusi (2015**)**, Z.W. Zhang et al.(2018).

Aluminum Alloys are alloys in which aluminum is the predominant metal. Several properties set aluminum alloys apart from other metals and alloys. First, aluminum is lighter than all other engineering metals except magnesium and beryllium. It has a density of about 2700 kg/m3. A second important property of aluminum is its thermal and electrical conductivity. It has about 60% of the conductivity of pure copper (IACS). Because of its lower density, aluminum has a higher conductivity than copper per unit mass. The third property that is responsible for the wide use of aluminum alloys is their corrosion resistance. Aluminum is not widely used for chemical resistance, but for applications involving atmospheric corrosion resistance, it is probably the most widely used metallic material. Architectural applications of aluminum are everywhere – railing, windows, frames, doors, flushing, and so on (Z.W. Zhang et al. (2018)).

## 2.1Ceramic as a reinforcement

The addition of ceramic reinforcements such as SiC, Al2O3, B4C, TiC, and AlN to the aluminum matrix, increase its wear resistance, strength, and hardness (A. A. Premnath et al. (2014), K. Kanthavel et al. (2016), M. O. Bodunrin et al.(2015), M. Kumar and A. M. Murugan(2017)). A small weight percentage of reinforcement produces a greater amount of mechanical and wear-resistances properties. For example, wear-resistance and mechanical property of aluminum can be improved by reinforcing with Al2O3, thus, they have been of greater significance under numerous applications (K. Kanthavel et al. (2016), M. Rahimian et al.(2010))

## 2.2 Solid lubricant as a reinforcement

To achieve good strength, self-lubrication, and frictional properties commonly used lubricant reinforcements are MoS2, Gr, BN, and CaF2. For instance, reinforcing aluminum metal matrix by graphite permits to create of a film segregating the wearing couple without any interference of additional lubricant (M. O. Bodunrin et al. (2015), A. Baradeswaran and A. E. Perumal, (2014), and X. Qu et al. (2018). The AMCs have poor wear resistance and frictional property and require additional reinforcements to possess improved properties (K. Kanthavel et al. (2016), A. Baradeswaran and A. E. Perumal, (2014)).

## 2.3 Statement of problem

In the modern industry, there is a high demand for materials with low weight and high specific strength particularly in the industry of aircraft, automobile, satellite, and military. The materials must have low density and high strength for applications in such industries. Aluminum is the world’s most abundant metal and the third most common element comprising 8% of the earth's crust. It has a density of around one-third of steel making it the lightest commercially available metal. However, its poor mechanical property such as low hardness, low compressive strength, low thermal stability, and low wear resistance limit it from advanced applications, especially under high-temperature working conditions. To overcome the limitation of the aluminum alloy, this experimental work deals with the development of the novel material, aluminum metal matrix hybridically reinforced by Al2O3 and Graphite particles identically for the reason that ceramics and solid lubricants are proved to improve the mechanical and tribological properties of the aluminum alloy. Fabrication of the composite was carried out through the powder metallurgy

process. The experiments were designed using L16 orthogonal array and Grey relation analysis. Microstructures of the sample were analyzed using SEM and Optical microscopy. The wear tests of the samples were carried out on Pin on Disc apparatus. The optimization of the process parameters for the optimum value of Actual density, Porosity, Hardness, Compressive strength and wear resistance were carried out using the Taguchi method and Grey relation analysis.

## 2.4 Objective

### 2.4.1 General objective

To experimentally investigate aluminum metal matrix composite reinforced with Aluminum oxide and Graphite microparticles.

### 2.4.2 Specific objective

- To fabricate aluminum metal composite material reinforced with $Al_2O_3$ and Graphite by powder metallurgy process route.
- To investigate the mechanical properties like actual density, theoretical density, porosity, compression strength, hardness and microstructure of the composite.
- To investigate the wear resistance and coefficient of friction of the composite.
- To examine the distribution of homogeneity of the reinforcement of aluminium oxide ($Al_2O_3$) and Graphite (Gr) by using Optical and Scanning Electron Microscope.
- To optimize process parameters and develop mathematical modeling using Taguchi method and grey relational analyses.

## 2.5 Significance of study

The finding of this study will reach out to the benefit of society considering that low weight, high strength material plays an important role in science and technology today. The greater demand for weight reduction for the conservative of the fuel and energy need the research for more effective fabrication. Weight reduction is the single greatest advantage of aluminum composite material usage. Low-weight plane is more fuel efficient because it requires less fuel to propel itself forward. The developed composite material has lower corrosion relative to the magnesium alloy. Consequently, the material isn’t prone to corrosion due to harsh

chemicals; they can also handle wide variations in temperature and exposure to severe weather. Having an improved wear resistance will also make them significant.

## 2.6 Scope of study

This study involves the experimental investigation of aluminum metal matrix composite hybridically reinforced with different weight percentage of $Al_2O_3$ and Graphite. First, the samples are fabricated by using powder metallurgy method. The experimental measurement made are actual density, theoretical density, porosity, hardness, are made at ceramic laboratory of material science department whereas the compression strength is measured at the laboratory of the design and manufacturing department of Adama science and technology. Finally wear resistance and coefficient of friction is measured at [b]Mechanical Engineering Department, NERIST, Itanagar,India. As a result, several improvements on the mechanical property are attained. Thus, the hardness, porosity, density, compression strength, Wear resistance actively exhibited increase whereas additionally, the scanning electron microscopy and the optical microscopy revealed the uniform distribution of the reinforcement into the matrix.

## 2.7 Limitation of the study

Through the experimental investigation several limitations have limited this research to be conducted as it is proposed. Those limitations are

- Non availability of nano-particles supply in Ethiopia.
- Due to the COVID-19 pandemic importing the materials from abroad was not possible.
- Non availability of vacuum ball milling in Adama science and technology.
- Non availability of high pressure hydraulic press.
- The instruments used for this research are from over five identical laboratories. Working in various laboratories caused waste of time and incur of extra cost.
- Tribometer are not available in Ethiopia. The available tribometer are not allowed for external researchers.

## 2.8 Beneficiary of the study

Aerospace industry, Automotive, Marine, Military, researchers and electronics industry will be the beneficiaries of this research.

## 2.9 Organization of the research

The organization of the thesis has been done as follows. Chapter one included Introduction in which the statement of problem background, objectives, the scope of the study, and the significance of the study are described. Chapter two includes the literature survey, a summary of the literature, and the research gaps. Chapter three encompasses the material and methods, which include the powder metallurgy, measurements of the mechanical, and the tribological property. Whereas chapter four deals with the results and discussion. This implies that the result and for every response in addition to this the optimization of parameters are included using the Taguchi method and the gray relational analyses. Chapter five includes the conclusion and recommendation. The interpretations of the obtained results are analyzed and recommendation for future work is directed.

# CHAPTER TWO

# LITERATURE REVIEW

## 2.1 Introduction

In the previous few decades research and progress in materials shifted from plain to composite materials, providing to the universal need for concentrated weight, quality, high performance and low cost in structural materials (V. Mohanavela et al. (2017)). A Composite material is the amalgamation of two or more material with diverse chemical property so as to form a resilient material (Z.W. Zhang et al. (2017)). Also metal matrix composites (MMC) advanced in latest years compromises a few exclusive mechanical properties such as, high strength, low density and high wear resistance, high stiffness, and other attractive properties. One of the significant purposes of MMC is to advance a material with a cautious amalgamation of stiffness and toughness so as to lessening the sympathy to and cracks and flaws at the same time upturn the dynamic and static properties. There is a requirement to increase the damage lenient properties predominantly ductility and fracture toughness in AMCs (V. Mohanavela et al. (2017)).

In today's time, every commerce, be it the automobile subdivision or the aircraft sector, the whole world needs a material of worthy strength. Besides, their weight ought to be reduced. When it comes to this sympathetic of material, the demand for aluminium in it increases. Conversely, strength is a problem with aluminium. It is factual that the density of aluminium is low; nevertheless, if its strength is compared with iron, its strength is also less. That is why the demand for composite material has greater than before in today's time. In present days, it is being manipulated that the strength of aluminium is nearly equal to iron deprived of increasing the weight. If recent research is seen, many researchers have also improved the strength of aluminium well (V. Umasankar et al. (2014)).

## 2.2 Aluminium matrix composite

AMCs refer to a class of light and high performance aluminum centric material systems (V. Mohanavela et al. (2017)). AMM composite are formed by uniformly distributing reinforcement in the metal matrix. Reinforcement is usually done to advance the mechanical properties of the metal matrix like strength, hardness, , temperature withstand capacity, environmental effect, wear resistance, , density, porosity, high specific strength and stiffness, low coefficient of

thermal expansion good corrosion and oxidation resistance, tribological properties, etc.[ K. K. Alaneme and K. O. Sanusi (2015**)**, Z.W. Zhang et al. (2018))**.**Being typically reinforced with of ceramic materials, the main short emergences reported on AMCs, are their low toughness and ductility in comparison to the unreinforced Al and alloys. The low ductility and toughness can arise from a combination of factors such as natural brittle nature of ceramic reinforcements; and the mostly poor wettability amid ceramics and metallic melts, which consequences in poor interface strength. The latter factor is often responsible for load transfer inefficiencies from the matrix to the reinforcements (K. K. Alaneme and K. O. Sanusi (2015**)**).

Particulate reinforced AMC are broadly used in automobile, aircraft, marine, transportation, aerospace and defense sectors because of their exceptional strength to weightiness ratio, good thermal conductivity and better wear resistance (S. Wakeel and A. A. Khan,(2017), K. K. Alaneme and K. O. Sanusi (2015**)**. It is mostly used in the industry of automotive components like drive shafts, connecting rods, and cylinder liners (S. Wakeel and A. A. Khan (2017)). Aluminum–matrix composites (AMCs) reinforced with particles reinforcements are finding increased use in automotive, military, aerospace and electricity industries due to their improved properties (R' S. Bhatia and Kudlipsingh (2013)). Production cost (M. T. Hayajneh et al. (2009)) recently has suggested a possible application of AMCs as bearing materials. Usually bearing materials should possess sufficient hardness and wear resistance, but at the same time their strength should sustain the applied load without deformation, also to have a considerable toughness, that can resist shock loading (V. Mohanavela, et al. (2017)).

## 2.3 Reinforcements of Aluminium matrix composite

The different reinforcing materials used in the development of AMCs can be classified into three broad groups, which are synthetic ceramic particulates, industrial wastes and agro waste derivatives. The final properties of the hybrid reinforcement depend on individual properties of the reinforcement selected and the matrix alloy. Moreover, the processing route adopted for synthesizing AMCs depends on the nature of the matrix alloy and reinforcing materials which also influence the final properties of AMCs. Based on the published articles studied, the discussion on the combinations of reinforcement used in the synthesis of hybrid AMCs is divided into three broad groups. These are hybrid AMCs with two synthetic ceramic materials; an agro

waste derivative combined with synthetic ceramic materials; and industrial waste combined with synthetic reinforcement (Sh. P. Dwivedi and A. Kumar (2020)).

Aluminium-based ceramic composites properties were pointed out by for the good strength, frictional properties and self-lubrication properties and mentioning commonly used lubricants such as $MoS_2$, BN, Gr and $CaF_2$. The AMCs possess less frictional and wear resistance property and needs additional reinforcements to improve the properties. Further, addition of ceramic reinforcement enhances tribological properties of the composite material and similarly ceramic materials of SiC, $Al_2O_3$, $B_4C$, TiC, and AlN improved wear properties and mechanical strength (A. A. Premnath et al. (2014 ), K. Kanthavel et al. (2016), M. O. Bodunrin et al. (2015), M. Kumar and A. M. Murugan (2017), Mohanavela et al. (2017)). Compared with other ceramic reinforcements, whiskers can retard the degradation in ductility of the matrix induced by the addition of reinforcement, which makes the composites a promising substitution for aluminium alloys. Therefore, whiskers such as TiB, $MgAl_2O_4$, MgO, $Al_{18}B_4O_{33}$ and $Al_2O_3$ were utilized to reinforce Al matrix composites because of the resulting combination of excellent properties of the Al matrix and the whiskers, such as high specific strength and stiffness, good wear resistance, elevated temperature stability, and even low (M. A Ibrahim et al. (2019), K. Kanthavel et al. (2016), G. Iacob et al. (2015)).

## 2.4 Methods of aluminium matrix composite fabrication

MMCs are manufactured by techniques like powder metallurgy, stir casting process, squeeze casting, In-situ process, ultrasonic cavitations process, spray forming, pressure less infiltration techniques, etc. Cost of fabrication remains a major disadvantage in MMC. The composite materials offer flexibility in selection of reinforcements to tailor the properties. Therefore, cost effective processing of composites plays a crucial role in expanding their applications. Light weight; low cost of processing of hybrid MMCs is yet to attract much attention from researchers by using high strength reinforcements such as $Al_2O_3$ and SiC (Karthick Ea et al. (2017)).Most commonly Hybrid reinforced AMCs like the single reinforced AMCs are generally produced via two routes viz.: solid route and liquid route. Solid route involves powder metallurgy techniques while liquid route, which entail compo-casting, squeeze casting and mostly stir casting techniques. Powder metallurgy techniques have become very important in the production of hybrid AMCs because composites having more volume fraction of the reinforcing particulates

can be produced via this technique. Also, hybrid reinforced AMCs reinforced with nano-sized particulates have been successfully fabricated using this technique. Near-net shaped products that do not require post fabrication machining are easily produced using powder metallurgy. This technique is gaining lots of attention because particle clustering, wettability and formation of unwanted phases, which are some of the problems associated with liquid metallurgy route, are easily avoided (Sh. P. Dwivedi and A. Kumar, (2020))

Nevertheless, Mazaheri et al. described friction stir processing as a novel technique for developing surface metal matrix composites (SMMCs). This has become necessary because metal matrix composites developed via stir casting and powder metallurgy are often reported to have increased strength and stiffness at the expense of ductility and toughness. Friction stir processing offers the opportunity of developing SMMCs with higher surface hardness and improved creep resistance while maintaining the ductility and toughness of the metallic substrates (V. Umasankar, et al. (2014)).

### 2.4.1 Powder metallurgy

Powder processing route is more widely used for the manufacture of MMC because it offers some advantages compared to other methods. One of the main advantages of this process is the lower temperatures unlike the case of casting route, uniform dispersions, near net shape manufacturing, economical advantage and absence of chemical reaction between the matrix and reinforcement phases while retaining the parent metal morphology (M. Rahimian et al. (2010), R' S. Bhatia and Kudlipsingh( 2015), and Karthick Ea et al. (2017)). Also, there is the possibility of incorporating many types of reinforcement phases in the same composite system. In addition, a higher fraction of reinforcement particles may be included in the composite when compared against the rheological limitations of casting processes. The mechanical properties of the powder metallurgy (PM) parts are comparable to wrought or cast alloy (Karthick Ea et al. (2017)). Parts produced by this technology require minimal finishing, and have technical/economic advantages which made them very attractive for many applications in industry (R' S. Bhatia and Kudlipsingh( 2015)).

### 2.4.2 Stir casting

Stir casting technique has remained the most investigated technique for fabricating AMCs owing to its simplicity, flexibility and commercial viability. Although concerns of homogenous

distribution of reinforcing particles, porosity, wettability, particle clustering, segregation, interfacial reactions and formation of detrimental secondary phases have been widely reported; methods to contain these problems have been well reported (Sh. P. Dwivedi and A. Kumar (2020)).In a normal practice of stir casting technique, cast metal matrix composites is produced by melting the matrix material in a vessel and then the molten metal is stirred thoroughly to form a vortex and the reinforcement particles are introduced through the side of the vortex formed. From some point of view this approach has disadvantages, mainly arising from the particle addition and the stirring methods. During particle addition there is undoubtedly local solidification of the melt induced by the particles, and this increase the viscosity of the slurry (D. K. Koli, et al (2013)).

## 2.5 Process control agents

J.S.S. Babu, et al. (2011) Executed milling process at 300 rpm using a toluene medium as a process control agent in order to avoid oxidation or sticking of powders on the wall of the vial. Likewise in order to avoid agglomeration of the powder and its deposition on the walls of the vial and balls experiments G. Iacob et al. (2015) conducted milling process using zinc stearate (1% of the powder mass) as process control agent. Zinc stearate also utilized as die wall lubrication (K. Kanthavel et al. (2016). In addition to this M. Rahimian et al. (2011) and N. Radhika and R. Subramaniam,(2013) mixed Aluminum and alumina powder in liquid ethanol environment. This acted as a PCA which reduced agglomeration and prevented oxidation of aluminum powder during mixing. Liquid ethanol was used as a process control agent.

## 2.6 Most of important parameters that influence the powder metallurgy

This is because most of the parameters put into consideration during the design of AMCs are linked with the reinforcing materials. A few of such parameters are reinforcement type, size, shape, modulus of elasticity, hardness, distribution in the matrix among others (Sh. P. Dwivedi and A. Kumar (2020)).The study of sintered aluminium metal matrix composite reinforced with different weight percentages of SiC particles has highlighted the significance of processing parameters on sintered density, hardness and consequent breaking load.

- Among the parameters, compacting pressure exhibits a positive influence on sintered density, while both sintering temperature and time, a reverse influence. The reinforcement percentage exhibits a marginal influence.

- The hardness of sintered MMC is positively influenced by compacting pressure, while others exhibit a reverse influence.
- Up to 10% reinforcement, the composite exhibit a microstructure with fairly uniform distribution of the reinforcement, with higher order reinforcement, agglomeration of reinforcement has been observed.
- For a given reinforcement percentage, the load deflection response is compacting pressure, largely temperature and sintering time duration specific.

## 2.7 Characterization of the AMC

The reinforcement distributions in composites under various fabrication conditions were examined using optical microscopy (Huvitz HR-300 series), scanning electron microscopy (FESEM, Leo Supra 55). Composite densities were measured at room temperature by the Archimedean principle. Distilled water was used as the liquid for the measurement and at least three specimens were tested to obtain an accurate average value. The harness of the aluminium composite material is characterized by Vickers micro hardness, Macro Rockwell hardness (S. Wakeel and A. A. Khan (2017) and Brinel hardness (N. Radhika and R. Subramaniam (2013)). Compression strength is measured by universal testing machine. Several researchers made determination of tribological property of aluminium matrix composite by pin on disc tribometer (N. Radhika and R. Subramaniam (2013), N. Radhika and R. Subramaniam (2013), and I. Aatthisugan et al. (2017)).

### 2.7.1 Measurements of experimental and theoretical density

The theoretical density of he developed sample is calculated by using the mixtures rule (A. A. Premnath et al. (2014)).

$$P_{th} = \rho_m V_m + \rho_{r_1} V_{r_1} + \rho_{r_2} V_{r_2} \quad (2.1)$$

Where, $V_m$ and $V_{r1}$ and $V_{r2}$ represent the volume fraction of matrix and reinforcements, whereas $\rho_m$, $\rho_{r_1}$ and $\rho_{r_2}$ are density of the matrix, density of the first reinforcement and the second reinforcement respectively.

I. Aatthisugan, et al. (2017) Calculated the actual density of the composite and pure Aluminum is calculated using Archimedes' principle. The cylindrical sample was weighed being suspended in distilled water and then ($W_w$) and weighed again in air ($W_a$),

The actual density was calculated according to Eq. (2.2)

$$\rho_a = \frac{W_a}{(W_a - W_w)} \rho_w \quad (2.2)$$

Where, $\rho_a$ is actual density and $\rho_w$ is density of water

The specimen was weighed using a photoelectric balance with an accuracy of 0.01 mg. In acquiescence with Eq. (1), the actual density of the entire specimen can be calculated; theoretical density ($\rho_t$) of the specimen is calculated by the ratio of mass to volume

### 2.7.2 Measurement of porosity

The porosity is calculated by the ratio of the actual density to theoretical density subtracted from one. The equation (3) utilizes the variation b/n the theoretical density and actual density to estimate the porosity of the sample. The porosity of each specimen can be calculated according to the following equation [M. Merola Sci. Eng. (1996), K. K. Alaneme and K. O. Sanusi (2015**)** and I. Aatthisugan, et al. (2017).

$$P = 1 - \left(\frac{\rho_a}{\rho_t}\right) \quad (2.3)$$

Where, P is the porosity of the material, $\rho_a$ is the actual density and $\rho_t$ is the theoretic density.

### 2.7.3 Measurement of hardness

Hardness is an important property which affects wear resistance of any metal. Nadika et al. (2013) Made hardness measurements using a standard Brinell hardness tester on the base metal and HMMC specimen. Specimen of 15 mm length was cut from the composite bar and the surfaces are polished using emery paper. In order to eliminate possible segregation effect, a minimum of three hardness readings are taken for each specimen at different locations of the test samples and the average is taken as the hardness value (Nadika et al(2013)). While (S. Wakeel and A. A. Khan, (2017)) determined the macro hardness of the plain matrix alloy and the developed composites by conducting Rockwell hardness testing at 15 kgf load which is applied constantly for a dwell time of 5seconds, in same manner for micro hardness is evaluated by conducting Vickers's hardness testing at 0.5 kgf load which is applied constantly for a dwell time of 10 seconds. The hardness of both types was performed over the polished specimens at five different locations and the average values are then obtained and they are reported consequently.

### 2.7.4 Measurement of compressive strength

The compression test was performed on these samples with computerized universal Testing Machine (UTM-Auto instrument)) at room temperature and ultimate compression strength of these samples was measured as per ASTM E9-09 standards. Since it is a computerized machine the ultimate compressive strength was recorded accurately. The test was conducted at a cross head speed of 1 mm/min (D. K. Koli et al. (2013)).

I. Aatthisugan et al. (2017) and K. Kanthavel et al. (2016) calculated the actual density of the composite and pure Aluminum by using Archimedes' principle. The cylindrical sample was weighed being suspended in distilled water and then ($W_w$) and weighed again in air ($W_a$), The density of the sintered samples was determined using Archimedes principle.

The actual density was calculated according to Eq. (2.4)

$$\rho_a = \frac{W_a}{(W_a - W_w)} \rho_w \tag{2.4}$$

Where, $\rho_a$ is actual density and $\rho_w$ is density of water

The specimen was weighed using a photoelectric balance with an accuracy of 0.01 mg. In acquiescence with Eq. (1), the actual density of the entire specimen can be calculated; theoretical density ($\rho_t$) of the specimen is calculated by the ratio of mass to volume.

### 2.7.5 Microstructure analysis

I. Aatthisugan et al. (2017) Prepared and polished the specimens for observation of the Microstructure. The initial polishing was done by using emery paper in the order of grits The specimens were prepared using standard hand polishing using 220, 600, 800 and 1000-grit silicon carbide papers respectively and final buffing was done using liquid alumina to get a mirror like finish. Keller's reagent was used as an etchant to observe features. The microstructure was observed using Optical Inverted Microscope. The microstructure was observed at a distance of 2, 8 and 14 mm from the outer diameter of the cast in order to study the variation of reinforcement particles. Likely Nadika et al. (2013) investigated the grain structures, size, shape and distribution of reinforced particles using Optical microscope. In other aspect S. Das et al. (2020) made SEM studies were on polished specimens to investigate the presence of reinforcement distribution, and matrix reinforcement grain size and gain morphology. In addition to this K. Kanthavel, et al. (2016) investigated the microstructures, material combination, wear

and friction properties by scanning electron microscopy; Metallographic analysis offers a dominant quality control as well as an important analytical tool.

### 2.7.6 Wear resistance measurement

Nadika et al. (2013) made dry sliding wear tests by using pin-on-disc as per ASTM G99 standard. The counter disc material was EN31 steel. Before testing, pins and disc surface were cleaned with acetone. All of the tests were performed on various applied loads of 5, 10, 20 and 50 N with sliding speeds of 1 m/s. A varying sliding distances of 500, 1000 and 2000 m were employed. After each test, the specimen and counter face disk were cleaned with organic solvents to remove traces. The pin was weighed before and after testing to an accuracy of 0.1 mg to determine the amount of wear loss. In a similar manner N. Radhika and R. Subramaniam, (2013) made a tribological determination on pin-on-disc test apparatus to evaluate the dry sliding wear characteristics of hybrid composite specimens. The sliding wear tests are conducted as per ASTM G 99-04 under lubricated, dry laboratory conditions at room temperature. Specimens of size 10 mm diameter and 30 mm length are cut from the cast samples machined and then polished metal graphically. Each specimen is thoroughly cleaned by acetone solution, dried, and then accurately weighed using a single pan electronic weighing machine with an accuracy of 0.0001 g. The contact surface of the cast sample (pin) has to be flat and will be in contact with the rotating disk. The tests are carried out by varying the applied load and sliding speed for a constant sliding distance of 2,100 m. During the test, the pin is pressed against a rotating EN32 steel disc with a hardness of 65 HRC by applying load that acts as counterweight and balances the pin. All the specimens followed a same track of 110 mm diameter with a tangential force. At the end of each test, the final weight of the pin is measured, after cleaning with acetone. The difference between the initial and final weight of the pin gives the weight loss due to sliding wear. The volume loss due to wear is calculated by the use of corresponding density values of the pin. The wear rate of the composite pins is then calculated (ratio of volume loss to sliding distance)

## 2.8 Taguchi optimization method

The Taguchi method is a statistical approach that is widely used to optimize process parameters and to improve the quality of manufactured products (Fei et al. (2013)). The method has been employed with great success in experimental designs for problems with multiple parameters due

to its practicality and robustness (Ahmad et al. (2016). Taguchi methods of experimental design provide a simple, efficient and systematic approach for the optimizing testing parameters and finding out their contribution on target parameters(N. Radhika and R. Subramaniam (2013)).The method uses a unique design of orthogonal arrays to provide a reduced variance for the experiment with the optimum setting of process parameters (Ahmad et al. (2016)). In the Taguchi method, a design parameter is considered significant if its influence is large compared with the experimental error as estimated by the analysis of variance (ANOVA) statistical method. Mean-response graphs were plotted using ANVW-31 software and the percentage of contribution of testing parameters was determined by ANOVA analysis [39].In the competitive market, industries face challenges in bringing high quality products. Taguchi method is one of the most efficient tools which can be used to reduce the number of variations in parameters through robust design of experiments (DOE) (N. Radhika and R. Subramaniam, 2013) .Taguchi recommends analyzing the mean response for each run in the inner array, and he also suggests analyzing variation using an appropriately chosen signal-to-noise ratio (S/N).These S/N ratios are derived from the quadratic loss function and among the three quality exhibition. The optimal setting is the parameter combination that has highest S/N ratio. The statistical analysis of the data is performed by analysis of variance (ANOVA) to study the contribution of the factor and interactions and to explore the effects of each process on the observed value ( R. Arunachalam et al. ( 2019)).The advantage of Taguchi's optimization method is that it allows the optimization of the process parameter with a minimum number of experiments. Because of these advantages, as well as off-line quality control, the Taguchi method has been successfully used in the optimization of process parameters in several manufacturing processes (Fei et al. (2013)).

## 2.9 Hybrid Taguchi and Grey Relational Analysis optimization

The traditional Taguchi technique can optimize only a single response variable under the effect of multiple parameters. Therefore, this technique is combined with grey relational analysis (GRA) to optimize multi-process parameters for multiple response variables that this research tends to address. GRA is widely used to convert multiple response variables into a single grey relational grade ( Fei et al. (2013)). In this method, signal-to noise (S/N) ratio is used to represent a performance characteristic and the largest value of S/N ratio is considered. Based on the objective of the experiment, any one of the S/N ratios, namely lower-the-better, the higher-the-

better or the nominal-the-better is selected for further analysis. Grey system theory developed by Prof. Deng in 1982 has proved to be a useful tool in dealing with poor, incomplete and uncertain information. GRA based on the grey system theory can also be used to solve the complicated interrelationships among the multiple performance characteristics effectively. GRA is used to obtain a grey relational grade to evaluate such multiple performance characteristics. As a result, optimization of complicated multiple performance characteristics can be converted into optimization of a single grey relational grade. The procedure that involved the grey relational method is as follows:

1. Experimental results are normalized between zero and one.
2. Grey relational coefficients are calculated from the normalized data. This coefficient helps to distinguish between the desired and actual experimental data.
3. Grey relational grade is calculated by averaging the grey relational coefficients. Grey relational grade is treated as the overall response of the process instead of the multiple responses of wear rate and coefficient of friction.
4. ANOVA for the input parameters is calculated with the grey relational grade to find which parameter has a significant influence on the abrasive wear performance as well as its percentage of contribution.
5. Optimum parameter levels for abrasive wear performance are then selected.
6. Confirmation experiment is conducted to verify the optimum wear parameters obtained (S Dharmalingaml et al. (2013)).

## 2.10 Literature survey on the aluminium matrix composite

G. Straffelin et al. (1997) studied the Influence of matrix hardness on the dry sliding behavior of 20 vol.% $Al_2O_3$-particulate-reinforced 6061 A1 metal matrix composite. The author revealed that if the hardness of the materials is increased by a treatment, their wear rate also increases, because of the occurrence of subsurface softening and the formation of surface mixed scales prone to leaving the Tribological system. On the other hand, the as-extruded composite is characterized by a lower matrix hardness thus reducing its wear rate.

O. Yılmaza and S. Buytozb (2001) revealed that the abrasive wear rates of composites decreased more rapidly with increase in $Al_2O_3$ volume fraction in tests. At the same time the results show that the beneficial effects of hard $Al_2O_3$ particles on wear resistance far

surpassed that of the sintered porosity in the compo casting metal-matrix composites (MMCs). Finally, it was seen that wear rate of the composites decreased considerably with graphite additions.

A. Forn et al. (2003) investigated the Spinel effect on the mechanical properties of metal matrix composite AA6061/($Al_2O_3$)p.. The authors suggest a decohesion between matrix and reinforcement, that involves a loss of mechanical properties. A fractographic study reveals that the fracture of the reinforced material takes place in the matrix–$Al_2O_3$ particles interface. The fracture mechanism seems to be influenced by spinel presence surrounding the aluminium oxide particle surface. In spite of the spinel attendance, one can notice that the aluminium matrix composite AA6061/($Al_2O_3$)p in the T6 condition, that is, submitted to age hardening treatment, suffers a remarkable mechanical behavior improvement.

Y. Sahin et al. (2005) made optimization of testing parameters on the wear behavior of metal matrix co-behavior based on the Taguchi method. This experimental result demonstrates that the abrasive grain size was the major parameter on abrasive wear, followed by reinforcement size. The sliding distance and applied load, however, were found to have a neglecting effect. Moreover, the optimal combination of the testing parameters could be predicted. The predicted weight loss of the composite samples was found to lie close to that of the experimentally observed ones.

Peng Yu et al. ( 2005) Structure, thermal and mechanical properties of in situ Al-based metal matrix composite reinforced with $Al_2O_3$ and TiC submicron particles The results indicated that fined $Al_2O_3$ particles and large inter-metallic $Al_3Ti$ plates were in situ formed in the Al–10 wt.% TiO2 sample during HIPing. However, the introduction of C to the Al–TiO2 system was beneficial to eliminate large inter-metallic Al3Ti plates. In this case, $Al_2O_3$ and TiC submicron particles were in situ formed in the Al–10 wt.% $TiO_2$–1.5 wt.% C sample. Three-point-bending test showed that the strength and the strain-at-break of the HIPed Al–10 wt.% $TiO_2$–1.5 wt.% C sample were significantly higher than those of its Al–10 wt.% $TiO_2$ counterpart. The improvement was derived from the elimination of bulk $Al_3Ti$ inter-metallic plates and from the formation of TiC submicron particles. DSC measurements and thermodynamic analysis were carried out to reveal the reaction formation mechanisms of in situ reinforcing phases. The DSC results generally correlated well with the theoretical predictions. Finally, the correlation between the structure-property relationships of in situ composites is discussed.

M. T. Hayajneh et al. (2009) revealed that the models for the thrust force and cutting torque were identified by using the alumina ($Al_2O_3$) particles contents, graphite (Gr) particles contents, cutting feeds (F) and spindle speeds (N) as input data and thrust force and cutting torque as the output data. A minimum error model was obtained through exhaustive search of the optimal learning parameters which leaded to build a feed forward back propagation neural network with two hidden layers and five hidden neurons on each hidden layer. The ANN model was verified experimentally by further experimentation using different sets of inputs. The results of these experiments were in a good agreement with those predicted using the ANN model.

M. Rahimian et al. (2010) Investigation of particle size and amount of alumina on microstructure and mechanical properties of Al matrix composite made by powder metallurgy. The authors revealed that as the alumina particle size decreases compressive strength, yield strength, hardness and elongation increase and factors such as, distribution homogeneity microstructure grain size and wear resistance in matrix decreases.

A. Manna et al. (2010) made experimental study on fabrication of Al–Al2O3/Grp metal matrix composites. The author observed that that the hardness of the composite is increased with the increase in reinforced particle volume fraction. Both tensile strength and impact strength are decreased with increase in reinforced volume fraction. The prepared composite plates are welded by gas welding with Al–Si-base filler metal.

Z. Mei-juan et al. (2010) studied the Microstructures and wear properties of graphite and Al2O3 reinforced AZ91D-Cex composites. The results reveal that Ce enriches around the boundaries of graphite particles and forms $Al_3Ce$ phase with Al. The addition of Ce refines the microstructures of the composites. With the increase of Ce content, the grain size becomes smaller and the wear resistance of the composite is improved. At low load, the composites have similar worn surface. At high load, the composite with 1.0% Ce has the best wear resistance due to the existence of $Al_3Ce$ phase. The $Al_3Ce$ phase improves the thermal stability of the matrix so the graphite particles can keep intact, which can still work as lubricant. At low load, the wear mechanism is abrasive wear and oxidation wear. At high load, the wear mechanism changes to delamination wear for all the composites

G. B. V. Kumar et al. (2011) It Mechanical and Tribological Behavior of Particulate Reinforced Aluminum Metal Matrix Composites – a review has been studied and concluded that the density

of the composites increases, and wear rate decrease with the incorporation of the hard ceramic reinforcement into the matrix material.

A. Manna1et al. (2011) observed that the hardness of the composite is increased with the increase in reinforced particle volume fraction. Both tensile strength and impact strength are decreased with increase in reinforced volume fraction on fabrication of Al-$Al_2O_3$/Grp metal matrix composites.

J. S. S. Babu et al. (2011) made a research in which the results of Taguchi analysis indicate that wear loss increases with increasing load and sliding distance, but it is reduced with increasing sliding speed. Coefficient of friction decreases with increasing applied load and sliding speed whereas it increases with increasing sliding distance. The composites with 10 vol.% and 15 vol.% of fiber had the lowest wear loss and friction because of the mixture effect of GNFs and $Al_2O_3$sf. However, due to the effect of agglomerated GNFs, there was an increase in wear loss and friction at 20 vol.%

V. N. Gaitonde et al. (2012) Some Studies on Wear and Corrosion Properties of Al5083 / Al2O3 /Graphite Hybrid Composites by using stir casting synthesis. The authors unveiled that the addition of reinforcement improves the hardness and reduces corrosion and wear rates.

S. Rajesh et al. (2012) executed modeling and optimization of sliding specific wear and coefficient of friction of aluminum based red mud metal matrix composite using Taguchi method and response surface methodology. In this investigation the use of Taguchi method presented for minimizing the specific wear and coefficient of friction in red mud based aluminum MMC. Response Surface Methodology (RSM) is also employed to develop mathematical model for specific wear rate and coefficient of friction. A plan of experiments, based on L27 Taguchi design method, the orthogonal array, signal- to- noise ratio, and analysis of variance (ANOVA) are employed to investigate the influence of parameters like applied load, sliding velocity, % of reinforcement and hardness of the counterpart material. Pin on Disc apparatus is used to conduct the experiment to analyze the effect of input parameters on output performance characteristics. From the analysis of signal to noise ratio (S/N) and ANOVA, the optimal combination levels and the effect of input parameter on output response are obtained. RSM is employed to develop mathematical model, capability of the model is good in prediction of results and results are very

closer to the measured value. Analysis of variance (ANOVA) technique is applied to check the validity of the developed model.

S. A. Sajjadi et al. (2012) made Comparison of microstructure and mechanical properties of A356 aluminum alloy/Al2O3 composites fabricated by stir and compo-casting processes. The results of microstructural study revealed uniform distribution, grain refinement and low porosity in micro and nano-composite specimens. The mechanical results showed that the addition of alumina (micro and nano) led to the improvement in yield strength, ultimate tensilestrength, compression strength and hardness. It was indicated that type of fabrication process and particle size were the effective factors influencing on the mechanical properties

A. Devaraju et al. (2013) revealed that Aluminum alloy base surface hybrid composites were fabricated by incorporating with mixture of (SiC + Gr) and (SiC + $Al_2O_3$) particles of 20 μm in average size on an aluminum alloy 6061-T6 plate using friction stir processing (FSP). It was observed that the addition of Gr particles rather than Al2O3 particles with SiC particles, decreases the micro hardness but immensely increases the dry sliding wear resistance of aluminum alloy 6061-T6 surface hybrid composite. The observed micro hardness and wear properties are correlated with microstructures and worn micrographs.

M. Nagaral et al. (2013) studied the mechanical behaviour of aluminium 6061 reinforced with $Al_2O_3$ & graphite particulate hybrid metal matrix composites by liquid metallurgy. Mechanical properties like hardness and tensile strength of Al6061 alloy was increased by addition $Al_2O_3$ particles. The Micro-Vickers hardness of the Al6061-6wt% Al2O3 was found to decrease with addition of graphite content in the composite but the effect of graphite content on tensile strength of the composite was less.

D. K. Koli et al. (2013).This authors reviewed the characterization of mechanical properties with production routes of powder metallurgy and castings for aluminium matrix-$Al_2O_3$ composites. Reinforcing aluminium matrix with much smaller particles, submicron or nano-sized range is one of the key factors in producing high-performance composites, which yields improved mechanical properties. A uniform distribution of the $Al_2O_3$ reinforcement phase in the Al matrix can be obtained by high-energy ball milling of Al–$Al_2O_3$ blends. Nearly 92% increase in the hardness and 57% increase in the tensile strength were obtained in the nano-composites as compared to the commercially pure aluminium. Ultrasonic assisted casting and powder

metallurgy methods are becoming more common for the production of Al-$Al_2O_3$ composites. Agglomeration of the reinforcing particles along with the increasing volume percentage is still a challenging task in composites materials manufacturing.

M. Uthayakumar et al. (2013) research study emphasizes on the dry sliding wear behavior of aluminum reinforced with 5% SiC and 5% $B_4C$ hybrid composite using a pin on disc tribometer. Wear performance of the hybrid composites were evaluated over a load ranges of 20–100 N, at the sliding velocities from 1 to 5 m/s. Detailed metallurgical examination and energy dispersive analysis were carried out to assess the effect of SiC and $B_4C$ particles on the wear mechanisms. The Focused Ion Beam (FIB) technique is used to characterize the tribo layers that have been formed at the worn surfaces of composites. The experimental results show that the hybrid composites retain the wear resistance properties up to 60 N loads and sliding speed ranges 1–4 m/s. The enhancement of wear resistance with small amount of SiC and B4C is achieved by the cooperating effect of reinforcement particles

M. Uthayakumar et al. (2013) Wear performance of Al–SiC–$B_4C$ hybrid composites under dry sliding conditions the authors revealed that the hybrid composites retain the wear resistance properties up to 60 N loads and sliding speed ranges 1–4 m/s. The enhancement of wear resistance with small amount of SiC and $B_4C$ is achieved by the cooperating effect of reinforcement particles.

X. Qu et al. (2013) revealed that result of the perfect lattice matching between gamma-Al2O3 and the Al matrix, the gamma-$Al_2O_3$ whisker is a desired reinforcement for the Al matrix, improving the ultimate tensile strength and hardness to 217 MPa and 43.5 HV, respectively, with a satisfactory ductility of 11%. Differential scanning calorimetry analysis shows that the growth of the whisker occurred at 550–650 °C, and the ball milling energy has a significant effect on whisker growth.

K. Kumar et al .(2014)investigated the processing and tensile testing of 2024 al matrix composite reinforced with $Al_2O_3$ nano-particles using mechanical stir casting process generally results poor distribution of nano particles having high porosity in the matrix. The tensile strength of Al2024/1 % wt $Al_2O_3$ nano composite has improved by 43% as compare to the Al2024 alloy.

A. A. Premnath et al.(2014) reinforced aluminium with graphite and alumina and analyzed the mechanical and tribological property. The density and hardness increase with increase in weight

percentage of Al2O3. The as shown on the fig reinforcing particles are evenly distributed in the matrix.

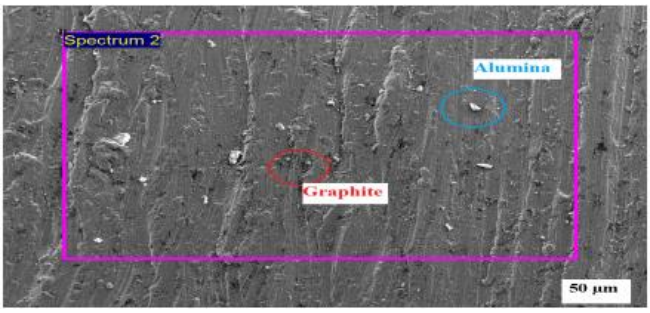


Figure 2.1 SEM images of uniform distribution of the alumina and graphite particles (A. A. Premnath et al.(2014)

From the analysis of variance (ANOVA), load is the dominant factor that affects the specific wear rate of hybrid composites followed by speed and weight fraction of $Al_2O_3$. Based on desirability approach, the improvement in the wear resistance of the composites became more prominent at high speed, high load and high weight fraction of $Al_2O_3$. The worn surface of the pin was examined using scanning electron microscope (SEM) which indicates that the wear mechanism of composites is mostly abrasive wear followed by oxide wear.

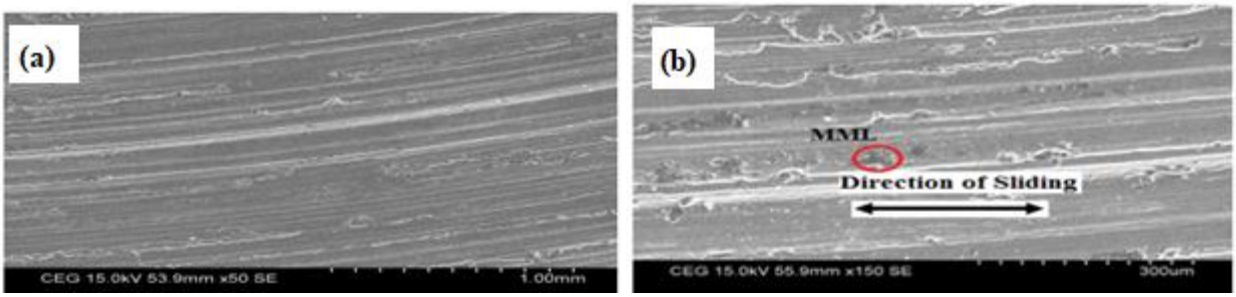


Figure 2.2 (a). SEM micrograph of Al/$Al_2O_3$/Gr at s = 2.46 (m/s), f = 30 (N) and w = 15 (%) Figure 2.2 (b) SEM micrograph of Al/$Al_2O_3$/Gr at load of 10 N (A. A. Premnath et al.(2014))

Baradeswaran and A. Elaya Perumal (2014)unveiled that The hardness, tensile strength, flexural strength and compression strength of the Al 7075–$Al_2O_3$–graphite hybrid composites are found to be increased by increased weight percentage of ceramic phase. The wear properties of the hybrid composites containing graphite exhibited the superior wear-resistance properties

D. M. Nuruzzaman et al. (2014) Fabricated the three sample of alumina aluminum matrix (Al-$Al_2O_3$) having 10%, 20% and 30% of Alumina ($Al_2O_3$) and calculated the effect on different

mechanical properties. These specimens were fabricated under the different load of 15 and 20 ton. Basically in this study effect of volume fraction of $Al_2O_3$ and compaction load on the properties of $Al/Al_2O_3$ was calculated. Now taking different samples, it was observed that increasing the load from 15 ton to 20 ton increases the density of Al-composite. On increasing the volume fraction of Alumina, the density increases but after sintering process it was observed that for the compaction load of 20 ton , the increase in density of composite was somehow less than that of the composite under the load of 15 ton. It was calculated through the Rockwell hardness tester that average hardness under the 20 ton compaction load is greater than that of composite under 15 ton compaction load and densities of composite under 20 ton load is higher than the specimen under 15 ton.

G. Iacobet al. (2015) Studies on wear rate and micro-hardness of the $Al/Al_2O_3/Gr$ hybrid composites produced via powder metallurgy it was observed that the micro-hardness improve when increasing the milling time and the reinforcement content due to presence of hard $Al_2O_3$ particles. The authors also observed a low wear rate exhibited by the $Al/Al_2O_3/Gr$ hybrid composites due to presence of $Al_2O_3$ and Gr which they acted as load bearing elements and solid lubricant respectively. The observed wear rate and micro-hardness have been correlated with micro structural analysis

Shivakumar N. et al. (2015) investigated Synthesize and characterization of nano sized $Al_2O_3$ reinforcing ZA-27 aluminium composite. The authors unveiled that homogeneity of the composite is well labeled using ANOVA the minimum wear loss weight percentage combination is identified additionally increase in $Al_2O_3$ resulted decrease in wear loss. Minimum wear rate and coefficient of friction were found to be the optimal parameter combination of the abrasive wear at an applied load of 20 N, sliding speed 1.5 m/s and abrasive medium 1000 mesh and 2 wt% MoS2. Grooving, ploughing and micro-cutting along with fracture and delamination during abrasive wear of the composite surfaces were confirmed using SEM analysis. Wear rate decreased with increase in sliding speed and molybdenum disulphide content, but increased with load and abrasive size.

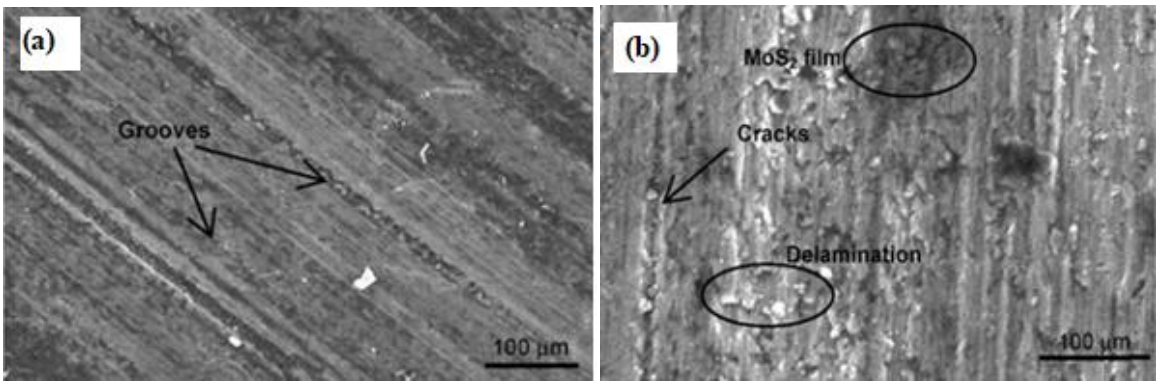


Figure 2.3 a) Worn surface of Al alloy/10 wt% Al2O3 /4 wt%MoS2 composite at 40 N load at a sliding speed of 1 m/s with abrasive size of 320 mesh. Figure 2.3 b) Worn surface of Al alloy/10% $Al_2O_3$/2% MoS2 tested at 60 N load at a sliding speed of 0.5 m/s with 120 mesh abrasive size (Shivakumar N. et al. (2015)

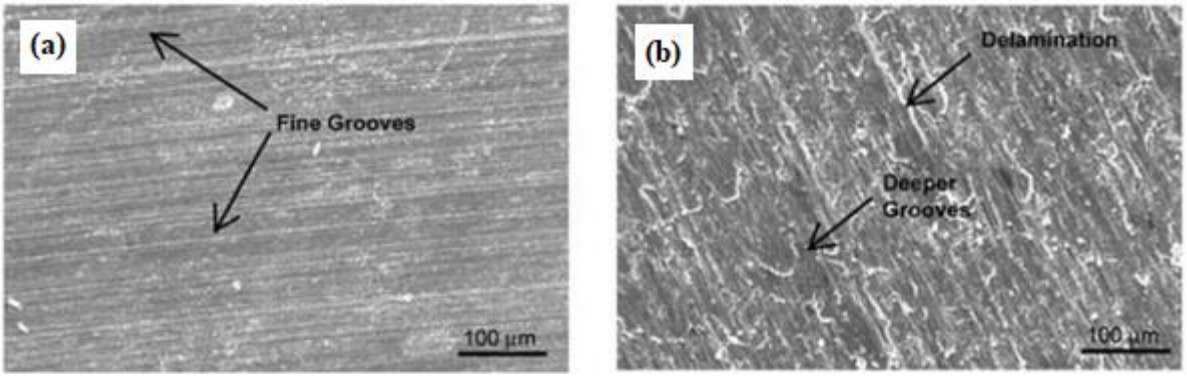


Figure 2.4 a) SEM images of fine grooves. Figure 2.4 b) SEM images of deep grooves and determination (Shivakumar N. et al. (2015))

Coefficient of friction increased with load but decreased with increase in sliding speed and molybdenum disulphide content. Whereas Hybrid aluminium composites with 10 wt% Al2O3 with 2 wt% MoS2 hybrid MMCs gave the best wear performance for the optimized abrasive wear parameters obtained.

S.Velicˇkovic et al. (2016) executed Optimization of tribological properties of aluminum hybrid composites using Taguchi design In this experimental proved that, as the weight percentage of graphite particle increase the tribological property also improve. The microstructure shows that the SiC and graphite are uniformly distributed. A worn surfaces analysis by SEM and EDS implies that Fe presence and MML layer formation. Adhesive wear mechanism is observed mainly.

S. V.˘kovic et al. (2016) made Optimization of tribological properties of aluminum hybrid composites using Taguchi design By applying analysis of variance, it was determined that the best tribological properties has A356/10SiC/3Gr hybrid composite. It was also found that the greatest impact on specific wear rate has load with the percentage effect of 69.163%, then sliding speed with 14.426% and the interaction between wt.% graphite and load. The dominant wear mechanism is adhesive wear as confirmed by scanning electron microscopy with energy dispersive spectroscopy (SEM-EDS)

S. N. Alam and L. Kumar (2016)Mechanical properties of aluminium based metal matrix composites reinforced with graphite nanoplatelets 2016 Results of the wear test show that there was a significant improvement in the wear resistance of the composites up to the addition of 3 wt% of xGnP in the Al matrix. The hardness of the various Al-xGnP composites also shows improvement upto the addition of 1 wt% xGnP beyond which there was a decrease in the hardness of the composites. The tensile strength of the Al-xGnP composites continuously reduced with the addition of xGnP due to the formation of Al4C3 particles at the interface of the Al and xGnP in the composite.

K. Kanthavel et al. (2016) made study of Tribological properties on $Al/Al_2O_3/MoS_2$ hybrid composite processed by powder metallurgy. SEM, EDX, and pin-on-disc wear tester is used to analyze The microstructures, material combination, wear and friction respectively. The newly developed aluminium with a combination of 5% (Al2O3) and 5% (MoS2) showed significant improvements in Tribological properties. The test unveiled that that sliding speed of 1.5 m/s, applied load of 5 N and with sliding distance of 1000 m result in minimum coefficient of friction as 0.117 and wear loss of 0.0102 g

V. Mohanavel et al. (2017) investigated the mechanical behavior of hybrid composite (AA6351+Al2O3+Gr) fabricated by stir casting method Optical microphotographs depict the nearly homogeneous distribution of the reinforcement particles in the base metal matrix. The hardness, the tensile strength and the flexural strength are found to increase in the AA6351 base matrix alloy with the increase in c reinforcement. The mechanical properties of the AA6351 alloy are significantly improved after the dispersion of Al2O3/Gr particles.

R. S. Bhatia and K. Singh (2017) revealed that boron carbide interface cracks produced greater wettability of particles and perfect interface was observed between Alumina and graphite

particles and this increased micro hardness of surface with further reinforcements on the experimental Analysis of Aluminium Metal Matrix Composite using Al2O3/B4C/Gr Particles fabricated by stir casting.

M. D. Selvam, and N.M.Sivaram (2017) investigated the Optimal Parameter Design by Taguchi Method for Mechanical Properties of Al6061 Hybrid Composite Reinforced With Fly Ash/Graphite/Copper. The experimental results showed significant changes in each composition. Both the tensile strength and hardness tend to increase when compared to unreinforced Al6061. A mathematical model representing the tensile strength is developed using regression analysis with the help of MINITAB software

I.Aatthisugan et al. (2017) studied the Mechanical and wear behavior of AZ91D magnesium hybrid composite reinforced with boron carbide and graphite the authors revealed that the addition of both a hard reinforcement (e.g., B4C) and soft reinforcement (e.g., graphite) significantly improves the wear resistance of magnesium composites. These entire results designate that the hybrid magnesium composites can be considered as an excellent material where high strength, ultimate tensile strength and wear-resistant components are of major importance, primarily in the aerospace and automotive engineering sectors.

Karthick Ea, et al. (2017) analyzed the Processing, Microstructure and Mechanical Properties of $Al_2O_3$ and SiC Reinforced Magnesium Metal Matrix Hybrid Composites, the author revealed that magnesium metal matrix composites (MMC) hardness increased from 64.53 to 75.16 HV, which was mainly due to the presence of reinforcements Al2O3 and SiC along with precipitates. Addition of alumina and silicon carbide on magnesium alloy influenced the hardness of MMC.

.M.A Ibrahim et al. (2019) reviewed the mechanical Properties of Aluminium Matrix Composite Including SiC/Al2O3 by Powder Metallurgy- hardness/compressive strength and tensile/ultimate tensile strengths increased with increasing the amount of reinforcements, sintering time, temperature, compaction load and reduced size of the reinforcements.

Sh. P. Dwivedi et al. (2020) investigated the Development of graphite and alumina reinforced aluminium based composite material. The authors revealed that two reinforcements have been used to increase the mechanical properties of aluminum. The first reinforcement that has been taken is named graphite and the second reinforcement is named alumina. Stir casting technique has been used to make composite. From the microstructure image, it is understood that the

reinforcement is well integrated into the matrix. Whereas tensile strength and hardness increased by the addition of graphite and alumina consequently due to the poor wettability toughness has decreased.

## 2.11 Summary of the literature

From the literature review the following summary are revealed by several researchers.

- With the increase in the weight percentage of $Al_2O_3$ the micro hardness, compressive strength, wears resistance and tensile strength increase.
- Most of the researches are done without utilizing optimization of parameters. The few researches done on optimization are done by Taguchi with its dis-advantage of optimizing only one parameter at a time.
- Increase in weight percentage of graphite content cause increase in density, wear resistance, corrosion resistance, nevertheless the micro hardness, friction rate, ductility, ultimate tensile strength.
- By using powder metallurgy for the fabrication of the sample uniform distribution of the reinforcement particles can be achieved.
- The magnesium content in most of the aluminium matrixa induce oxidation during sintering process.
- The reinforcement cause improvement on the hardness and wear resistance of the composite while simultaneously it decrease the ductility and fracture toughness of the samples. Due to the poor wettability and emanation between the melted matrix and the reinforcing matrix.

Many researchers have already made an experimental investigation on the Aluminium matrix reinforced by Aluminium oxide and graphite they have revealed the above conclusion. But still no experimental investigation is made on parametric optimization by utilizing hybrid Taguchi and grey relation analysis on aluminium matrix composite reinforced by alumina nada graphite particles.

## 2.12 Research gaps

Several researchers have done experimental investigation of the aluminium matrix composite reinforced by aluminium oxide and graphite particles. Nevertheless, none experimental investigation is done on aluminium reinforced by aluminium oxide and graphite by hybrid

Taguchi and GRG. The low magnesium content in the aluminium alloy have positive impact on the sintering condition of the composite by reducing the poor wettability  emanation that can be caused by the oxidation of the aluminium matrix composite during sintering process. In addition to this many researchers have used Taguchi optimization method to analyze the optimal condition of the parameters. Even though they optimized some parameters, they could not reduce the dis-advantage of the Taguchi method which is optimization of one parameter at a time. But this research has overcome this dis-advantage by making optimization of parameters by hybrid Taguchi and grey relational analyses.

# CHAPTER THREE

# MATERIALS AND METHODOLOGY

## 3.1 Introduction

This chapter describes the materials and method used for the fabrication of composites. For this study, the materials such as aluminium alloy powder, aluminium oxide, graphite, and toluene and Keller reagent are utilized in order to manufacture the composite material specimen. Argon gas is utilized in the sintering process to control the sintering condition and distilled water, ethanol are utilized for cleaning purpose.

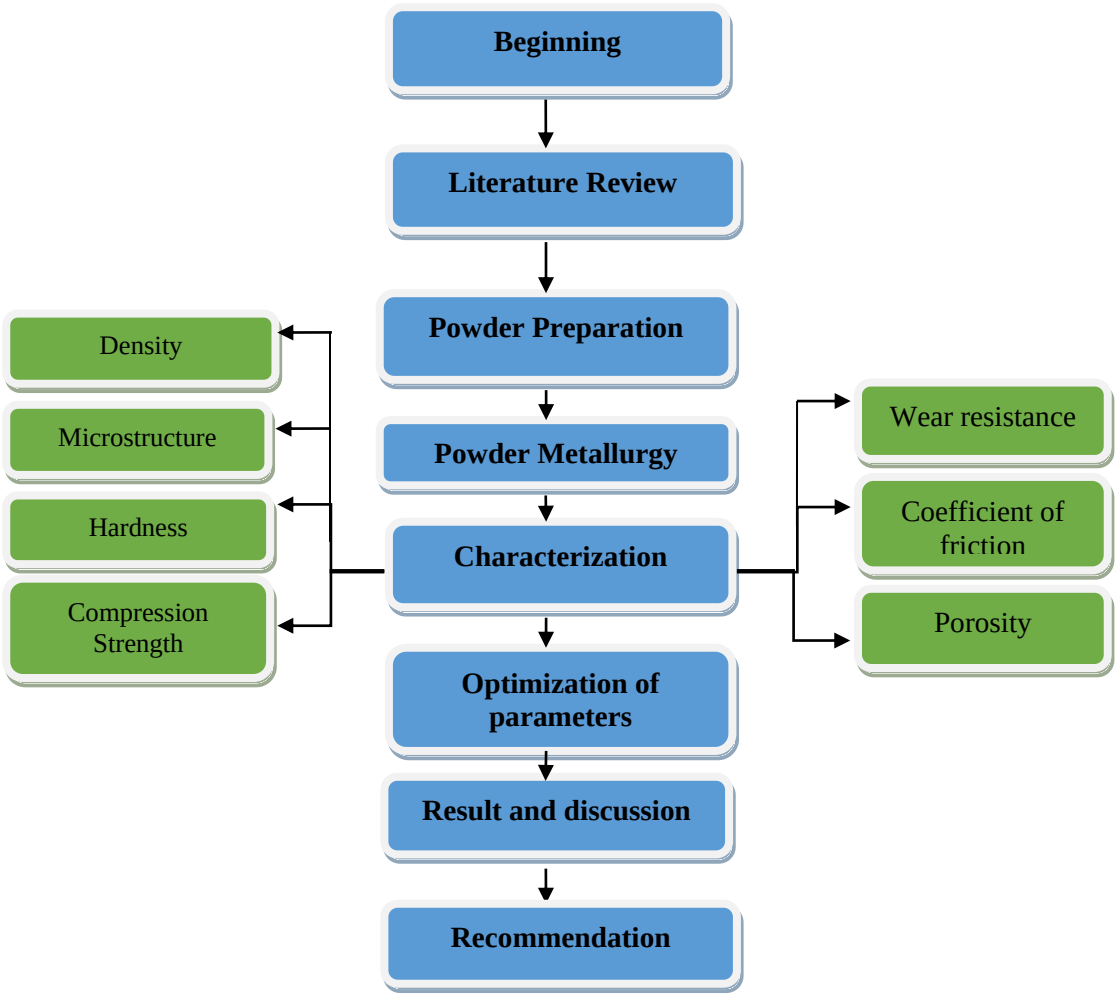


Figure 3.1 Flow chart of methodology

## 3.2 Materials and methods

Aluminium powder (from blulux.co India) with 99.8 % purity, Graphite powder, Aluminium Oxide powder (from trust chemical laboratories), Toluene, Ethanol are bought from Addis Abeba Yeshadam trading PLC with an average particle size of 50-250µm is used as a matrix in this experiment.

Table 3.1Chemical composition of the aluminium

| **Content** | **Aluminum** | **Iron** | **Copper** | **Silicon** | **Manganese** | **Magnesium** | **Zinc** |
|---|---|---|---|---|---|---|---|
| **Weight percentage** | 99.8% | 0.17% | 0.00159% | 0.0313% | 0.0023% | 0.0016% | 0.0053% |

Aluminium oxide ($Al_2O_3$) powder with 70-250 meshes size is chosen as reinforcement owing to its high hardness and low co-efficient of thermal expansion, highly wear resistant, good mechanical properties, high temperature strength and thermal shock resistance.

Table3.2 Properties of aluminium oxide [14].

| **Property** | |
|---|---|
| Density (g/cm3 | 3.9 |
| Modulus of elasticity (Gpa) | 380 |
| Poisson's ratio | 0.22 |
| Tensile strength (Mpa) | 282 – 551 |
| Fracture toughness (Mpa) | 4.2 – 5.9 |
| Thermal expansion Coefficient of(10-6(˚C)-1) | 7.4 |
| Thermalconductivity(W/m-k) | 39 |

Graphite powder is Graphite is a solid lubricant, which permits high corrosion resistance and almost reduces the friction coefficient, disintegrates the wear products, accelerates heat abstraction and increases seizure resistance.

Table 3.3 Properties of graphite [14].

| Property | |
|---|---|
| Bulk density | 1.3 – 1.95 g/cc |
| Porosity | 0.7% - 53% |
| Modulus of elasticity | 8 – 15 Gpa |
| Compressive strength | 20 – 200 Mpa |
| Coefficient of thermal expansion | 1.2 – 8.2 × 10-6 C |
| Thermal conductivity | 25 – 470 W/m˚K |
| Specific heat capacity | 710 – 8130 J/m˚K |
| Electrical resistivity | 5 × 10-6 – 30 × 10-6 Ω·m |

Additional instruments utilized during the experimentations are beaker, measuring cylinder, electric precision weight balance shaker, milling machine, milling balls, punch and dies, hydraulic press, furnace, toluene, ethanol, glycerol, argon gas filled gas cylinder, copper tube, Keller reagent, diamond suspension, sand paper, vicker hardness testing machine, scanning electron microscope, optical microscope and tribometer.

Table 3.4 materials needed for the experiment

| **Exp .no** | **Materials** | **Quantity** | **Unit** |
|---|---|---|---|
| **1** | Aluminium alloy powder | 2 | kg |
| **2** | Graphite | 0.5 | kg |
| **3** | Aluminium oxide | 1 | kg |
| **4** | Toluene | 2 | lit |
| **5** | Ethanol | 3 | lit |
| **6** | Keller reagent | 0.2 | lit |
| **7** | Diamond suspension | 0.25 | lit |
| **8** | Argon gas | 10 | Mpa |
| **9** | Glycerol | 10 | lit |

Table 3.5 Apparatus used for the experiment

| S.no | Apparatus | Quantity | unit |
|---|---|---|---|
| **1** | Beaker | 8 | - |
| **2** | Glass jar | 3 | - |
| **3** | Sand paper | 12 | - |
| **4** | Copper tube | 1 | m |
| **5** | Gas cable | 8 | m |
| **6** | Rubber gloves | 15 | pairs |
| **7** | Safety glass | 1 | - |

Table 3.6 Testing equipment during the experimental investigation

| No | Equipment |
|---|---|
| **1** | Shaker |
| **2** | Electric weight balance |
| **3** | Ball milling |
| **4** | Hydraulic press |
| **5** | Electric resistance furnace |
| **6** | Vicker hardness testing machine |
| **7** | Optical microscope |
| **8** | Scanning electron microscope |
| **9** | Universal testing machine |
| **10** | Tribometer |

## 3.3 Process parameters

The process parameters are aluminum oxide weight percentage which is expected to increase the mechanical property of the composite material. Whereas the graphite weight percentage added is expected to create lubricant film on the inter layer of the composite material to increase the wear resistance of the composite material. In addition to this the compaction pressure is proved to enhance the strength of the material by reducing the void space between the particles.

Nevertheless compaction time and milling time is also considered as parameters because the more the size of the powder is reduced the more its strength is increased. In this experimental investigation all the parameters are utilized to investigate the effect or influence of each parameter and optimize relative to the responses observed.

### 3.3.1 Aluminium oxide weight percentage

In several research metal matrixes composite material are reinforcement by low weight percentage (0-5%) and higher weight percentage (0-30%). In this research higher weight percentage is chosen in order to achieve higher strength whereas, lower weight percentage is chosen for graphite particle to reduce the impact of graphite weight percentage, which is reducing the toughness of the composite material. The weight percentage of aluminium is designed on four levels.0 weight percentage to investigate the effect of graphite particle without aluminium oxide; the next is 10%, 20% and 30%.

### 3.3.2 Graphite weight percentage

Graphite reinforcement is known as a solid lubricant, which makes them very important for wear resistance and lower coefficient of friction. But due to their side effect on the toughness of the materials if the weight percentage of the graphite is more than 5% the toughness of the material will be very low. Subsequently the weight percentage of the graphite particle is from 0 wt% to 4.5 wt% with the range of1.5%

### 3.3.3 Compaction pressure

Compaction pressure is the most important parameter in the powder metallurgy production process. On the process of the compaction the pressure is the major factor to enhance the mechanical property of the composite. The powders mixed and milled simultaneously on ball milling stage, the powders are subjected to compaction pressure of 45Mpa, 50Mpa, 55Mpa and 60Mpa

### 3.3.4 Compaction time

The compaction time of this composite production is from 15 min to 60 min with range of the 15min.

### 3.3.5 Milling time

Milling time is a process of reducing the micro size of the powders. Aluminium matrix composite form an oxide layer when the temperature of the milling jar is higher than 400 $^0$C, to control this condition the timing of the milling is bounded to 120min specifically, the milling time was from 30min, 60min, 90min and 120 min.

## 3.4 Design of experiment

The experimental design of the investigation is done by the Minitab 19 statistical software with five factors and four level of experiment. Taguchi's which is one of DOE application is used to analyze the effect of multitudinous parameters and their comportment by performing minimum number of experimentations and to observe their effect on a specific behavior. It can conjointly determine the optimum condition for the experiment to give better result (Nadika et al. (2013), N. Radhika and R. Subramaniam (2013)). As stated by Taguchi It have three major phases and they are: planning, conducting and analysis. The optimized parameters are determined by Signal to Noise ratio (S/N ratio) (N. Radhika and R. Subramaniam (2013)).Fabrication of the sample is done by powder metallurgy using hydraulic press at various parameters. In this process five parameters ($Al_2O_3$wt %, Gr wt%, compaction pressure, compaction time, milling time) are considered. In the Taguchi DOE concept, the preference of orthogonal array depends on total degrees of freedom of the process parameters. Degree of freedom is accounted or defined as the number of comparisons in between the parameters required to optimize each parameter (factor) with the selected levels. The Degree of freedom for the orthogonal array must be greater than or equal to the preferred number of control factors ( S. Dharmalingaml et al. (2013)). In this study, the degree of freedom required is fifteen. To study the influence of these five factors at different four levels on the mechanical property of the composite, L16 orthogonal array is used for design of experiment.

Table 3.7 The experimental design of the whole powder metallurgy process.

| Test Runs | Aluminum oxide wt% | Graphite wt% | Compaction pressure (Mpa) | Compaction time (s) | Milling Time (s) |
|---|---|---|---|---|---|
| **1** | 0 | 0.0 | 45 | 900 | 1800 |
| **2** | 0 | 1.5 | 50 | 1800 | 3600 |
| **3** | 0 | 3.0 | 55 | 2700 | 5400 |
| **4** | 0 | 4.5 | 60 | 3600 | 7200 |
| **5** | 10 | 0.0 | 50 | 2700 | 7200 |
| **6** | 10 | 1.5 | 45 | 3600 | 5400 |
| **7** | 10 | 3.0 | 60 | 900 | 3600 |
| **8** | 10 | 4.5 | 55 | 1800 | 1800 |
| **9** | 20 | 0.0 | 55 | 3600 | 3600 |
| **10** | 20 | 1.5 | 60 | 2700 | 1800 |
| **11** | 20 | 3.0 | 45 | 1800 | 7200 |
| **12** | 20 | 4.5 | 50 | 900 | 5400 |
| **13** | 30 | 0.0 | 60 | 1800 | 5400 |
| **14** | 30 | 1.5 | 55 | 900 | 7200 |
| **15** | 30 | 3.0 | 50 | 3600 | 1800 |
| **16** | 30 | 4.5 | 45 | 2700 | 3600 |

## 3.5 Selection of the orthogonal array

One of the major objectives of this experimental investigation is to evaluate the effect of the parameters at different four levels. The design of experiment has to enable the system to reveal the effect of the reinforcement monolithically. The orthogonal array that is compatible with four levels and five factors is L16 orthogonal array.

## 3.6 Optimization of parameter

Optimization of parameters are done by utilizing minitab19 statistical soft ware. Frist the response parameters are converted into S/N ratio. The S/N ratio is cooperated in to grey relational analysis and converted into the normalizing sequence, the deviation sequence which is used to calculate the grey relational coefficient is calculated from the normalizing sequence. Finally the GRG value which is used on the Taguchi optimization for optimization purpose is calculated from the gray relation coefficient.

## 3.7 Data Analysis and Optimal Setting

Data analysis and optimal setting is executed by utilizing the minitab19 statistical soft ware.

The results obtained from various experimentations are analyzed in detail and are discussed in the following subsections.The experimental investigation data such as aluminium oxide weight percentage, graphite weight percentage, compaction pressure, compaction time and milling time are transformed into Signal-to-Noise (S/N) ratio. Signal to noise ratio is interpreted as the ratio of the mean value of the signal to the standard deviation of noise value. It is used to arbitrate the rank of input process factors or parameters. There are 3 types of quality indicative, namely larger is better, smaller is better and nominal is best ( Fei et al.(2013).

For actual density, theoretical density and porosity, wear loss and coefficient of friction ‘smaller is better’ characteristic is used, shown in Eq. (3.12), since low density and porosity is required for the enhancement of low weight high strength material

‘Smaller is better’ characteristics (Fei et al. (2013).

$$S/N = -10 \log\left(\text{sum}\left(\frac{y^2}{n}\right)\right) \tag{3.1}$$

For compression strength and micro hardness ‘larger is better’ quality exhibitive is used.

‘Larger is better’ characteristics (Fei et al.(2013).

$$S/N = 10 \log \text{sum}\left(\frac{1}{y^2}/n\right) \tag{3.2}$$

Where, y is the required data ($Al_2O_3$ %wt, Gr %wt, compaction pressure, compaction time and milling time) and n is the number of observations. The process parameters and their four levels used for development of Aluminium metal matrix composites have been shown in table 3.8. The experimental results of response parameters with their corresponding S/N ratio have been listed

in distinctive subtitle. After the execution of the design of the experiment the experimental response is changed into the S/N ratio and using grey relational analysis, the S/N ratio of several factors are changed into one row of grey relational grade response. Using the grey relational grade Taguchi analysis will take place after the Taguchi analysis; from the analysis the mean effect plot for means the optimal condition is analyzed.

Table 3.8 .Process parameters and their level for Aluminium metal matrix composites.

| **Process Parameters** | Notation | Level 1 | Level 2 | Level 3 | Level 4 |
|---|---|---|---|---|---|
| **$Al_2O_3$ weight percentage** | A | 0 | 10 | 20 | 30 |
| **Gr weight percentage** | B | 0 | 1.5 | 3 | 4.5 |
| **Compression pressure(Mpa)** | C | 45 | 50 | 55 | 60 |
| **Compression time(min)** | D | 15 | 30 | 45 | 60 |
| **Milling time(min)** | E | 30 | 60 | 90 | 120 |

### 3.7.1 Analysis of Variance

Analysis of variance for the investigation is calculated by minitab19 software using the grey relational grade as a response parameter for several experimental responses.

### 3.7.2 Confirmation experiment

Once the optimal combination of process parameters and their levels was obtained, the final step is to verify the predicted result against experimental results .if the optimal combination of parameters and their levels coincidently match with one of the experiment in the orthogonal array and then no confirmation test is required.

## 3.8 Powder Metallurgy

The method of processing AMCs has been categorized into ex-situ whereby reinforcements are added into the matrix and in situ in which there is production of hard particles by reaction process (M. A Ibrahim et al (2019). The basic process of powder metallurgy consists of three major stages. Primarily, the primary material is physically mixed and milled in existence of process control agent. Ball milling is performed to achieve better mechanical properties. On the second stage the mixed powder is injected into a die and compacted on a press to produce a

weakly cohesive structure close to the dimensions of the object ultimately to be manufactured. Finally heat treatment takes place where the product is sintered by applying high temperature, long setting times (D. K. Koli et al. (2013)).

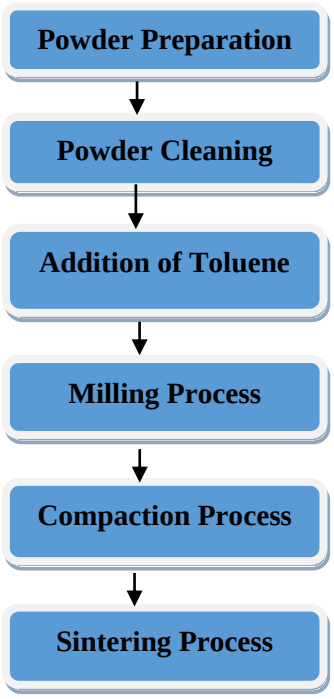


Figure 3.2 Flow chart of powder metallurgy

Likewise in this experimental investigation fundamental process of PM reside three supreme stages. First and foremost, the powders are cleaned by ethanol from different kinds of contamination. After cleaning process the powder composed of different weight percentage of reinforcement are physically milled and mixed in the existence of toluene which is used to prevent the process from oxidation. The milling process is executed at 340rpm with a ball to powder ratio of 1:2 by ball milling machine (Fristsch Pulverisette Germany) by utilizing zirconium balls for physical size reduction. The ball size used is eight balls with 10mm diameter and ten balls with 2.5mm diameter ball. At miscellaneous milling time (30min, 60min, 90min and 120min).Subsequently, on the next stage, the milled and mixed powder is impregnated into a die and compressed by a press at various compaction pressure(45Mpa, 50Mpa, 55Mpa and 60Mpa)and various compaction time (15min, 30min, 45min, 60min). After compaction process the weakly cohesive structure specimen is ejected by the press from the mold with close to the dimensions of 5mm length and 20mm diameter. Ultimately, sintering process is engaged under argon gas atmosphere to prevent the oxidation of the samples at high temperature. The heat

treatment took place at 600 ℃ for 1 hour, under constant temperature and cooled to the atmosphere temperature under argon gas controlled furnace.

Table 3.9 Advantages and disadvantages of powder metallurgy

| Advantages | Disadvantages |
|---|---|
| Porosity can be controlled | Expensive Tooling and equipment |
| Impressive mechanical properties are achieved | Parts can have low ductility |
| Near net shapes can be obtained | Expensive powder materials |

Generally powder metallurgy can be classified into three stages.

The experimental

- Milling process
- Compaction process
- Heat treatment /sintering

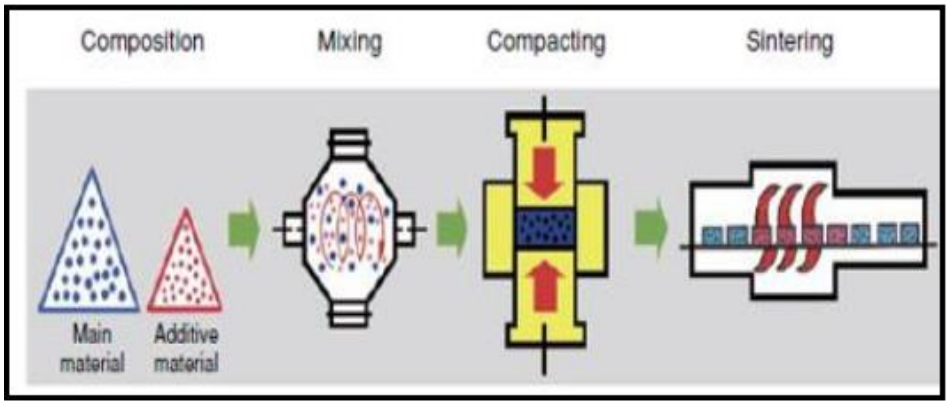


Figure 3.3 Powder metallurgy process steps (M. A Ibrahim et al. (2019)).

### 3.8.1 Milling process

Milling process is done on the ball milling machine (Fristsch Pulverisette Germany) for different milling time. First the powder weighed and added to the matrix material by using weight balance according to the design of experiment. All the samples are milled at 340 rpm, With 20:1 ball to powder weight ratio. The balls used are steel balls with two types of ball size in diameter of 20mm and 10mm respectively. The total times of milling are 24 hours. In this process the 100g powder with different weight percentage of reinforcement are added to the steel jar in the

presence of 10% toluene which is used as a process controlling agent. After milling process is done the mixture exposed to the environment to be vaporized and dried. Finally the dried powders are restored in the plastic jar. After the drying the powder are added into a shaker. Ranging from 350 micron to 50 micron.50 micron is utilized for the experimentation.

### 3.8.2 Compaction process

Compaction process is done using hydraulic press (POSTECH Hydraulic press Korea).First the powder is poured into a mold press a process in which the milled powders are uni-axially loaded by different pressure glycerol is used as a die lubrication to decrease die wear. The mold used on this investigation has 20mm diameter die hole and 19.8±1mm punch diameter. Consequently after the powder is poured into the mold will uni-axially loaded under hydraulic press at different compaction pressure and compaction time. All the samples are prepared with different parameters. With ≅ 20 mm diameter and 5mm length

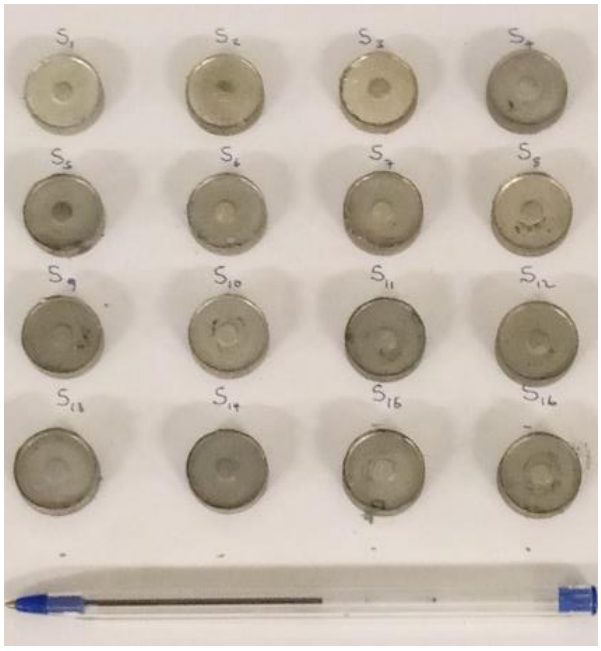

Figure 3.4 samples prepared by hydraulic press.

### 3.8.3 Sintering process

Sintering process took place in special mold that is prepares by the size of the samples to prevent the distortion that may occur due to relatively high sintering temperature. Sintering process is

done at 600 for 45 minute in argon controlled condition. The gas injected into the electric furnace at 15bar/min.

## 3.9 Characterization of mechanical and tribological property

The reinforcement distributions in composites under various fabrication conditions were examined using optical microscopy (Huvitz HR-300 series), scanning electron microscopy (Jeol, Japan; Model: 6410). Composite densities were measured at room temperature by the Archimedean principle. Distilled water was used as the liquid for the measurement and at least three specimens were tested to obtain an accurate average value. The Vickers micro hardness (HVS-50) of composites was measured using a square-based pyramid indenter under a load of 10kg with a dwell time of 10s. Compression strength is measured by universal testing machine. Tribological property is measured by tribometer.

### 3.9.1 Theoretical Density measurement

The theoretical density of he developed sample is calculated by using the mixtures rule (A. A. Premnath,et al. (2014))

$$\rho_{th} = \rho_m V_m + \rho_{r_1} V_{r_1} + \rho_{r_2} V_{r_2} \text{ (1)} \quad (3.3)$$

Where, $V_m$ and $V_{r1}$ and $V_{r2}$ represent the volume fraction of matrix and reinforcements, respectively whereas $\rho_m$, $\rho_{r_1}$ and $\rho_{r_2}$ are density of the matrix, density of the first reinforcement and the second reinforcement respectively.

### 3.9.2 Actual density measurement

The actual density of the composite and pure Aluminum is calculated using Archimedes' principle. The cylindrical sample was weighed being suspended in distilled water and then ($W_w$) and weighed again in air ($W_a$), (I. Aatthisugan et al. (2017)

The actual density was calculated according to Eq. (3.4)

$$\rho_a = \frac{W_a}{(W_a - W_w)} \rho_w \quad (3.4)$$

Where, $\rho_a$ is actual density and $\rho_w$ is density of water

The specimen was weighed using a photoelectric balance with an accuracy of 0.01 mg. In acquiescence with Eq. (3.2), the actual density of the entire specimen can be calculated; theoretical density ($\rho_t$) of the specimen is calculated by the ratio of mass to volume.

### 3.9.3 Porosity measurement

The porosity of each specimen can be calculated according to Eq. (3.5) (I. Aatthisugan et al. (2017), K. K. Alaneme and K. O. Sanusi (2015**)**)

$$P = 1 - \left(\frac{\rho_a}{\rho_t}\right) \tag{3.5}$$

Where, P is the porosity of the material, $\rho_a$ is the actual density and $\rho_t$ is the theoretic density.

### 3.9.4 Hardness measurement

The hardness of the specimens is measured by vicker hardness testing machine (HVS-50) with test force of 10kgf and 10 sec of dwelling time.The hardness of the composite samples was determined using Vickers hardness tester (HVS-50, Buehler, USA). A diamond pyramid with a square base having an included angle of 136° ± 0.5 was used as an indenter. The diamond indenter was forced into the surface of the composite samples at a constant indentation load of 10 kgf with a dwell time of 10s. The surface-projected diagonal lengths of the resulting impression of each sample were then measured immediately after unloading using an upright optical. The flat surface was indented at five different locations and the average of the mean diagonal lengths of five indentations was calculated.

$$HV = \frac{Constant \times Testforce}{Surfaceareaofindentation}$$

$$= \frac{0.102 \times 2F\left(sin\frac{136^\circ}{2}\right)}{d^2} \tag{3.6}$$

Where, F is a test force, d is diagonal of the indentation and 136°is the angle between the opposite surface at the vertex, which is pressed into the surface of the test piece.

### 3.9.5 Compression strength measurement

The compression strengths of the specimens are measured by universal testing machine with test force of 10kgf and 10 sec of dwelling time. The compression test was performed on cylinder shaped AMC specimens bearing a dimension of 5 mm radius and 5 mm fabricated (Fig.3.5) fabricated as per ASTM C773-88. The test was carried out at ambient temperature on a FIE make universal testing machine (UTM) (Model: UTE-20).

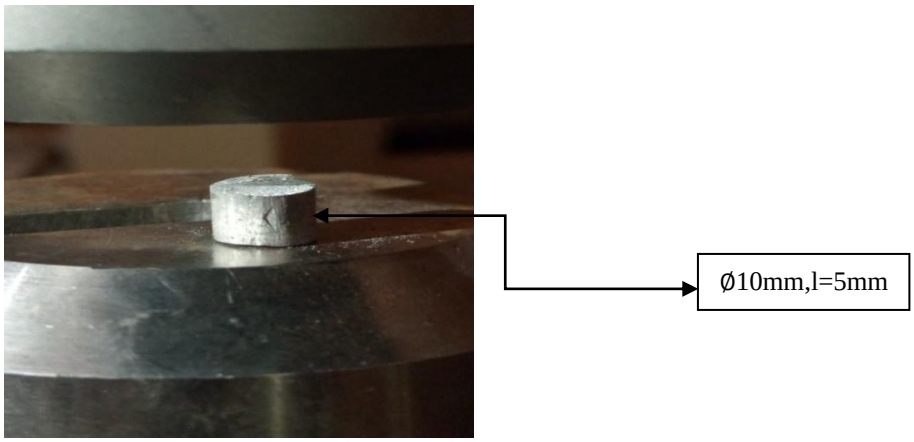


Figure 3.5 Sample dimension for compression testing according to ASTM C773-88.

### 3.9.6 Wear test

The tribological determination is done on Pin-on-Disc test apparatus, to evaluate the dry sliding wear characteristics of hybrid composite specimens. The sliding wear tests are conducted as per the wear testing machine sample size under lubricated, dry laboratory conditions at room temperature. Specimens of area of 6mm×6mm and 18mm length of mm are cut from the samples machined and then polished metal graphically

Volume loss is calculated by Eqn (3.7) ( O.Yilmag and S.buytog (2001)

$$Volume\ loss = \frac{m_1 - m_2}{\rho} \times 1000mm \tag{3.7}$$

$$Wear\ rate = \frac{V}{L} mm^3/_m \tag{3.8}$$

Whereas coefficient of friction is calculated using the following formula by taking the friction force calculated by the tribometer.

$$\text{Coefficient of friction} = \frac{F_r}{F_n} \tag{3.9}$$

Each specimen is thoroughly cleaned by acetone solution, dried, and then accurately weighed using a single pan electronic weighing machine with an accuracy of 0.0001g. During the test, the pin is pressed against a rotating steel disc with a hardness of 65 HRC by applying load that acts as counterweight and balances the pin. All the specimens followed a same track of 100 mm diameter with a tangential force. At the end of each test, the final weight of the pin is measured, after cleaning with acetone. The difference between the initial and final weight of the pin gives the weight loss due to sliding wear. The volume loss due to wear is calculated by the use of corresponding density values of the pin. The wear rate of the composite pins is then calculated

(ratio of volume loss to sliding distance). Dry Wear testing is done by pin on disc wear measuring apparatus to investigate the wear volume loss depending on many parameters. In this test four parameters ($Al_2O_3$ wt%, Gr wt%, Load, Speed, Sliding distance) are considered. To study the influence of these five factors at different four levels on the wear loss of aluminium matrix composite, L16 orthogonal array is used for design of experiment. Wear testing sample is prepared as per the sample compatible the wear testing machine with tribometer standard.

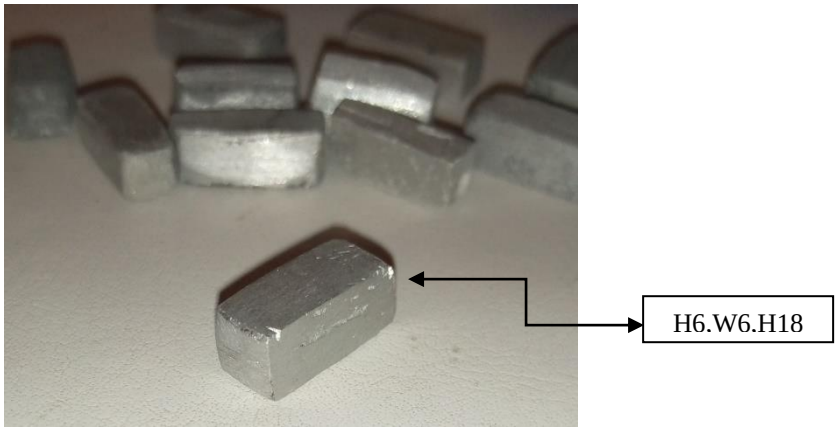


Figure 3.6 Sample prepared for wear test.

Table 3.8 The design of experiment for the wear and coefficient of friction test

| **Test run** | **Al2O3 wt%** | **Gr Wt%** | **Load(N)** | **Speed m/s** | **Sliding distance(m)** |
|---|---|---|---|---|---|
| **1** | 0 | 0.0 | 10 | 0.4 | 502 |
| **2** | 0 | 1.5 | 20 | 0.6 | 754 |
| **3** | 0 | 3.0 | 30 | 0.8 | 1005 |
| **4** | 0 | 4.5 | 40 | 1.0 | 1256.6 |
| **5** | 10 | 0.0 | 20 | 0.8 | 1005 |
| **6** | 10 | 1.5 | 10 | 1.0 | 1256 |
| **7** | 10 | 3.0 | 40 | 0.4 | 502 |
| **8** | 10 | 4.5 | 30 | 0.6 | 754 |
| **9** | 20 | 0.0 | 30 | 1.0 | 1256.6 |
| **10** | 20 | 1.5 | 40 | 0.8 | 1005 |
| **11** | 20 | 3.0 | 10 | 0.6 | 754 |
| **12** | 20 | 4.5 | 20 | 0.4 | 502 |
| **13** | 30 | 0.0 | 40 | 0.6 | 754 |
| **14** | 30 | 1.5 | 30 | 0.4 | 502 |
| **15** | 30 | 3.0 | 20 | 1.0 | 1256.6 |
| **16** | 30 | 4.5 | 10 | 0.8 | 1005 |

## 3.10 Taguchi and Grey Relation Analysis (GRA)

There are number of optimization techniques that deal with friction and wear behavior of composites among all the foresaid techniques, Grey Relational Analysis (GRA) is used for multi-objective optimization problems. Complex problems having minimal information can be solved by grey theory, it is an evaluation technique based on the random uncertainty of small samples. The 'white' systems means, the system which has complete information, whereas in a 'black' system has no known information. Any system lies between these two that is a 'grey' system with limited information.

### 3.10.1 Normalizing sequence

The Taguchi method optimizes single response at one time, whereas GRA optimizes multiple responses at a time. In the GRA optimization process, the measured values of k and COF are normalized between 0 and 1. The purpose of this normalization is to remove the variations in the range of responses. In order to normalize the two quality characteristics, i.e. k and COF, with 'lower-the-better' quality characteristics, the following equation was used (S. Das et al. (2020)).

$$\boldsymbol{X_i^*(j) = \frac{maxx_i(j) - X_i(j)}{maxx_i(j) - minX_i(j)}} \quad (3.10)$$

### 3.10.2 Determination of deviation sequence

Where $\Delta_{0i}(j)$ is deviation sequence data and $X_0(j)$ is the experimental result for the $0^{th}$ experiment using jth response. $\boldsymbol{x_i^*(j)}$ Is the experimental result for the $i^{th}$ experiment using $j^{th}$ response (S. Das et al. (2020)).

$$\boldsymbol{\Delta_i(j) = |X_0^*(j) - x_i^*(j)|} \quad (3.11)$$

### 3.10.3 Determination of grey relational coefficient

Where $\boldsymbol{\Delta_i(j)}$ is the absolute value of the difference between $\boldsymbol{X_0^*(j)}$ and $\boldsymbol{x_i^*(j)}$, $\boldsymbol{\Delta max}$ and $\boldsymbol{\Delta min}$ are global maximum and global minimum values in different data series. Generally, the distinguishing coefficient (n) = 0.5 is taken.. After the responses are normalized, the grey relational coefficient (GRC) was calculated using the equation (S. Das et al. (2020)).

$$\boldsymbol{\xi_i(j) = \frac{\Delta min + \xi\, \Delta max}{\Delta_i(j) + \xi \Delta max}} \quad (3.12)$$

$\boldsymbol{\xi}$ is usually considered as 0.5

### 3.10.4 Determination of grey relation grade

The mean of the GRC of each quality characteristics was used to estimate grey relational grade (GRG) as depicted on Equa 3.13. (S. Das et al. (2020)).

$$\gamma_i = \frac{1}{n}\sum_{j=1}^{n} \xi_i(j) \tag{3.13}$$

### 3.10.5 Determination of optimal parameters

In this experiment the optimization of parameter is done by the Taguchi optimization method on minitab19 statistical software and grey relational analysis method is used to change the responses into one AS/N ratio .and the GRG value is used to optimize the parameters. This method enables as to optimize several parameters at a time. Grey Relational Grade was calculated for each experiment data and considered as response for the next analysis. At this stage, the best quality characteristic ‘smaller the best’ and ‘larger the best’ has been used for further analysis, as it give the best performance of hardness, compressive strength and smaller is better is used for porosity, density, wear loss and coefficient of friction. The GRG obtained is analyzed by Analysis of Variance (ANOVA) and it provides the statistical significance of input process parameter over an output and their results were shown in

### 3.10.6 Prediction of GRG under optimal parameters

Next step is to determine and confirm the development of quality characteristics by the optimal parametric combination by using minitab19 software. The predicted optimal condition can be calculated by software to get optimized parameters.

# CHAPTER FOUR

# RESULTS AND DISCUSSION

## 4.1Introduction

In this chapter, the results of the experimental works have been discussed in detail. In different sub section, density, porosity, hardness test result, compressive test result, mean effect of parameters on the density, porosity, hardness, compressive strength, wear loss and coefficient of friction ,hybrid grey relational and Taguchi analysis of optimization of actual density and porosity, hybrid grey relational analysis and Taguchi of hardness and compressive strength, hybrid grey relational analysis and Taguchi method of optimization of wear loss and coefficient of friction, microstructure result friction are explained.

## 4.2 Density of the composite

The composite densities are presented in Table 4.1. It is observed that the composite densities increased with increase in wt. % of aluminium oxide particles. While both the actual density and theoretical density decrease with the weighty percentage of the graphite particle .The hybrid reinforcement mix containing aluminium oxide and graphite particles, both had slightly lower densities compared to composite containing aluminium oxide particles. The lower densities reported for the hybrid mix compositions are due to the lower density of graphite (2230kg/cm$^3$). And the increase in density of the hybrid composite is due to the higher density of the aluminum oxide (3900 kg/m$^3$)

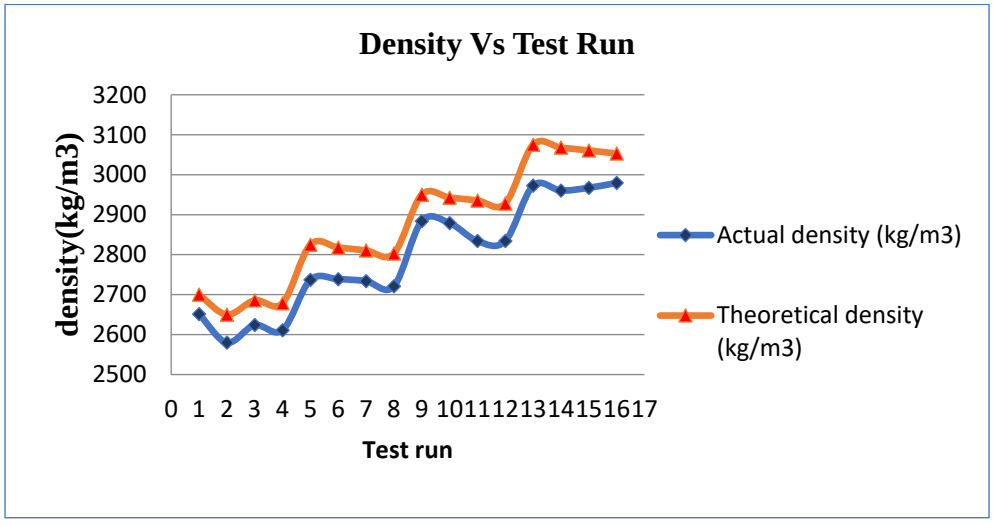


Figure 4.1 The graph of density versus experimental test run.

As it is shown on the Figure 4.1 graph as the weight percentage of the Aluminium Oxide increase the theoretical and actual density of the composite increase. The graph also reveals that the density decrease with the weight percentage of graphite and increased with an increase on the aluminium oxide weight percentage. Increment on the density of has negative impact on the service properties of the developed composite material. The density of the composite increase with the increase in weight percentage of reinforcement and an increase of the hardness, compressive strengths and wear resistance of the material is intended to make the material advanced in mechanical property.

Table 4.1 Actual density and theoretical density with variable aluminium oxide and graphite reinforcement.

| **Exp.No** | **$Al_2O_3$ wt%** | **Gr Wt%** | **Actual density ($kg/m^3$)** | **Theoretical density ($kg/m^3$)** |
|---|---|---|---|---|
| **1** | 0 | 0.0 | 2651.4 | 2700.0 |
| **2** | 0 | 1.5 | 2580.0 | 2650.0 |
| **3** | 0 | 3.0 | 2623.83 | 2685.6 |
| **4** | 0 | 4.5 | 2610.9 | 2678.4 |
| **5** | 10 | 0.0 | 2736.71 | 2825.0 |
| **6** | 10 | 1.5 | 2738.61 | 2817.8 |
| **7** | 10 | 3.0 | 2733.87 | 2810.6 |
| **8** | 10 | 4.5 | 2720.8 | 2803.0 |
| **9** | 20 | 0.0 | 2883.92 | 2950.0 |
| **10** | 20 | 1.5 | 2878.94 | 2942.8 |
| **11** | 20 | 3.0 | 2834.02 | 2935.6 |
| **12** | 20 | 4.5 | 2834.01 | 2928.0 |
| **13** | 30 | 0.0 | 2972.6 | 3075.0 |
| **14** | 30 | 1.5 | 2960.42 | 3067.8 |
| **15** | 30 | 3.0 | 2967.25 | 3060.6 |
| **16** | 30 | 4.5 | 2979.42 | 3053.0 |

The actual density of the composite increase with in weight percentage of aluminium oxide is because the density of aluminium oxide is 31.64% greater than density of aluminium alloy and 43.79% greater than density of graphite. Unlikely, as weight percentage of graphite and milling time increase the actual density decrease. Graphite reinforcement decreases the actual density because the density of graphite is 17.77% lower than aluminium alloy and 43%lower than density of the aluminium oxide. The optimal condition to attain low actual density is undertaken

to be 0% of aluminium oxide reinforcement 4.5% of graphite reinforcement, 50Mpa compaction pressure, 30 min compaction time, 120 min milling time.

### 4.2.1 Analysis of mean effect plot of actual density

Figure 4.2 show the main effect plot for means of porosity. The graph implies that the optimum condition for the actual density is 20% $Al_2O_3$, 4,5%Gr ,compaction pressure of 60mpa,45 minute of compaction time and30 minute of milling time. Additionally the composite with 0%wt of al2o3 and gr showed less density.


Figure 4.2 Main effect plot of actual density

### 4.2.2 Response table for means of actual density

Table 4.2 is the response table of the actual density shows that $Al_2O_3$ Weight Percentage has highest contribution in increasing the density of the composite with delta number of 0.732.this because the aluminium oxide is added with higher range of weight percentage while, milling time is the second contributing factor in increasing the factor. The third ranker contributing factor is compaction time with delta number of 0.589.likely the compaction pressure and Gr Weight Percentage take the fourth and fifth rank with delta number of 0.361 and 0.236 respectively.

Table 4.2 Response Table for Means

| Level | $Al_2O_3$Wt% | Gr Wt% | Compression Pressure | Compression Time | Milling Time |
|---|---|---|---|---|---|
| 1 | 2.340 | 2.649 | 2.645 | 2.835 | 2.509 |
| 2 | 2.899 | 2.780 | 3.006 | 3.090 | 2.913 |
| 3 | 2.770 | 2.885 | 2.743 | 2.501 | 3.151 |
| 4 | 3.072 | 2.768 | 2.688 | 2.655 | |
| Delta | 0.732 | 0.236 | 0.361 | 0.589 | 0.643 |
| Rank | 1 | 5 | 4 | 3 | 2 |

### 4.2.3 Analysis of variance for actual density

From table 4.3 which is the ANOVA table of actual density, the following interpretation can be made. If the p value is less than or equal to 0.05 it indicates that the higher level of significance which implies that $Al_2O_3$ weight percentage has high contribution on increasing the actual density of the composite. The last column of the ANOVA table shown in table 4.3 indicates the percentage of contribution (Pc) in which $Al_2O_3$ weight percentage has the highest level of contribution (33.42%) followed by milling time (31.95%), Compression time (20.04%) and compression pressure (10.28%).

Table 4.3 Analysis of variance for actual density

| Source | DF | Seq SS | Adj SS | Adj MS | F | P | Pc |
|---|---|---|---|---|---|---|---|
| $Al_2O_3$wt% | 3 | 12.5006 | 12.5006 | 4.1668 | 148.99 | 0.060 | 33.42% |
| Gr wt% | 3 | 1.5726 | 1.5726 | 0.5242 | 18.74 | 0.168 | 4.2% |
| Compression pressure | 3 | 3.8467 | 3.8467 | 1.2822 | 45.85 | 0.108 | 10.28% |
| Compression time | 3 | 7.4959 | 7.4959 | 2.4986 | 89.34 | 0.078 | 20.04% |
| milling time | 2 | 11.9484 | 11.9484 | 5.9741 | 213.61 | 0.048 | 31.95% |
| Residual Error | 1 | 0.0280 | 0.0280 | 0.0279 | | | 0.074% |
| Total | 15 | 37.3922 | | | | | 100% |

## 4.3 Porosity of the composite

Table 4.4indicate that the variation of porosity samples. It can be understood from Figure 4.3 that the porosity of the composites increased with the increase in weight percent of reinforcements. The increase in porosity of composite and hybrid composite poor wettability low compaction pressure of the experimentation. The increment on porosity with increase on the reinforcement is induced due to the low working pressure. The working pressure during compaction should be more than 200Mpa to reduce the porosity.

Table 4.4 Tabular description of the design of experiment with porosity response

| **Test runs** | Aluminium oxide wt% | Grwt% | Compn pressure (Mpa) | Compn time (s) | Milling Time (s) | Porosity (%) | **S/N ratio** |
|---|---|---|---|---|---|---|---|
| **1** | 0 | 0.0 | 45 | 900 | 1800 | 1.9 | -5.5751 |
| **2** | 0 | 1.5 | 50 | 1800 | 3600 | 2.64 | -8.4321 |
| **3** | 0 | 3.0 | 55 | 2700 | 5400 | 2.3 | -7.2346 |
| **4** | 0 | 4.5 | 60 | 3600 | 7200 | 2.52 | -8.0280 |
| **5** | 10 | 0.0 | 50 | 2700 | 7200 | 3.125 | -9.8970 |
| **6** | 10 | 1.5 | 45 | 3600 | 5400 | 2.81 | -8.9741 |
| **7** | 10 | 3.0 | 60 | 900 | 3600 | 2.73 | -8.7233 |
| **8** | 10 | 4.5 | 55 | 1800 | 1800 | 2.93 | -9.3374 |
| **9** | 20 | 0.0 | 55 | 3600 | 3600 | 2.24 | -7.0050 |
| **10** | 20 | 1.5 | 60 | 2700 | 1800 | 2.17 | -6.7292 |
| **11** | 20 | 3.0 | 45 | 1800 | 7200 | 3.46 | -10.7815 |
| **12** | 20 | 4.5 | 50 | 900 | 5400 | 3.21 | -10.1301 |
| **13** | 30 | 0.0 | 60 | 1800 | 5400 | 3.33 | -10.4489 |
| **14** | 30 | 1.5 | 55 | 900 | 7200 | 3.5 | -10.8814 |
| **15** | 30 | 3.0 | 50 | 3600 | 1800 | 3.05 | -9.6860 |
| **16** | 30 | 4.5 | 45 | 2700 | 3600 | 2.41 | -7.6403 |

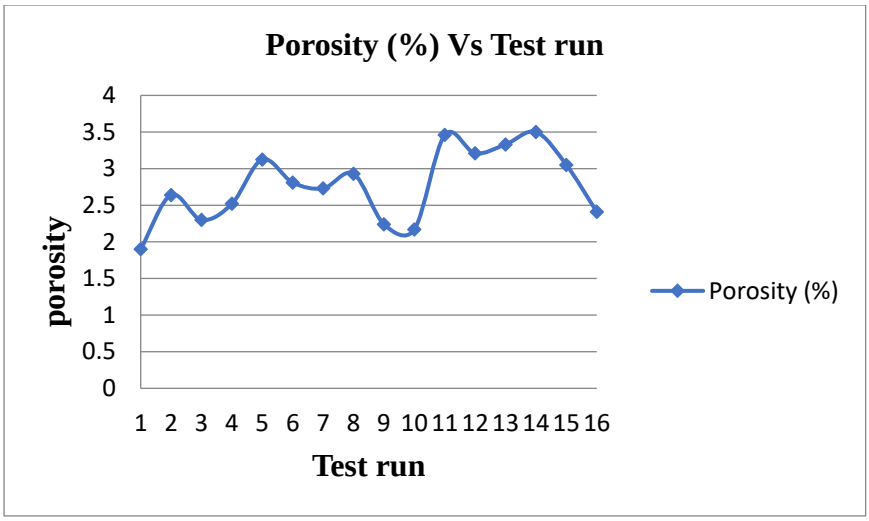


Figure 4.3 Graph of porosity as function of test run

### 4.3.1 Analysis of mean effect plot of porosity

Figure 4.4 show the main effect plot for means show that the optimum condition for the actual density is 20% Al2O3,4,5%Gr ,compaction pressure of 45 mpa,45 minute of compaction time and30 minute of milling time. Additionally the composite with 0%wt of Al2O3 and Gr showed less porosity.


Figure 4.3 Main effect plots for means of porosity

### 4.3.2 Response table for means of porosity

The response table of the porosity show that $Al_2O_3$ Weight Percentage has highest contribution in increasing the density of the composite with delta number of 0.732.while milling time is the second contributing factor on porosity of the composite with 0.643 delta number. The third ranker contributing factor is compaction time with delta number of 0.589.likely the compaction pressure and Gr Weight Percentage take the fourth and fifth rank with delta number of 0.361 and 0.236 respectively.

Table 4.5 Response table for means of porosity

| Level | $Al_2O_3$ weight percentage | Gr weight percentage | Compression pressure | Compression time | Milling time |
|---|---|---|---|---|---|
| 1 | 2.340 | 2.649 | 2.645 | 2.835 | 2.509 |
| 2 | 2.899 | 2.780 | 3.006 | 3.090 | 2.913 |
| 3 | 2.770 | 2.885 | 2.743 | 2.501 | 3.151 |
| 4 | 3.072 | 2.768 | 2.688 | 2.655 | |
| Delta | 0.732 | 0.236 | 0.361 | 0.589 | 0.643 |
| Rank | 1 | 5 | 4 | 3 | 2 |

### 4.3.3 Analysis of variance of porosity

The percentage of contribution of the ANOVA table shown in table 4.6 indicates the percentage of contribution (Pc) in which milling time has the highest level of contribution (33.54%) followed by $Al_2O_3$ wt% (32.76%), Compression time (20.47%) and compression pressure (8.83%).

Table 4.6 Analysis of Variance for Means

| Source | DF | Seq SS | Adj SS | Adj MS | F | P | Pc |
|---|---|---|---|---|---|---|---|
| Al2O3 wt% | 3 | 1.17193 | 1.17193 | 0.390643 | 3472.38 | 0.012 | 32.76% |
| Gr wt% | 3 | 0.11213 | 0.11213 | 0.037377 | 332.24 | 0.040 | 3.13% |
| Compression pressure | 3 | 0.31600 | 0.31600 | 0.105335 | 936.31 | 0.024 | 8.83% |
| Compression time | 3 | 0.76830 | 0.76830 | 0.256102 | 2276.46 | 0.015 | 21.47% |
| milling time | 2 | 1.20864 | 1.20864 | 0.604321 | 5371.74 | 0.010 | 33.54% |
| Residual Error | 1 | 0.00011 | 0.00011 | 0.000113 | | | 0.0031 |
| Total | 15 | 3.57712 | | | | | |

## 4.4 Analysis of hardness test

Hardness is the confrontation of a material to deform, indentation or scratching the basic goal of hardness is to enumerate the resistance of a material to plastic deformation. Load during hardiness test is 10 kg (99.1N) on three trials on the sample. For each test, three reputations are followed and an average value was taken. All the experimental data is tabulated in the table 4.7.

Table 4.7 Tabular description of the design of experiment and Vicker hardness measurement result

| **Test runs** | **1st trial** | **2nd trial** | **3rd trial** | **Average** | **S/N ratio** |
|---|---|---|---|---|---|
| **1** | 242.96 | 241.71 | 232.33 | 239.00 | 47.5680 |
| **2** | 251.5 | 225.2 | 231.4 | 235.90 | 47.4546 |
| **3** | 218.1 | 238.9 | 243.2 | 233.40 | 47.3620 |
| **4** | 212.7 | 227.33 | 232.5 | 224.18 | 47.0119 |
| **5** | 303.27 | 281.73 | 285 | 290.00 | 49.2480 |
| **6** | 294.87 | 290.13 | 279.6 | 288.20 | 49.1939 |
| **7** | 303.36 | 267.81 | 269.23 | 279.80 | 48.9370 |
| **8** | 270.13 | 269.7 | 276.17 | 272.00 | 48.6914 |
| **9** | 311.09 | 333.01 | 318.84 | 320.98 | 50.1296 |
| **10** | 326.56 | 321.21 | 309.2 | 318.99 | 50.0755 |
| **11** | 319.56 | 319.18 | 309.2 | 315.98 | 49.9932 |
| **12** | 319.04 | 324.81 | 307.15 | 317.00 | 50.0212 |
| **13** | 269.27 | 279.12 | 346.21 | 298.20 | 49.4902 |
| **14** | 289.56 | 312.2 | 287.23 | 296.33 | 49.4355 |
| **15** | 280.9 | 287.47 | 276.13 | 281.50 | 48.9896 |
| **16** | 277.13 | 241.10 | 241.28 | 253.17 | 48.0682 |

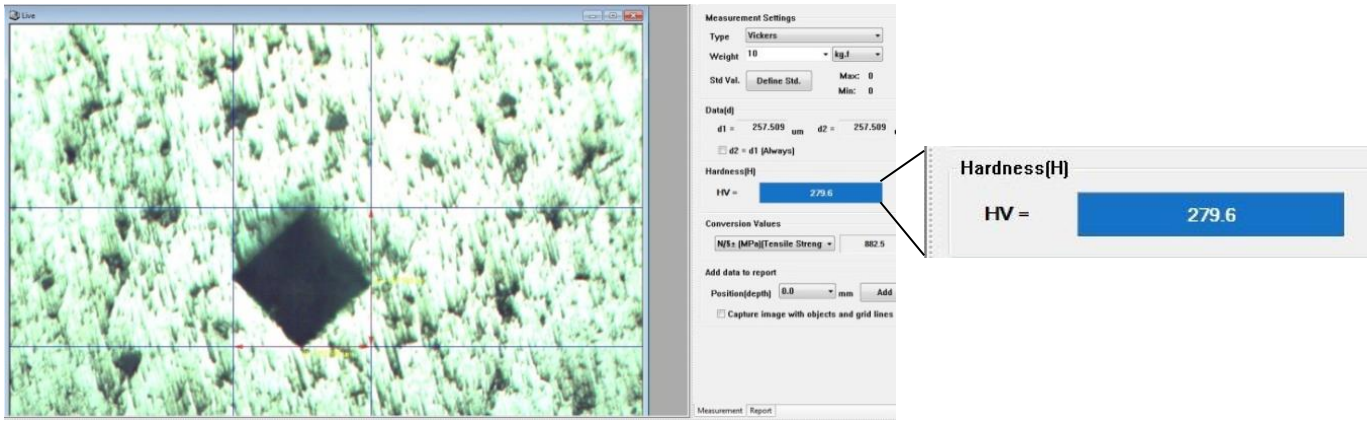


Figure 4.4 Measurement of the indented sample number 6 with10wt% $Al_2O_3$ and 1.5 wt% Gr.

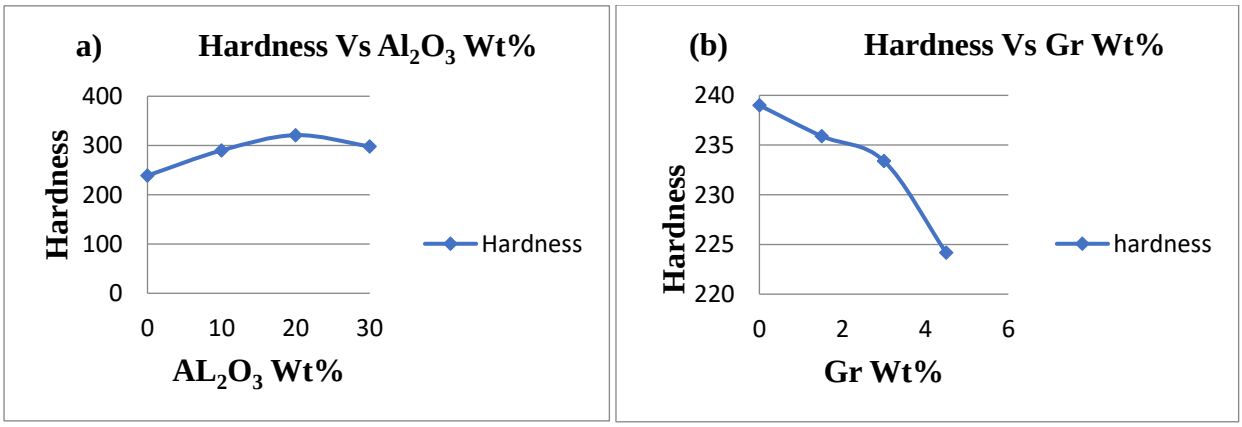


Figure 4.5 a) Show the Vickers hardness versus Al2O3 wt% figure 4.5 b) show the hardness versus graphite wt%

Table 4.7 and figure 4.5 show that with increase in the weight percentage of graphite, the hardness of the composite increase. When the reinforcement of graphite particle increase from 0 to 4.5 with range of 1.5 the hardness of the composite decrease from 239 to 224.18.Likewise the hardness of the composite increase from 239 to 320 with increase in the weight percentage of aluminium oxide from 0-20 and decline after 20Wt% reinforcement. This result is in well agreement with (G. Iacob et al.(2015), A. Baradeswaran and A. E. Perumal,( 2014)).

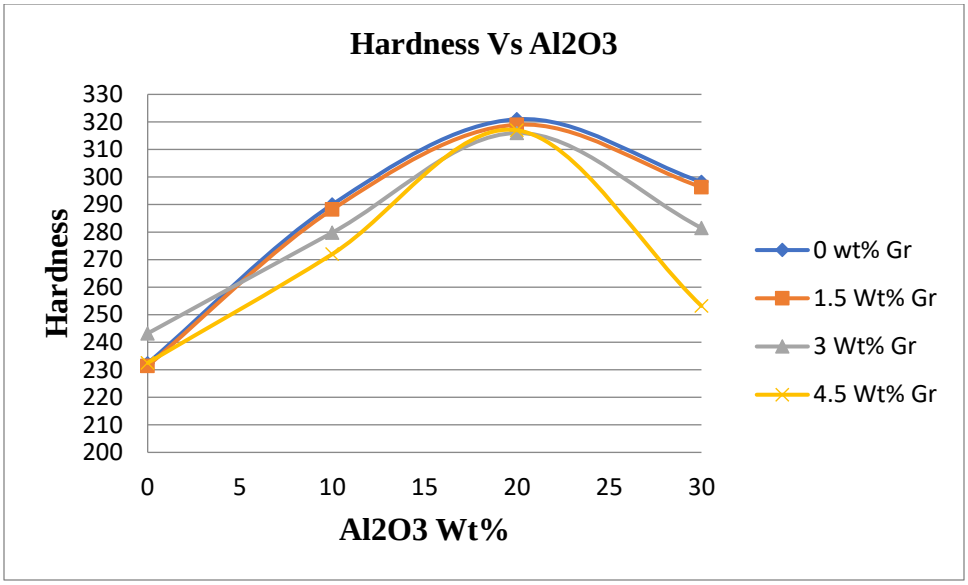


Figure 4.6 Graph of hardness versus weight percentage of aluminium oxide

Figure 4.6 shows that with an increase in weight percentage of the aluminum oxide reinforcement the hardness of the composite material increase. Due to the poor wettability and de-bonding between the reinforcement particles and the matrix material increased due to the low compaction pressure, the hardness of the hybrid composite decrease after 20% of $Al_2O_3$ reinforcement. Additionally the introduction of the solid lubricant into the matrix material induced decrement on the hardness of the composite.

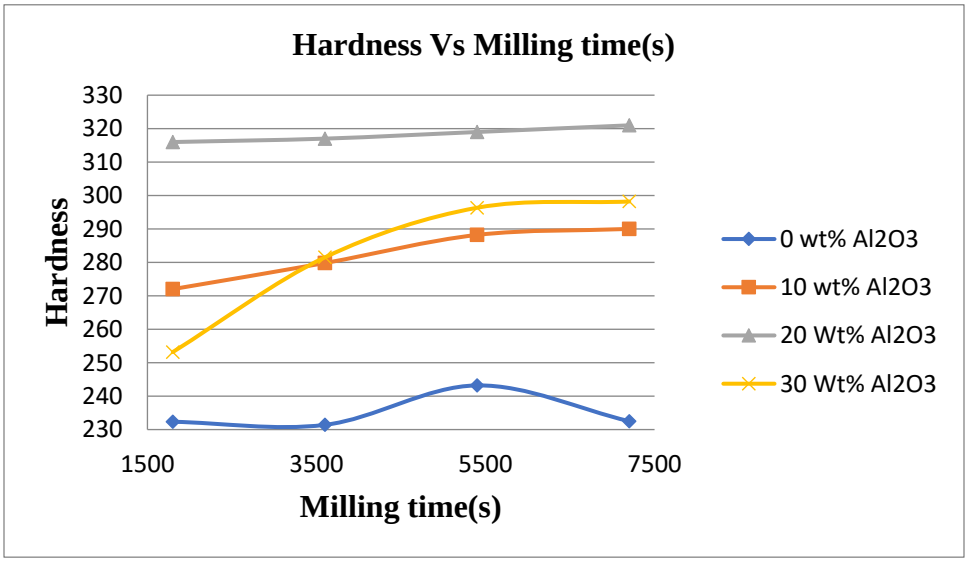


Figure 4.7 Graph of hardness versus milling time

Regarding the milling time figure 4.7 can be interpreted from the graph the hardness of the composite material increase with increase in the milling time. Above all experimental setup the

composite with 30% $Al_2O_3$ weight percentage show higher improvement with increase in milling time. This implies that with increase in milling time the hardness of the composite material increase. This caused by decrement on the particular size of powder during milling process which allow well integration between the reinforcement and matrix material.

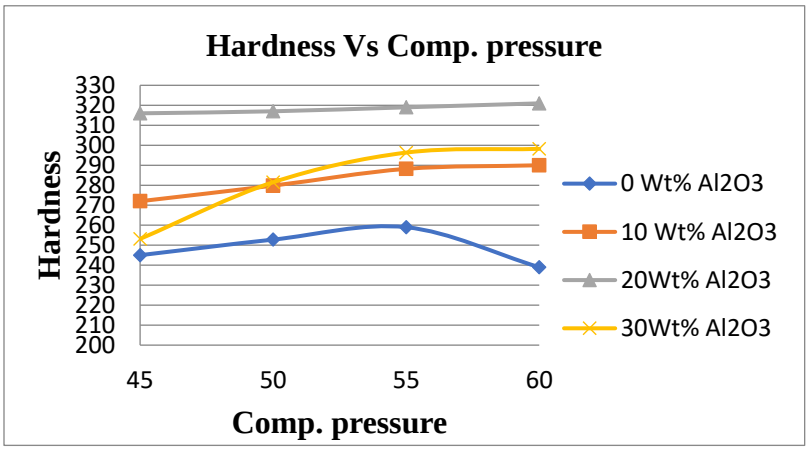


Figure 4.8 Graph of hardness versus compaction pressure

Concerning the compaction pressure the hardness of the composite resulted increment with an increase in compaction pressure. The hybrid composite with 10% of aluminum oxide reinforcement and various percentage of graphite reinforcement show higher increase with increase in compaction time. This caused due to low reinforcement of aluminum oxide reinforcement. The low reinforcement can be benefited from the low pressure due to requirement of high pressure for high level of weight percentage of reinforcement.

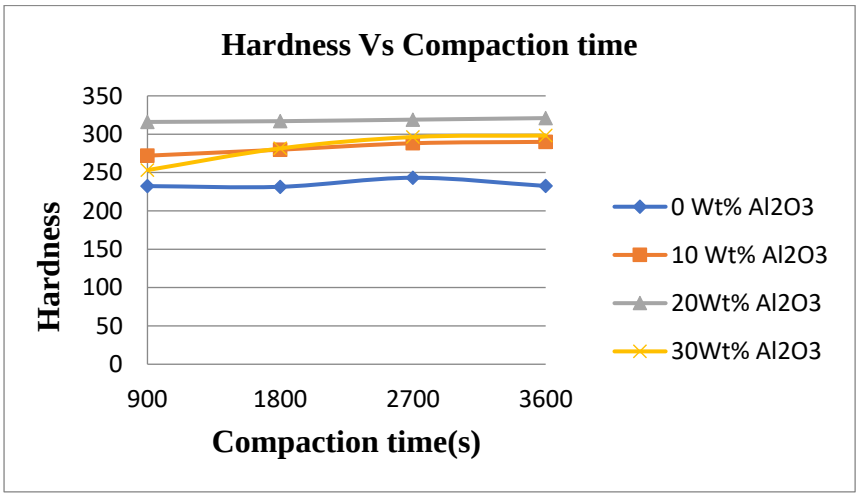


Figure 4.9 Graph of hardness versus compaction time

Even though he compaction time doesn't have much effect relative to the other factors, composite with 10% Wt $Al_2O_3$ reinforcement increased slightly.

### 4.4.1 Analysis of main effect plot of hardness

Figure 4.10 show the main effect plot for means show that the optimum condition for the actual density is 20% $Al_2O_3$,1.5%Gr ,compaction pressure of 60mpa,45 minute of compaction time and 60 minute of milling time.


Figure 4.10 Main effect plot of hardness

### 4.4.2 Response table for means of hardness

The response table of the actual density presented in table 4.8 show that $Al_2O_3$ Weight Percentage has highest contribution in increasing the hardness of the composite with delta number of 102.8.while milling time is the second contributing factor in increasing the hardness of the composite with delta number of 8.the third ranker contributing factor is compaction time with delta number of 6.9. Likely the compaction pressure and Gr Weight Percentage take the fourth and fifth rank with delta number of 6.2 and 3.7 respectively.

Table 4.8 Table of response of means of hardness

| Level | $Al_2O_3$ Wt% | Gr Wt% | Compression pressure | Compression time | Milling time |
|---|---|---|---|---|---|
| 1 | 248.9 | 302.4 | 298.2 | 296.8 | 296.5 |
| 2 | 282.5 | 300.9 | 299.6 | 298.2 | 304.5 |
| 3 | 318.2 | 298.7 | 299.3 | 302.9 | 304.1 |
| 4 | 351.8 | 299.5 | 304.4 | 303.6 | |
| Delta | 102.8 | 3.7 | 6.2 | 6.9 | 8.0 |
| Rank | 1 | 5 | 4 | 3 | 2 |

### 4.4.3 Analysis of variance of hardness

The percentage of contribution in table 4.9 implies that the $Al_2O_3$ weight percentage has the highest level of contribution (89.93%) followed by Gr Wt %( 6.24%), Milling time (1.55%),Compression time (20.04%) and compression pressure (10.28%).

Table 4.9 Analysis of variance of hardness

| Source | DF | Seq SS | Adj SS | Adj MS | F | P | Pc |
|---|---|---|---|---|---|---|---|
| **Al2O3 Wt%** | 3 | 14670.8 | 14670.8 | 4890.25 | 83.54 | 0.08 | 89.93% |
| **Gr Wt%** | 3 | 1019.3 | 1019.3 | 339.78 | 5.8 | 0.294 | 6.24% |
| **Compression pressure** | 3 | 132.1 | 132.1 | 44.03 | 0.75 | 0.668 | 0.80% |
| **Compression time** | 3 | 179 | 179 | 59.68 | 1.02 | 0.605 | 1.09%1 |
| **milling time** | 2 | 253.1 | 253.1 | 126.57 | 2.16 | 0.433 | 1.55% |
| **Residual Error** | 1 | 58.5 | 58.5 | 58.54 | | | 0.35% |
| **Total** | 15 | 16312.9 | | | | | |

## 4.5 Analysis of compressive strength

The compressive strength is done by using universal testing machine and samples are shown in Figure 4.11the sample length ids 5mm with diameter of 10mm.the samples are subjected to the controlled room axial load until it is failed. The compressive strength of the sample and elongation of the sample are calculated by the machine**.**

Table 4.10 Graphical representation of the design of experiment and compression test result

| Test runs | Aluminium oxide wt% | Graphite wt% | Compaction pressure (Mpa) | Compaction time (s) | Milling Time (s) | Compression strength(Mpa) | S/N ratio |
|---|---|---|---|---|---|---|---|
| **1** | 0 | 0.0 | 45 | 900 | 1800 | 155 | 43.8066 |
| **2** | 0 | 1.5 | 50 | 1800 | 3600 | 142.3 | 43.0641 |
| **3** | 0 | 3.0 | 55 | 2700 | 5400 | 122.07 | 41.7322 |
| **4** | 0 | 4.5 | 60 | 3600 | 7200 | 119.23 | 41.5277 |
| **5** | 10 | 0.0 | 50 | 2700 | 7200 | 208.28 | 46.3730 |
| **6** | 10 | 1.5 | 45 | 3600 | 5400 | 197.5 | 45.9113 |
| **7** | 10 | 3.0 | 60 | 900 | 3600 | 189.23 | 45.5398 |
| **8** | 10 | 4.5 | 55 | 1800 | 1800 | 191.23 | 45.6311 |
| **9** | 20 | 0.0 | 55 | 3600 | 3600 | 261.56 | 48.3514 |
| **10** | 20 | 1.5 | 60 | 2700 | 1800 | 257.26 | 48.2074 |
| **11** | 20 | 3.0 | 45 | 1800 | 7200 | 249.58 | 47.9442 |
| **12** | 20 | 4.5 | 50 | 900 | 5400 | 231.71 | 47.2989 |
| **13** | 30 | 0.0 | 60 | 1800 | 5400 | 146.76 | 43.3322 |
| **14** | 30 | 1.5 | 55 | 900 | 7200 | 122.34 | 41.7514 |
| **15** | 30 | 3.0 | 50 | 3600 | 1800 | 116.2 | 41.3041 |
| **16** | 30 | 4.5 | 45 | 2700 | 3600 | 109.78 | 40.8105 |

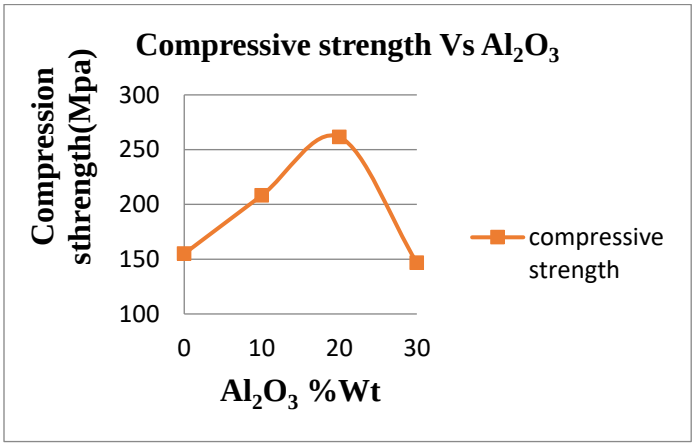


Figure 4.11 Variation of compressive strength as a function of $Al_2O_3$Wt%

From the figure 4.11 it is observed that, the compressive strength of the composite material increase with increase in the weight percentage of aluminium oxide. As the weight percentage of the aluminium oxide increase from 0% to 30% with range of 10, the hardness of the composite increased from 239 to 318. This result is in well agreement with [9].

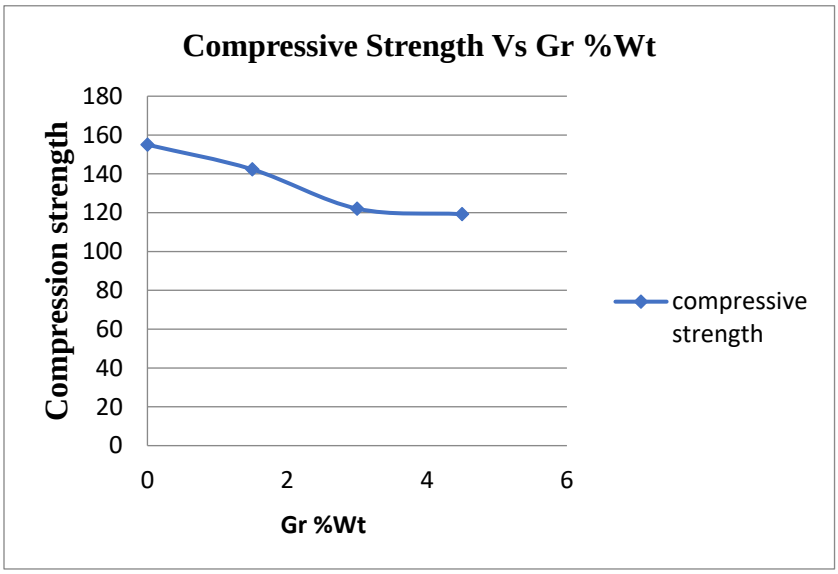


Figure 4.12 Variations in compressive versus Graphite weight percentage

The graph shows that with increase in the weight percentage of graphite the compressive strength of the composite decrease. Specifically as the reinforcement of graphite particle increase from 0 to 4.5 with range of 1.5 the compressive strength of the composite decrease from 155 to119.

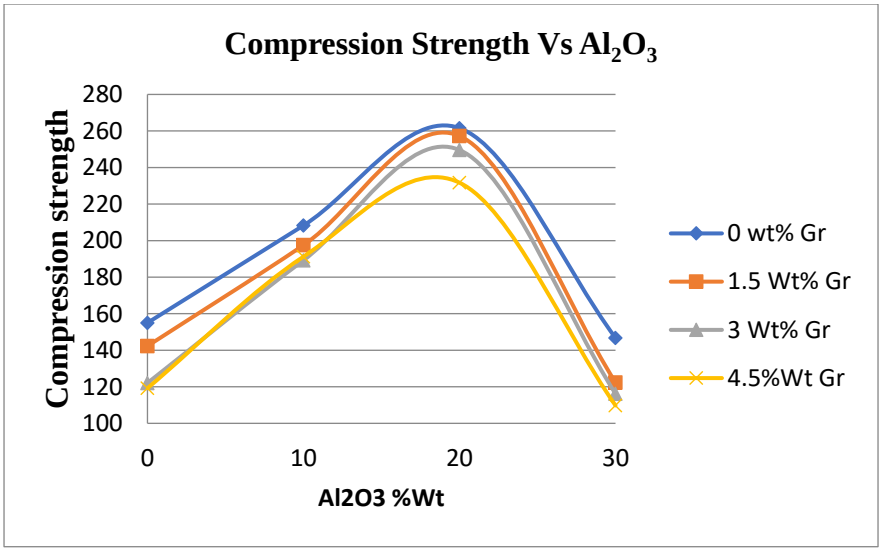


Figure 4.13 Variations in compressive strength versus $Al_2O_3$weight percentage

Figure 4.13 show that with increase in weight percentage of the aluminum oxide reinforcement the compression strength of the composite material increase up to 20% weight percentage and formerly decline due to the creation of poor wettability and de-bonding between the reinforcement particles and the matrix material increased due to the incompatibility between the reinforcement percentage and the pressure. Additionally the introduction of the solid lubricant into the matrix material induced a decrement on the compression strength of the composite material. The hardness of the composite is decreased with increase in the weight percentage of the composite material.

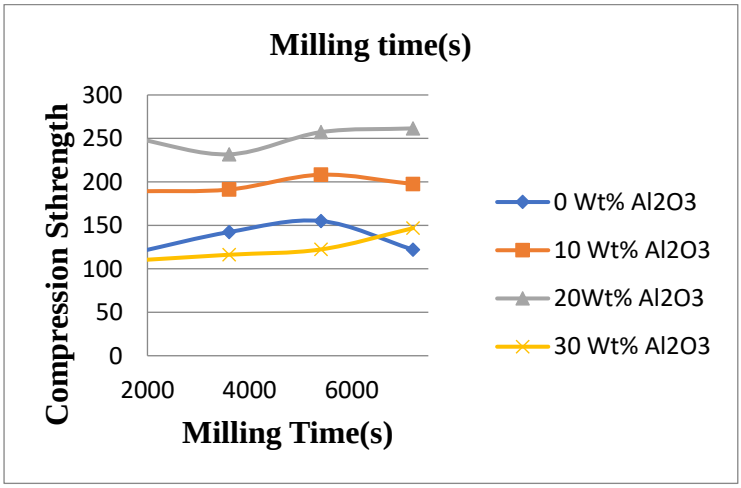


Figure 4.15 Variations in compressive strength as a function of milling time

As it can be interpreted from the figure4.15 the milling time of course have a constructive impact on the compressive strength of the composite material. All the samples compressive strength show increase with increase in the milling time. Specifically samples with20Wt% Al2O3 show better increment than the others sample.

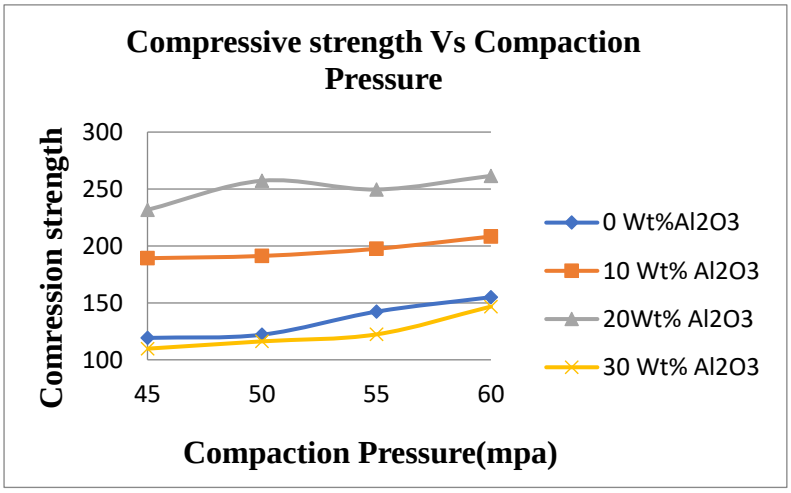

Figure 4.16 Variations in compressive strength versus $Al_2O_3$ weight percentage

As to the compaction pressure the compressive strength of the composite show increase with increase in compaction pressure. This caused due to low reinforcement of aluminum oxide reinforcement. The low reinforcement can be benefited from the low pressure due to requirement of high pressure for high level of weight percentage of reinforcement.

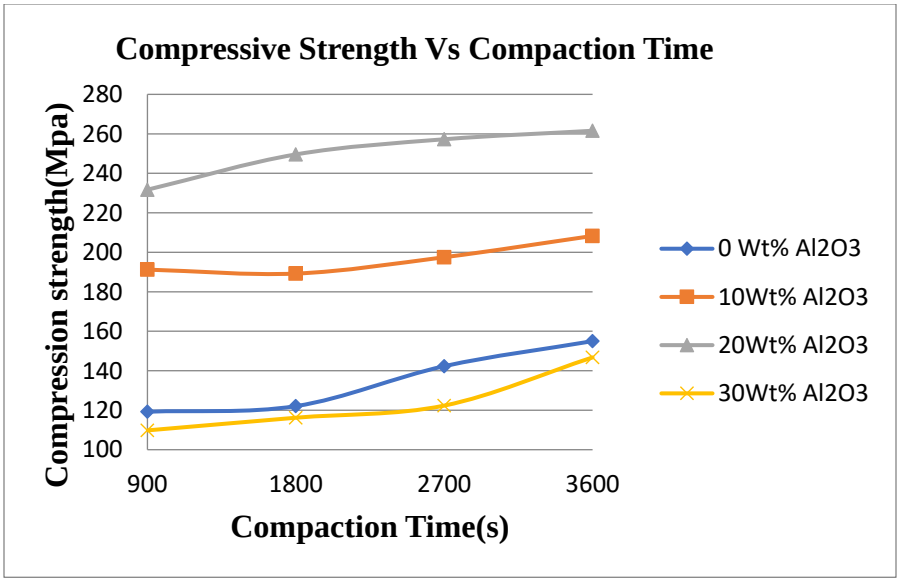


Figure 4.17 Variations in compressive strength as a function of $Al_2O_3$ Wt%

It can be understood from the Figure 4.17 that the compressive strength the increase in the compaction time induces increment on the compressive strength. Specifically, the composite with 0 Wt% of $Al_2O_3$ increase with better rate with increase in compaction time

### 4.5.1 Analysis of mean effect plot of compression strength

As it can be interpreted from the Figure 4.18, the optimum condition for the actual density is 20%$Al_2O_3$, 1.5%Gr, compaction pressure of 60mpa and 30 minute of compaction time and 30 minute of milling time.


Figure 4.18 Main effects plot for means of compressive strength.

### 4.5.2 Response Table for Means of compressive strength

The response table of the compression strength show that $Al_2O_3$ Weight Percentage has highest contribution in increasing the hardness of the composite with delta number of 126.3.While milling time is the second contributing factor in increasing the hardness of the composite with delta number of 29.9.the third ranker contributing factor is compaction time with delta number of 8.8. Likely the compaction pressure and milling time take the fourth and fifth rank with delta number of 3.8 and 3.3 respectively.

Table 4.11 response table for means of compressive strength

| Level | Al2O3 Wt% | Gr Wt% | Compression pressure | Compression time | Milling time |
|---|---|---|---|---|---|
| 1 | 134.7 | 192.9 | 178.0 | 174.6 | 177.8 |
| 2 | 196.6 | 179.8 | 174.6 | 182.5 | 174.5 |
| 3 | 250.0 | 169.3 | 174.3 | 174.3 | 174.9 |
| 4 | 123.8 | 163.0 | 178.1 | 173.6 | |
| Delta | 126.3 | 29.9 | 3.8 | 8.8 | 3.3 |
| Rank | 1 | 2 | 4 | 3 | 5 |

### 4.5.3 Analysis of variance of compressive strength

The last column of the ANOVA table shown in table 4.12 indicate that the percentage of contribution (Pc) in which $Al_2O_3$ weight percentage has the highest level of contribution (94.52%) followed by graphite weight percentage (4.7%), Compression time (0.47%) and compression pressure (0.11%).

Table 4.12 Analysis of variance of compressive strength

| Source | DF | Seq SS | Adj SS | Adj MS | F | P | Pc |
|---|---|---|---|---|---|---|---|
| Al2O3 Wt% | 3 | 41361.3 | 41361.3 | 13787.1 | 389.86 | 0.037 | 94.52% |
| Gr Wt% | 3 | 2059.2 | 2059.2 | 686.4 | 19.41 | 0.165 | 4.7% |
| Compression pressure | 3 | 51.6 | 51.6 | 17.2 | 0.49 | 0.753 | 0.11% |
| Compression time | 3 | 208.0 | 208.0 | 69.3 | 1.96 | 0.473 | 0.47% |
| milling time | 2 | 39.6 | 39.6 | 19.8 | 0.56 | 0.687 | 0.09% |
| Residual Error | 1 | 35.4 | 35.4 | 35.4 | | | 0.08% |
| Total | 15 | 43755.0 | | | | | |

## 4.6 Analysis of the wear loss

The wear rates of all the composites produced are presented in table 4.13. It is observed that the best wear resistance was obtained with the use of composites containing 10%, 20% and 3-4.5% graphite. Specifically it is observed that for all composite series produced, the composites without graphite exhibited greater wear susceptibility in comparison to the composite grades containing graphite. The presence of graphite is reported to help reduce the wear rate of the composites by providing a solid lubricating layer between the composite and the rubbing hard counter surface. However, it is noted that the wear resistance increased with increase in the graphite content from 0.5 to 4.5 wt%. It is also observed that the effect of aluminium oxide on wear susceptibility was not as consistent as the case of graphite but generally for the composites containing aluminium oxide there was on the average an increase in wear resistance with increase in aluminium oxide content. Nevertheless the aluminium oxide content of 30 weight percentage showed low wear resistance. Due to the poor wettability and de-bonding occurred in

between the grain boundary due to low working pressure. This is caused by non availability of high pressure hydraulic press. The hydraulic press used for this investigation is not compatible with composites of high weight percentage of reinforcement.

Table 4.13 Graphical representations of DOE and wear loss.

| Test runs | Aluminium oxide wt% | Gr wt% | Compn pressure (Mpa) | Compaction time (s) | Milling Time (s) | Wear loss($mm_3$/m) | S/N ratio |
|---|---|---|---|---|---|---|---|
| **1** | 0 | 0.0 | 45 | 900 | 1800 | 0.0033 | 49.63 |
| **2** | 0 | 1.5 | 50 | 1800 | 3600 | 0.0027 | 51.373 |
| **3** | 0 | 3.0 | 55 | 2700 | 5400 | 0.0023 | 52.765 |
| **4** | 0 | 4.5 | 60 | 3600 | 7200 | 0.00225 | 52.956 |
| **5** | 10 | 0.0 | 50 | 2700 | 7200 | 0.0022 | 53.152 |
| **6** | 10 | 1.5 | 45 | 3600 | 5400 | 0.0018 | 54.895 |
| **7** | 10 | 3.0 | 60 | 900 | 3600 | 0.00235 | 52.579 |
| **8** | 10 | 4.5 | 55 | 1800 | 1800 | 0.0022 | 53.152 |
| **9** | 20 | 0.0 | 55 | 3600 | 3600 | 0.0028 | 51.057 |
| **10** | 20 | 1.5 | 60 | 2700 | 1800 | 0.00277 | 51.150 |
| **11** | 20 | 3.0 | 45 | 1800 | 7200 | 0.0021 | 53.556 |
| **12** | 20 | 4.5 | 50 | 900 | 5400 | 0.0022 | 53.152 |
| **13** | 30 | 0.0 | 60 | 1800 | 5400 | 0.0044 | 47.131 |
| **14** | 30 | 1.5 | 55 | 900 | 7200 | 0.00425 | 47.43 |
| **15** | 30 | 3.0 | 50 | 3600 | 1800 | 0.0038 | 48.404 |
| **16** | 30 | 4.5 | 45 | 2700 | 3600 | 0.0035 | 49.119 |

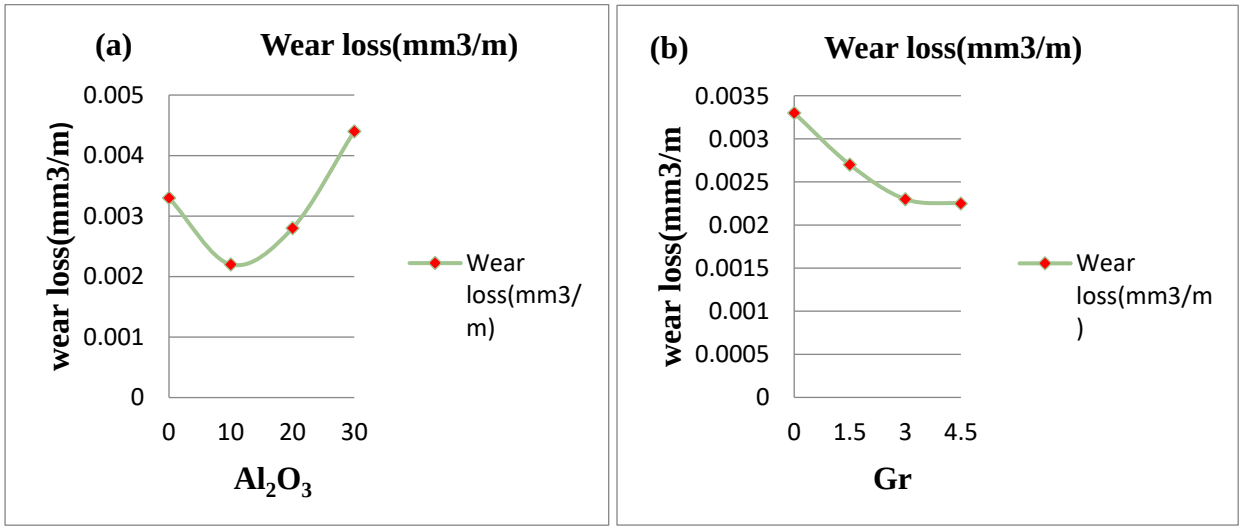


Figure 4.19 a) Variations in weight loss as a function of $Al_2O_3$Wt%.b) Variations in weight loss as a function of Gr Wt%

Figure 4.19 show that with increase in the weight percentage of graphite the wear loss of the composite decreased. Increase in weight percentage aluminum oxide reinforcement results in decrement on the wear loss up to 20%Wt $Al_2O_3$ and an increase is observed with increase in %Wt $Al_2O_3$ beyond 20%Wt reinforcement. Figure 4.19(b) show that, as the graphite reinforcement particle increase from 0 to 4.5 with range of 1.5 the wear loss of the composite decreased from 0.0033 to 0.00225. Likewise, the wear loss of the composite material developed decrease with increase in the weight percentage of aluminium oxide.

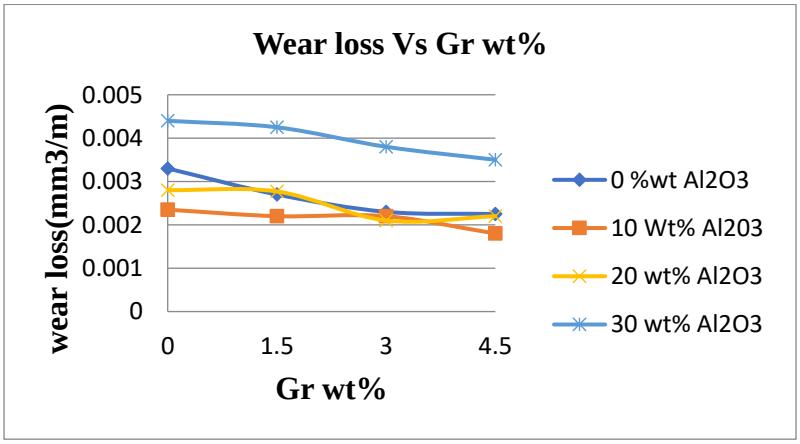


Figure4.20.Variations in weight loss function of Gr Wt% at various Wt% of $Al_2O_3$

Tallying of the graphite reinforcement is designated to increase the wear resistance of the composite material. As it can be construed from the figure 4.20 with increase in the weight percentage of the graphite particle, the wear loss of the composite decreased. The aluminium alloy matrix with 0 Wt% $Al_2O_3$ and various amount of graphite weight percentage show high wear loss decrement.

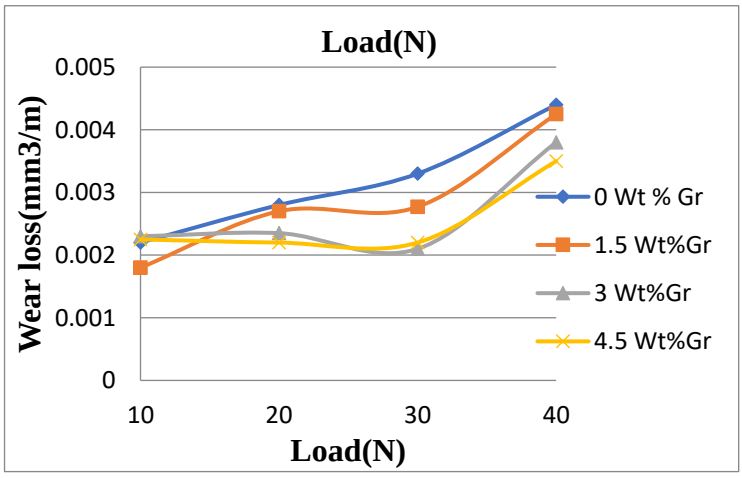


**Figure 4.21**Variation of the wear loss as a function of load at different Wt% of Gr

From the figure it can be understood that with increasing load the wear loss increase. Additionally the composite with graphite content achieved low wear loss.as the graphite reinforcement weight percentage increase the wear loss decrease. From the graphical interpretation the composite with 3 and 4.5 Wt% Gr show low wear rate at 30N load. This result is in good agreement with (M. Rahimian et al. (2010), K. K. Alaneme and K. O. Sanusi (2015))

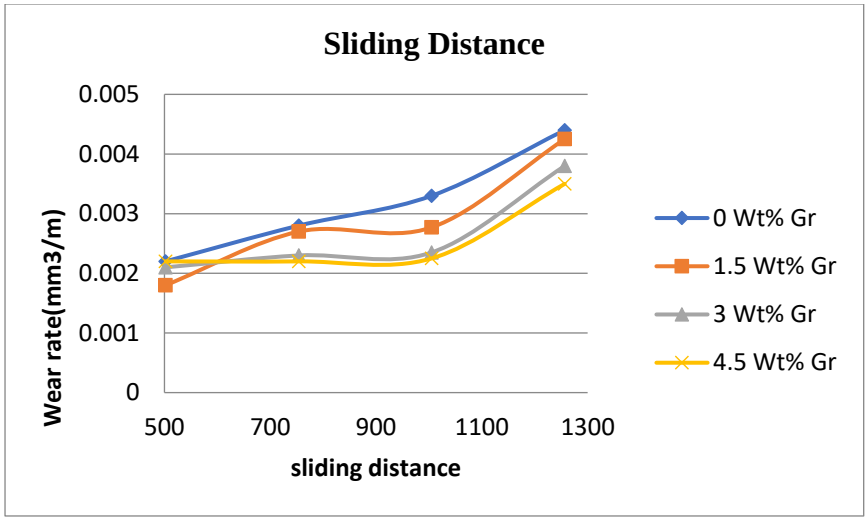


Figure 4.22 Variations in weight loss as a function of sliding distance at different Wt% of Gr.

As fig 4.22 depicts the wear loss increased with increasing sliding distance. The composite with 4.5Wt%Gr show low wear loss. The results reveal that with increasing graphite content the wear loss decrease. In this case, the above results are in line with other scholars (M. Rahimian et al. (2010), M. Rahimian, et al. (2011)).

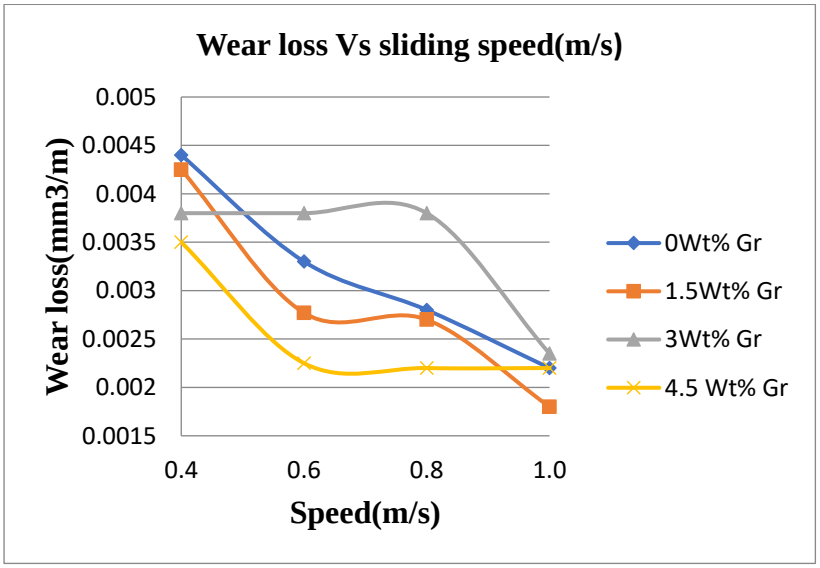


Figure 4.23 Variations in weight loss as a function of sliding distance at different Wt% of Gr.

As the sliding speed increase from 0.4 m/s to 1.0 m/s the wear loss of the composite decrease from 0.0044 to 0.00235.the samples with 1.5 and 4.5 Gr Wt% show high reduction on wear loss. The sample with 3 Wt% of Gr show minimum reduction as sliding speed increase from 0.4 to 0.8 and as sliding increase from 0.8 to 1 m/s the sample show high wear loss reduction. This could be due to other factors affection such as load and sliding distance.. The result implies that the wear loss decrease with increasing graphite reinforcement into $Al_2O_3$ –Al composite [9, 10].

### 4.6.1 Mean effect plot of wear loss

Fig show the main effect plot for means show that the optimum condition for the wear loss is 10% Al2O3, 4.5%Gr, 10N load and 1m/s sliding velocity minute of compaction time and 30 minute of milling time. This means at this condition low wear rate takes place.

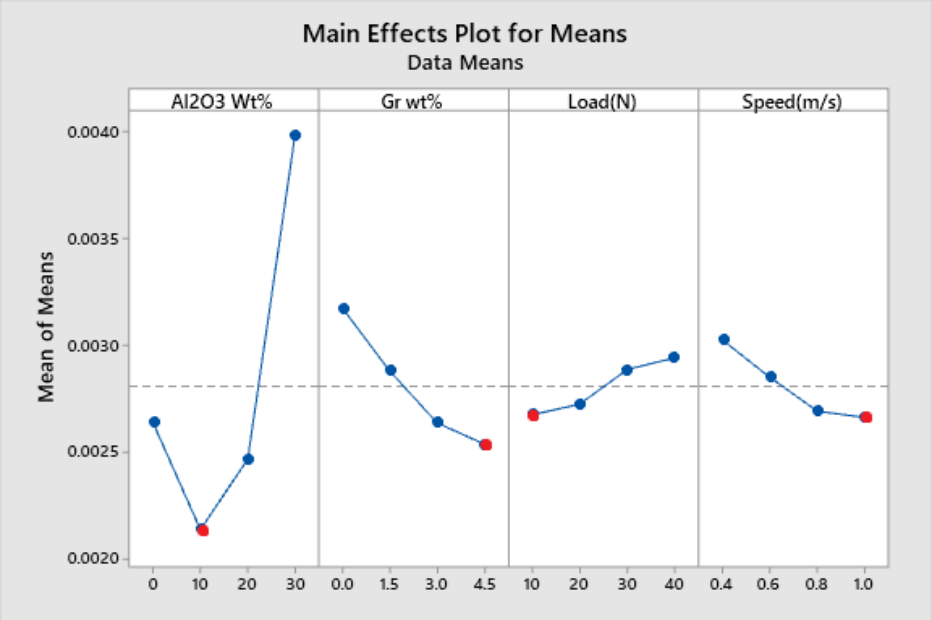


Figure 4.24 Main effect plot of wear loss

### 4.6.2 Response table for means of wear loss

The response table of the wear loss show that $Al_2O_3$ Weight Percentage has highest influence in decreasing the wear loss of the composite with delta number of 0.00185.While graphite weight percentage is the second contributing factor in decreasing the wear loss of the composite with delta number of 0.000638.the third ranker contributing factor is sliding speed, with delta number of 0.000363. Likely the load takes the fourth rank with delta number of 0.000267 and 3.3 respectively.

Table 4.25 Response table for mean of wear loss

| Level | $Al_2O_3$ wt% | Gr wt% | Load | Speed |
|---|---|---|---|---|
| 1 | 0.002638 | 0.003175 | 0.002675 | 0.003025 |
| 2 | 0.002138 | 0.002880 | 0.002725 | 0.002850 |
| 3 | 0.002468 | 0.002637 | 0.002888 | 0.002693 |
| 4 | 0.003988 | 0.002537 | 0.002942 | 0.002662 |
| Delta | 0.001850 | 0.000638 | 0.000267 | 0.000363 |
| Rank | 1 | 2 | 4 | 3 |

### 4.6.3 Analysis of variance for means of wear loss

As it is can be understood from the ANOVA table the percentage of contribution of the last column of the ANOVA table shown in table 5 indicates the percentage of contribution (Pc) in which load has highest percentage of contribution by 45%

Table 4.26 Analysis of variance for means of wear loss.

| Source | DF | Seq SS | Adj SS | Adj MS | F | P | Pc |
|---|---|---|---|---|---|---|---|
| $Al_2O_3$Wt% | 3 | 0.013669 | 0.013669 | 0.004556 | 0.69 | 0.614 | 16% |
| Gr Wt% | 3 | 0.036019 | 0.036019 | 0.012006 | 1.83 | 0.316 | 31% |
| Load | 3 | 0.000569 | 0.000569 | 0.000190 | 0.03 | 0.992 | 45% |
| Speed | 3 | 0.020769 | 0.020769 | 0.006923 | 1.06 | 0.483 | 6% |
| Residual Error | 3 | 0.019669 | 0.019669 | 0.006556 | | | 0.09% |
| Total | 15 | 0.090694 | | | | | |

## 4.7 Analysis of coefficient of friction

As the harder $Al_2O_3$ particles protrude from the softer aluminium matrix, the CoF value increases with increase in harder aluminum oxide content. In general, from the current study it could be established that CoF of the specimens reinforced with Gr particles was lower than the CoF of aluminum matrix specimens reinforced with $Al_2O_3$ particles. The decrement on the Coef with increase in weight percentage of Gr is mainly due to the lubrication effect of Gr particles which

tends to form a lubricant layer between sliding elements. Amongst every one of the conditions studied, aluminium composite exhibited less CoF, whereas pure aluminium alloy obsessed the maximum CoF value. Coefficient of friction is calculated from frictional force that is calculated by the machine and the load applied on the sample. The graph shows that CoF decrease with increase in weight percentage Gr%. As the weight percentage of Al2O3 increase from 0to 20 the CoF decrease. When the weight percentage of aluminium oxide increase from 20 to 30 the coefficient of friction increase from 0.46 to 0.53.

Table 4.27 The graphical representation of DOE and result of Coefficient of friction with S/N ratio.

| **Test runs** | **$Al_2O_3$ wt%** | **Gr wt%** | **Compaction pressure (Mpa)** | **Compaction time (s)** | **Milling Time (s)** | **CoF** | **S/N ratio** |
|---|---|---|---|---|---|---|---|
| **1** | 0 | 0.0 | 45 | 900 | 1800 | 0.66 | 3.61 |
| **2** | 0 | 1.5 | 50 | 1800 | 3600 | 0.49 | 6.196 |
| **3** | 0 | 3.0 | 55 | 2700 | 5400 | 0.41 | 7.744 |
| **4** | 0 | 4.5 | 60 | 3600 | 7200 | 0.37 | 8.636 |
| **5** | 10 | 0.0 | 50 | 2700 | 7200 | 0.46 | 6.745 |
| **6** | 10 | 1.5 | 45 | 3600 | 5400 | 0.39 | 8.179 |
| **7** | 10 | 3.0 | 60 | 900 | 3600 | 0.51 | 5.849 |
| **8** | 10 | 4.5 | 55 | 1800 | 1800 | 0.48 | 6.375 |
| **9** | 20 | 0.0 | 55 | 3600 | 3600 | 0.41 | 6.745 |
| **10** | 20 | 1.5 | 60 | 2700 | 1800 | 0.42 | 7.535 |
| **11** | 20 | 3.0 | 45 | 1800 | 7200 | 0.35 | 9.119 |
| **12** | 20 | 4.5 | 50 | 900 | 5400 | 0.38 | 8.404 |
| **13** | 30 | 0.0 | 60 | 1800 | 5400 | 0.53 | 5.514 |
| **14** | 30 | 1.5 | 55 | 900 | 7200 | 0.46 | 6.74 |
| **15** | 30 | 3.0 | 50 | 3600 | 1800 | 0.45 | 6.936 |
| **16** | 30 | 4.5 | 45 | 2700 | 3600 | 0.37 | 0.4 |

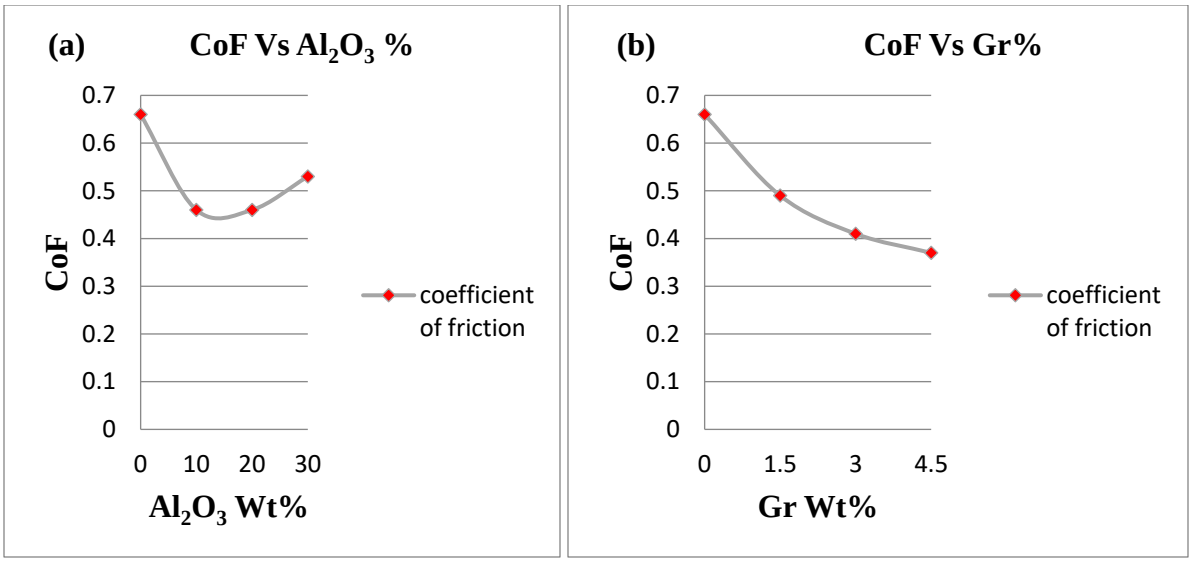


Figure 4.25 **a)** Variations in Cof as a function of $Al_2O_3$wt%. b) Variations in Cof as a function of Gr wt%.

Table 4.27 and the Figure 4.25 show that with increase in the weight percentage of graphite the coefficient of friction of the composite decrease. As the reinforcement of graphite particle increase from 0 to 4.5 with range of 1.5 the coefficient of friction of the composite increase from 0.66 to 0.37. Likewise, the coefficient of friction of the composite material developed decrease with increase in the weight percentage of aluminium oxide. As the weight percentage of the aluminium oxide increase from 0 to 20, the wear loss of the composite material decrease from 0.66 to 0.46.

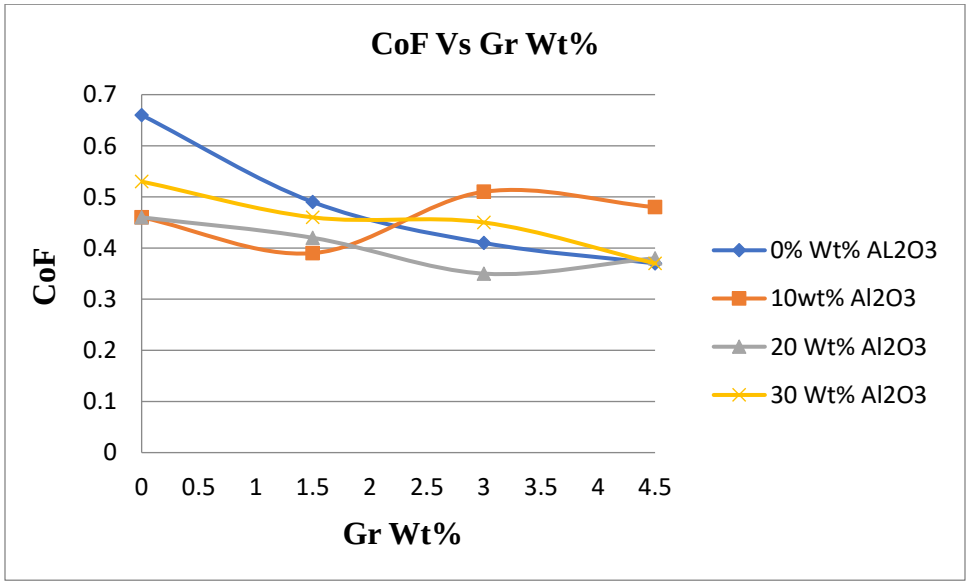


Figure 4.26Variations in CoF as a function of Gr weight percentage

Tallying of the graphite reinforcement is designated to decrease the CoF of the composite material. As it can be construed from the figure 4.26 with an increase in the weight percentage of the graphite particle, the CoF of the composite decreased. The aluminium alloy matrix with 20Wt% $Al_2O_3$ and various amount of graphite weight percentage show low CoF decrement

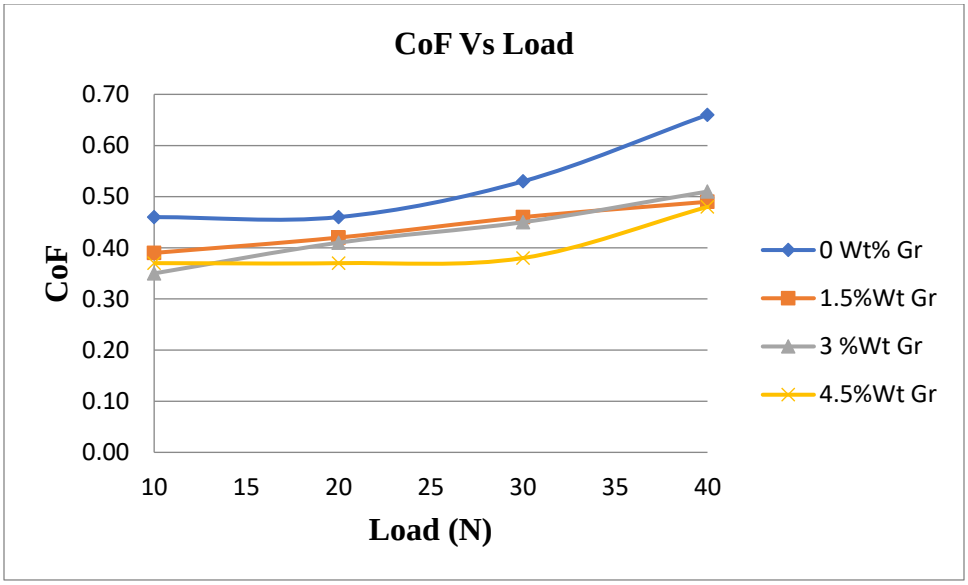


Figure 4.27 Variations in Cof of the composites as a function of load.

From the figure it can be understood that with increasing load the CoF increase. Additionally the composite with graphite content achieved low CoF. As the graphite reinforcement weight percentage increase the CoF decrease. From the graphical interpretation the composite with 3 and 4.5 Wt% Gr show low CoF at 30N load. This result is in good agreement with (M. Rahimian et al. (2010), A. Devaraju and A. Kumar, 2013)

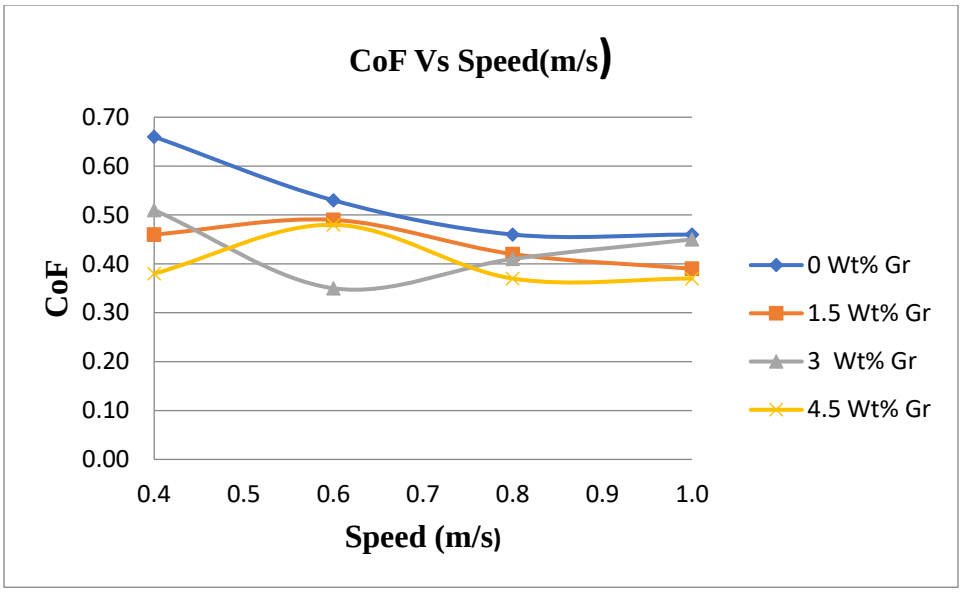


Figure 4.30 Variations in weight loss of the composites as a function sliding speed

As the sliding speed increase from 0.4m/s to 1m/s the CoF of the composite decrease. From the composite samples the experimental specimens with 3Wt% and 4.5Wt% revealed low coefficient of friction. The result implies that the Cof decreased with increasing graphite reinforcement into $Al_2O_3$ –Al composite the result is in line with (M. Rahimian et al. (2010), A. Devaraju and A. Kumar, 2013)

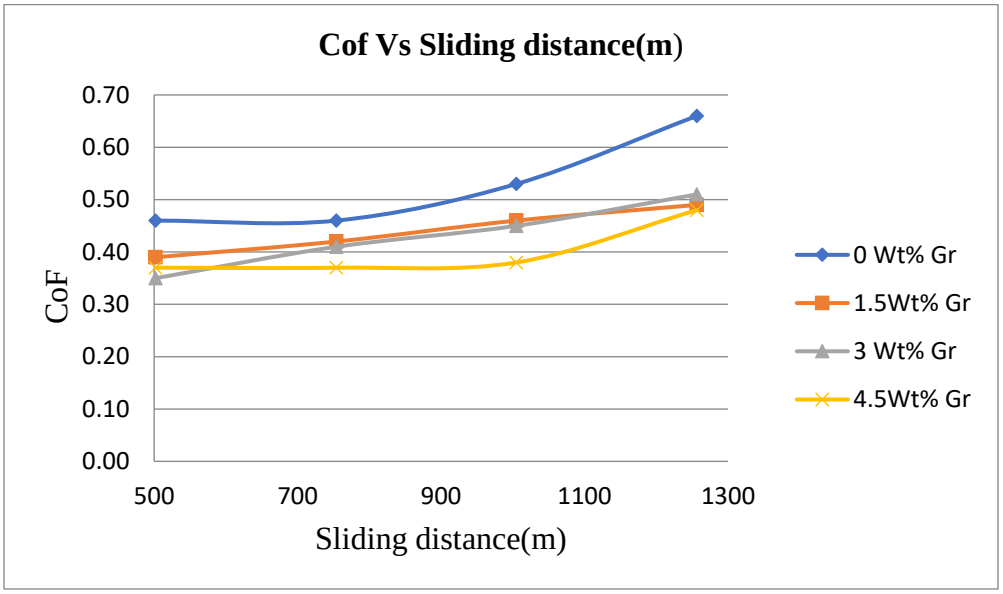


Figure 4.31Variations in CoF as a function sliding distance.

From the graph it can be understood that with increase in the sliding distance, the coefficient of friction increase. Above all the samples with 3Wt% and 4.5Wt% of Gr resulted a low coefficient ofr friction (M. Rahimian et al. (2010), A. Devaraju and A. Kumar, 2013).

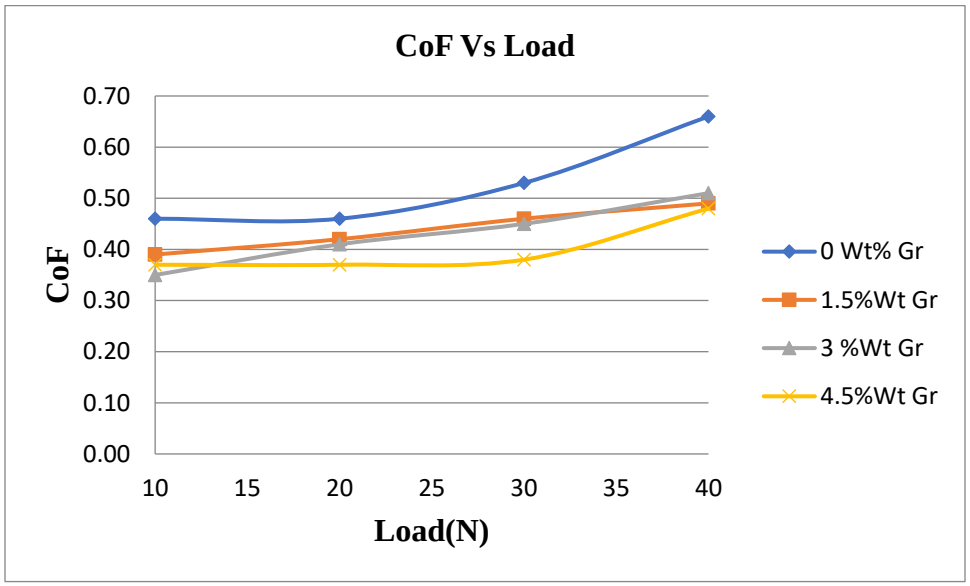


Figure 4.32Variations in CoF as a function of Load.

The fig revealed that with increase in the load the CoF increase. From the composite samples the experimental specimens with 3Wt% and 4.5Wt% of Gr revealed low coefficient of friction.

### 4.7.1 Analysis of mean effect plot of Coefficient of friction

Fig show the main effect plot for means show that the optimum condition for the wear loss is 20% weight percentage of aluminium oxide, 4.5% weight percentage of graphite reinforcement, 10N load and 0.8 m/s sliding velocity. This means at this condition optimum coefficient of friction takes place.


Figure 4.33 Main effect plots for means of CoF.

### 4.7.2 Analysis variance for coefficient of friction

The last column of the ANOVA table shown in table 4.28 indicates the percentage of contribution (Pc) in which $Al_2O_3$ weight percentage has the highest level of contribution (94.5%) followed by graphite weight percentage (4.7%), sliding speed (0.47%), load (0.11%)

Table 4.28 analysis of variance of coefficient of friction

| Source | DF | Seq SS | Adj SS | Adj MS | F | P | Pc |
|---|---|---|---|---|---|---|---|
| $Al_2O_3$ Wt% | 3 | 0.013669 | 0.013669 | 0.004556 | 0.69 | 0.614 | 94.5% |
| Gr Wt% | 3 | 0.036019 | 0.036019 | 0.012006 | 1.83 | 0.316 | 4.7% |
| load | 3 | 0.000569 | 0.000569 | 0.000190 | 0.03 | 0.992 | 0.11% |
| speed | 3 | 0.020769 | 0.020769 | 0.006923 | 1.06 | 0.483 | 0.47% |
| Residual Error | 3 | 0.019669 | 0.019669 | 0.006556 | | | 0.09% |
| Total | 15 | 0.090694 | | | | | |

## 4.8 Analysis of gray relational analysis of actual density and porosity

The consequences obtained from various researches are considered in detail and are discussed in the following subdivisions.The investigational analysis data such as alumina weight percentage, graphite weight percentage, compaction pressure, compaction time and milling time are transformed into Signal-to-Noise (S/N) ratio. Subsequently the response parameters of the wear loss and coefficient of friction are converted into S/N ratio using Taguchi analysis. The normalizing sequence for both parameters is calculated from the S/N ratio. By using the normalizing sequence value deviation sequence is calculated. The Gray relational coefficient for both parameters is calculated using the deviation sequence values. Finally the GRG is developed from the GRC.

Table 4.29 show that the GRG of actual and porosity of the composite material.

| Exp. no | Response parameters | | S/N ratio | | Normalizing sequence | | Deviation sequence | | Grey Relation Coefficient | | |
|---|---|---|---|---|---|---|---|---|---|---|---|
| | Actual Density | Porosity | Actual Density | Porosity | Actual Density | Porosity | Actual Density | Porosity | Actual Density | Porosity | GRG |
| **1** | 2651.40 | 1.900 | -5.575 | -5.575 | 0.000 | -1.051 | 1.000 | 2.051 | 0.333 | 0.939 | 0.636 |
| **2** | 2580.00 | 2.640 | -8.432 | -8.432 | 0.538 | -0.949 | 0.462 | 1.949 | 0.520 | 0.971 | 0.745 |
| **3** | 2623.83 | 2.300 | -7.235 | -7.235 | 0.313 | -0.992 | 0.687 | 1.992 | 0.421 | 0.957 | 0.689 |
| **4** | 2610.90 | 2.520 | -8.028 | -8.028 | 0.462 | -0.964 | 0.538 | 1.964 | 0.482 | 0.966 | 0.724 |
| **5** | 2736.71 | 3.125 | -9.897 | -9.897 | 0.814 | -0.897 | 0.186 | 1.897 | 0.729 | 0.988 | 0.859 |
| **6** | 2738.61 | 2.810 | -8.974 | -8.974 | 0.641 | -0.930 | 0.359 | 1.930 | 0.582 | 0.977 | 0.779 |
| **7** | 2733.87 | 2.730 | -8.723 | -8.723 | 0.593 | -0.939 | 0.407 | 1.939 | 0.551 | 0.974 | 0.763 |
| **8** | 2720.80 | 2.930 | -9.337 | -9.337 | 0.709 | -0.917 | 0.291 | 1.917 | 0.632 | 0.981 | 0.807 |
| **9** | 2883.92 | 2.240 | -7.005 | -7.005 | 0.269 | -1.000 | 0.731 | 2.000 | 0.406 | 0.954 | 0.680 |
| **10** | 2878.94 | 2.170 | -6.729 | -6.729 | 0.217 | -1.010 | 0.783 | 2.010 | 0.390 | 0.951 | 0.671 |
| **11** | 2834.02 | 3.460 | -10.78 | -10.782 | 0.981 | -0.866 | 0.019 | 1.866 | 0.964 | 0.999 | 0.981 |
| **12** | 2834.01 | 3.210 | -10.13 | -10.130 | 0.858 | -0.889 | 0.142 | 1.889 | 0.779 | 0.991 | 0.885 |
| **13** | 2972.60 | 3.330 | -10.45 | -10.449 | 0.918 | -0.878 | 0.082 | 1.878 | 0.860 | 0.995 | 0.927 |
| **14** | 2960.42 | 3.500 | -10.88 | -10.881 | 1.000 | -0.862 | 0.000 | 1.862 | 1.000 | 1.000 | 1.000 |
| **15** | 2967.25 | 3.050 | -9.686 | -9.686 | 0.775 | -0.905 | 0.225 | 1.905 | 0.689 | 0.985 | 0.837 |
| **16** | 2979.42 | 2.410 | -7.640 | -7.640 | 0.389 | -0.977 | 0.611 | 1.977 | 0.450 | 0.962 | 0.706 |

### 4.8.1 Analysis of mean effect plot of GRG of actual density, porosity

show the main effect plot for means show that the optimum condition for GRG of the actual density and porosity is 10% $Al_2O_3$, 4.5%Gr, compaction pressure of 60mpa and 45 minute of compaction time and 30 minute of milling time


Figure 4.34 main effect plots for means of GRG of actual density, porosity

### 4.8.2 Response table for means of GRG of actual density and porosity

The response table of the GRG of actual density and porosity shows that $Al_2O_3$ Weight Percentage has highest contribution in increasing the actual density and porosity of the composite with delta number of 0.5461. While graphite weight percentage is the second contributing factor in increasing the actual density and porosity of the composite with delta number of 0.1119.the third ranker contributing factor is compaction pressure with delta number of 0.0472. Likely the compaction time and milling time take the fourth and fifth rank with delta number of 0.0291and 0.0277 respectively.

Table 4.30 response table for means of GRG of actual density and porosity

| Level | $Al_2O_3$ Wt% | Gr Wt% | Compression pressure | Compression time | Milling time |
|---|---|---|---|---|---|
| 1 | 0.3830 | 0.6414 | 0.5618 | 0.5742 | 0.5760 |
| 2 | 0.5720 | 0.6111 | 0.5749 | 0.5905 | 0.5912 |
| 3 | 0.9291 | 0.5649 | 0.6011 | 0.5790 | 0.6037 |
| 4 | 0.4628 | 0.5294 | 0.6091 | 0.6032 | |
| Delta | 0.5461 | 0.1119 | 0.0472 | 0.0291 | 0.0277 |
| Rank | 1 | 2 | 3 | 4 | 5 |

### 4.8.3 Analysis of variance for gray relational analysis of actual density and porosity

The last column of the ANOVA table shown in table 4.31 indicates the percentage of contribution (Pc) in which milling time has the highest level of contribution (38.12) followed by Al2O3 weight percentage Compression time (30.9%) and compression time (23.66%).while the compaction pressure and Gr are the least contributors (4.78% and 2.32%)respectively.

Table 4.31 Analysis of variance for gray relational analysis of theoretical density, actual density, porosity

| Source | DF | Seq SS | Adj SS | Adj MS | F | P | Pc |
|---|---|---|---|---|---|---|---|
| $Al_2O_3$ Wt% | 3 | 0.058758 | 0.058758 | 0.019586 | 49.26 | 0.104 | 30.9% |
| Gr Wt% | 3 | 0.004410 | 0.004410 | 0.001470 | 3.70 | 0.361 | 2.32% |
| Compn pressure | 3 | 0.009091 | 0.009091 | 0.003030 | 7.62 | 0.259 | 4.78% |
| Compn time | 3 | 0.044970 | 0.044970 | 0.014990 | 37.70 | 0.119 | 23.66% |
| milling time | 2 | 0.072444 | 0.072444 | 0.036222 | 91.10 | 0.074 | 38.12% |
| Residual Error | 1 | 0.000398 | 0.000398 | 0.000398 | | | 0.2% |
| Total | 15 | 0.190072 | | | | | |

## 4.9 Analysis of GRG of wear loss and coefficient of friction

The results obtained from various experimentations are analyzed in detail and are discussed in the following subsections.The experimental investigation data such as alumina weight percentage, graphite weight percentage, compaction pressure, compaction time and milling time are transformed into Signal-to-Noise (S/N) ratio. After the response parameters of the wear loss and coefficient of friction are converted into S/N ratio using Taguchi analysis. The normalizing

sequence for both parameters is calculated from the S/N ratio. By using the normalizing sequence value deviation sequence is calculated. The Gray relational coefficient for both parameters is calculated using the deviation sequence values. Finally the GRG is developed from the GRC.

Table 4.32 Show that the GRG development for the actual and porosity of the composite material.

| **Test run** | **Response Parameters** | | **SN ratio** | | **Normalizing Sequence** | | **Deviation Sequence** | | **Grey Relational Coefficient** | | **Grey Relational Analysis** |
|---|---|---|---|---|---|---|---|---|---|---|---|
| | **Wear loss** | **CoF** | **Wear loss** | **CoF** | **Wear loss** | **CoF** | **Wear loss** | **CoF** | **Wear loss** | **CoF** | **GRG** |
| **1** | 0.0033 | 0.660 | 49.63 | 3.61 | 0.678 | 0.99 | 0.322 | 0.002 | 0.612 | 1.000 | 0.806 |
| **2** | 0.0027 | 0.490 | 51.373 | 6.196 | 0.453 | 0.529 | 0.547 | 0.471 | 0.480 | 0.517 | 0.499 |
| **3** | 0.0023 | 0.410 | 52.765 | 7.744 | 0.274 | 0.248 | 0.726 | 0.752 | 0.410 | 0.401 | 0.405 |
| **4** | 0.0022 | 0.370 | 52.956 | 8.636 | 0.249 | 0.086 | 0.751 | 0.914 | 0.402 | 0.355 | 0.379 |
| **5** | 0.0022 | 0.460 | 53.152 | 6.745 | 0.224 | 0.429 | 0.776 | 0.571 | 0.394 | 0.469 | 0.431 |
| **6** | 0.0018 | 0.390 | 54.895 | 8.179 | -0.001 | 0.169 | 1.001 | 0.831 | 0.335 | 0.377 | 0.356 |
| **7** | 0.0023 | 0.510 | 52.579 | 5.849 | 0.298 | 0.592 | 0.702 | 0.408 | 0.418 | 0.553 | 0.485 |
| **8** | 0.0022 | 0.480 | 53.152 | 6.375 | 0.224 | 0.496 | 0.776 | 0.504 | 0.394 | 0.500 | 0.447 |
| **9** | 0.0028 | 0.460 | 51.057 | 6.745 | 0.494 | 0.429 | 0.506 | 0.571 | 0.500 | 0.469 | 0.484 |
| **10** | 0.00277 | 0.420 | 51.150 | 7.535 | 0.482 | 0.286 | 0.518 | 0.714 | 0.494 | 0.413 | 0.454 |
| **11** | 0.0021 | 0.350 | 53.556 | 9.119 | 0.172 | 0.002 | 0.828 | 1.002 | 0.379 | 0.334 | 0.356 |
| **12** | 0.0022 | 0.380 | 53.152 | 8.404 | 0.224 | 0.128 | 0.776 | 0.872 | 0.394 | 0.366 | 0.380 |
| **13** | 0.0044 | 0.530 | 47.131 | 5.514 | 1.000 | 0.653 | 0.000 | 0.347 | 1.005 | 0.592 | 0.799 |
| **14** | 0.0042 | 0.460 | 47.43 | 6.74 | 0.961 | 0.43 | 0.039 | 0.57 | 0.933 | 0.47 | 0.701 |
| **15** | 0.0038 | 0.450 | 48.404 | 6.936 | 0.836 | 0.395 | 0.164 | 0.605 | 0.757 | 0.45 | 0.606 |
| **16** | 0.0035 | 0.370 | 49.119 | 8.636 | 0.744 | 0.086 | 0.256 | 0.914 | 0.665 | 0.355 | 0.510 |

### 4.9.1 Analysis of main effect of GRG of wear loss and coefficient of friction

Fig show the main effect plot for means show that the optimum condition for the actual density and porosity is 20 %$Al_2O_3$, 4.5%Gr, load 20N and sliding speed(m/s).

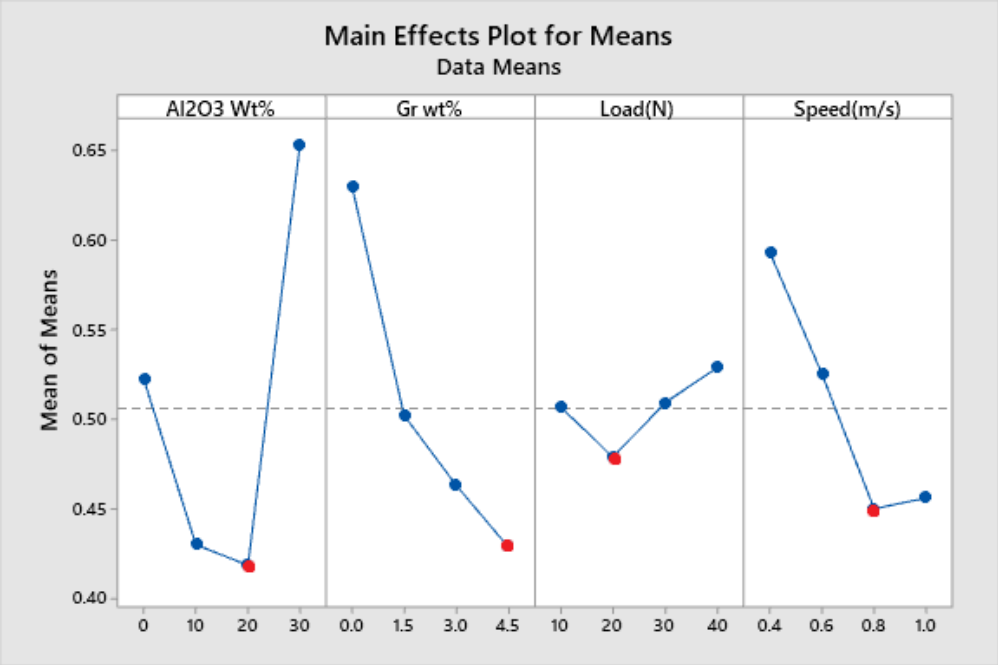


Figure 4.35 Main effects plot for means of GRG of wear loss and coefficient of friction

### 4.9.2 Response for means of GRG of wear loss and coefficient of friction

The response table of the compression strength shows that $Al_2O_3$ Weight Percentage has highest contribution in increasing the actual density and porosity of the composite with delta number of 0.5461. While graphite weight percentage is the second contributing factor in increasing the actual density and porosity of the composite with delta number of 0.1119.the third ranker contributing factor is compaction pressure with delta number of 0.0472. Likely the compaction time and milling time take the fourth and fifth rank with delta number of 0.0291 and 0.0277 respectively.

Table 4.33 Response for means of GRG of wear loss and coefficient of friction

| Level | $Al_2O_3$ Wt% | Gr Wt% | Load(N) | Speed(m/s) |
|---|---|---|---|---|
| 1 | 0.5221 | 0.6301 | 0.5071 | 0.5930 |
| 2 | 0.4300 | 0.5023 | 0.4789 | 0.5252 |
| 3 | 0.4186 | 0.4632 | 0.5094 | 0.4501 |
| 4 | 0.6538 | 0.4289 | 0.5291 | 0.4561 |
| Delta | 0.2351 | 0.2012 | 0.0502 | 0.1429 |
| Rank | 1 | 2 | 4 | 3 |

### 4.9.3 Analysis of variance of GRG of wear loss and coefficient of friction

Table 4.34 depict that the$Al_2O_3$ weight percentage has the highest level of contribution (43.93%) followed by graphite particle weight percentage (28.69%), speed (16.77%) and load (1.58%).

Table 4.34 Analysis of variance ofGRG of wear loss and coefficient of friction

| Source | DF | Seq SS | Adj SS | Adj MS | F | P | Pc |
|---|---|---|---|---|---|---|---|
| $Al_2O_3$ Wt% | 3 | 0.141999 | 0.141999 | 0.047333 | 4.87 | 0.113 | 43.93% |
| Gr Wt% | 3 | 0.092732 | 0.092732 | 0.030911 | 3.18 | 0.184 | 28.69% |
| Load | 3 | 0.005126 | 0.005126 | 0.001709 | 0.18 | 0.906 | 1.58% |
| Speed | 3 | 0.054219 | 0.054219 | 0.018073 | 1.86 | 0.312 | 16.77% |
| Residual Error | 3 | 0.029171 | 0.029171 | 0.009724 | | | 9.02% |
| Total | 15 | 0.323247 | | | | | |

## 4.10 Analysis of gray relational analysis of hardness and compressive strength

The results obtained from various experimentations are analyzed in detail and are discussed in the following subsections.The experimental investigation data such as alumina weight percentage, graphite weight percentage, compaction pressure, compaction time and milling time are transformed into Signal-to-Noise (S/N) ratio. After the response parameters are converted into S/N ratio using Taguchi analysis. The normalizing sequence is calculated from the S/N ratio. By using the normalizing sequence value deviation sequence ids calculated. The Gray relational coefficient is calculated using the deviation sequence. Finally the GRG is developed from the GRC.

Table 4.35 Analysis of variance ofgray relational analysis of hardness and compressive strength

| Test runs | Response parameters | | S/N ratio | | Normalizing sequence | | Deviation sequence | | Gray relational coefficient | | GRG |
|---|---|---|---|---|---|---|---|---|---|---|---|
| | Compn strength (Mpa) | Hardness | Compn strength (Mpa) | Hardness | Comprnzstrength (Mpa) | Hardness | Compn strength (Mpa) | Hardness | Compn strength (Mpa) | Hardness | |
| **1** | 155 | 239 | 43.81 | 47.56 | 0.39 | 0 | 0.602 | 1 | 0.453 | 0.333 | 0.39 |
| **2** | 142.3 | 245 | 43.06 | 47.78 | 0.29 | 0.084 | 0.701 | 0.915 | 0.416 | 0.353 | 0.38 |
| **3** | 122.07 | 252.8 | 41.73 | 48.05 | 0.12 | 0.190 | 0.877 | 0.809 | 0.362 | 0.381 | 0.37 |
| **4** | 119.23 | 259 | 41.52 | 48.26 | 0.09 | 0.272 | 0.904 | 0.727 | 0.355 | 0.407 | 0.38 |
| **5** | 208.28 | 290 | 46.37 | 49.24 | 0.73 | 0.655 | 0.262 | 0.344 | 0.655 | 0.592 | 0.62 |
| **6** | 197.5 | 288.2 | 45.91 | 49.19 | 0.67 | 0.634 | 0.323 | 0.365 | 0.607 | 0.577 | 0.59 |
| **7** | 189.23 | 279.8 | 45.54 | 48.93 | 0.62 | 0.534 | 0.372 | 0.465 | 0.572 | 0.517 | 0.54 |
| **8** | 191.23 | 272 | 45.63 | 48.69 | 0.64 | 0.438 | 0.360 | 0.561 | 0.580 | 0.471 | 0.52 |
| **9** | 261.56 | 320.9 | 48.35 | 50.13 | 1 | 1 | 0 | 0 | 1 | 1 | 1 |
| **10** | 257.26 | 318.9 | 48.21 | 50.07 | 0.98 | 0.978 | 0.019 | 0.021 | 0.963 | 0.959 | 0.96 |
| **11** | 249.58 | 315.9 | 47.94 | 49.99 | 0.94 | 0.946 | 0.053 | 0.053 | 0.902 | 0.903 | 0.90 |
| **12** | 231.71 | 317 | 47.29 | 50.02 | 0.86 | 0.957 | 0.139 | 0.042 | 0.781 | 0.921 | 0.85 |
| **13** | 146.76 | 298.2 | 43.33 | 49.49 | 0.33 | 0.750 | 0.665 | 0.249 | 0.428 | 0.667 | 0.54 |
| **14** | 122.34 | 296.3 | 41.75 | 49.43 | 0.12 | 0.729 | 0.875 | 0.270 | 0.363 | 0.648 | 0.50 |
| **15** | 116.2 | 281.5 | 41.30 | 48.98 | 0.065 | 0.554 | 0.934 | 0.445 | 0.348 | 0.529 | 0.43 |
| **16** | 109.78 | 253.1 | 40.81 | 48.06 | 0 | 0.195 | 1 | 0.804 | 0.333 | 0.383 | 0.35 |

### 4.10.1 Analysis of mean of GRG of hardness and compressive strength

Figure 4.12 show the main effect plot for means show that the optimum condition for Analysis of gray relational analysis of hardness and compressive strength is 20% $Al_2O_3$, 1.5%Gr, compaction pressure of 60mpa and 60 minute of compaction time and 120 minute of milling time.

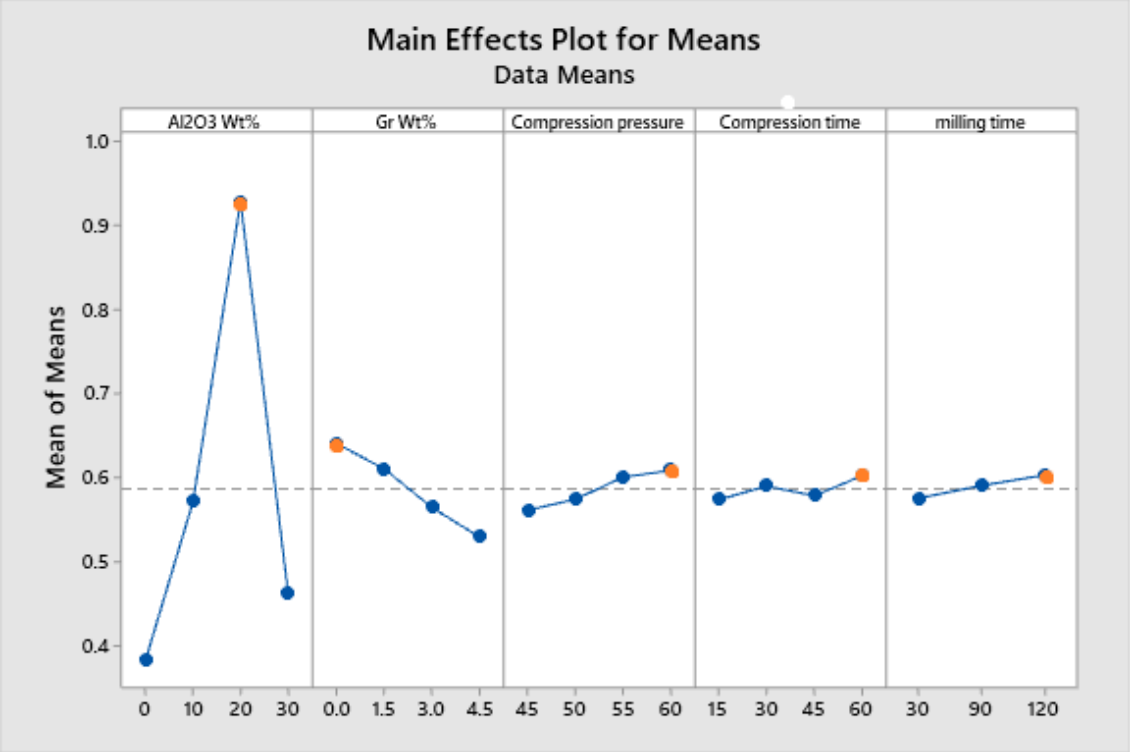


Figure 4.36 Main effects plot for means of GRG of hardness and compressive strength

### 4.10.2 Response table for means of GRG of hardness and compressive strength

The response table of the compression strength shows that $Al_2O_3$ Weight Percentage has highest contribution in increasing the hardness and compression strength of the composite with delta number of 0.5461. While graphite weight percentage is the second contributing factor in increasing the compression strength and hardness of the composite with delta number of 0.1119.the third ranker contributing factor is compaction pressure with delta number of 0.047 likely the compaction time and milling time take the fourth and fifth rank with delta number of 0.0291 and 0.0277respectively.

Table 4.36 Response table for means of GRG of hardness and compressive strength

| Level | $Al_2O_3$ Wt% | Gr Wt% | Compression pressure | Compression time | milling time |
|---|---|---|---|---|---|
| 1 | 0.3830 | 0.6414 | 0.5618 | 0.5742 | 0.5760 |
| 2 | 0.5720 | 0.6111 | 0.5749 | 0.5905 | 0.5912 |
| 3 | 0.9291 | 0.5649 | 0.6011 | 0.5790 | 0.6037 |
| 4 | 0.4628 | 0.5294 | 0.6091 | 0.6032 | |
| Delta | 0.5461 | 0.1119 | 0.0472 | 0.0291 | 0.0277 |
| Rank | 1 | 2 | 3 | 4 | 5 |

### 4.10.3 Analysis of variance of GRG of hardness and compressive strength

The last column of the ANOVA table shown in table 4.36 indicates the percentage of contribution (Pc) in which $Al_2O_3$ weight percentage has the highest level of contribution (43.92%) followed by graphite weight percentage (28.68%), sliding speed (16.77%) and load (1.58) respectively.

Table 4.36 Analysis of variance of GRG of hardness and compressive strength

| Source | DF | Seq SS | Adj SS | Adj MS | F | P | Pc |
|---|---|---|---|---|---|---|---|
| Al2O3 Wt% | 3 | 0.141999 | 0.141999 | 0.047333 | 4.87 | 0.113 | 43.92% |
| Gr Wt% | 3 | 0.092732 | 0.092732 | 0.030911 | 3.18 | 0.184 | 28.68% |
| load | 3 | 0.005126 | 0.005126 | 0.001709 | 0.18 | 0.906 | 1.58% |
| speed | 3 | 0.054219 | 0.054219 | 0.018073 | 1.86 | 0.312 | 16.77% |
| Residual Error | 3 | 0.029171 | 0.029171 | 0.009724 | | | 9.02% |
| Total | 15 | 0.323247 | | | | | |

## 4.11 Confirmation experiment

Once the optimal combination of process parameters and their levels was obtained, the final step is to verify the predicted result against experimental results .if the optimal combination of parameters and their levels coincidently match with one of the experiment in the orthogonal array and then no confirmation test is required.

Table 4.37 confirmation of the experiment

| No | Response | Predicted value | | Corresponding to optimum condition | |
|---|---|---|---|---|---|
| 1 | Density | 2872.36 | | 2834 | |
| 2 | Porosity | 2.11125 | | 2.24 | |
| 3 | Hardness | 327.565 | | 318.9 | |
| 4 | Compressive strength | 304.647 | | 257.26 | |
| 5 | Wear resistance | 0.311875 | | 0.0022 | |
| 6 | Coefficient of friction | 0.311875 | | 0.38 | |
| 7 | GRA OF actual density and porosity | **Density** | **Porosity** | **Density** | **Porosity** |
| | | 2872.36 | 2.24 | 2720.9 | 2.93 |
| 8 | GRA OF wear loss and coefficient of friction | **Wear loss** | **Cof** | **Wear loss** | **Cof** |
| | | 0.311875 | 0.38 | 0.0022 | 0.38 |
| 9 | GRA OF compressive strength and hardness | **Comp strength** | **Hardness** | **Comp strength** | **Hardness** |
| | | 304.647 | 327.565 | 261.56 | 320.19 |

## 4.12 Micro structural analysis

By using SEM analysis, the qualitative information on the distribution of particles, size and morphology of hybrid composite specimen after polishing process is observed. Figure 4.36shows the morphology of the hybrid composite powders Al/$Al_2O_3$/Gr mechanically milled. It is to be

noted that the particles size and the morphology were significantly changing with extending milling time. By extending milling time from 30 min to 120min the particle size decreases which induced better distributions of the reinforcement components, minimizing their agglomeration. Uniform distribution of the particles is obtained on the samples 10% and 20% weight percentage of aluminum oxide. In addition to this de-bonding and pores are observed on the composite with 30% weight percentage of aluminium oxide. More over agglomeration is obtained on the samples with low milling time. As it can be interpreted from the fig4.36 (a) the monolithic aluminum n alloy without reinforcement has induced flows and micro chips whereas fig 4.36 (f) show the graphite particle at 5 micrometer. It revealed that there is a cluster of graphite particle sticked together. Fig 4.36(h, g, i) show matrix reinforced by 10Wt% $Al_2O_3$ and 3Wt% Gr. From the SEM image uniform distribution of both reinforcements is attained. High compaction pressure applied on the 11 the sample made the surface dense and pores free. medium milling time has also improved the distribution and particle size is also reduced as it can be concluded from the Fig 4.36 (k at 100 µm, j at 50µm,l at 20 µm) is reinforced by 10% $Al_2O_3$ Wt% of $Al_2O_3$ and 3Wt% Gr. Sample number 12 which is milled for longer time showed uniform distribution of the $Al_2O_3$ Wt% and Gr wt% . Fig 4.36 (m at 200 µm, n at 100 µm, o at 50 µm) contain 20Wt% $Al_2O_3$ and 4.5 wt% Gr clearly show the evenly distribution of both reinforcements. the samples with high compaction pressure revealed five and dense surface whereas the samples with highest compaction time doesn't show that much effect that can be detected to the reinforcement of the particles. De bonding on the boundary of aluminium oxide and graphite is observed on the Fig 4.37 (m, n, o) reinforced by 30wt% $Al_2O_3$ and 4.5 % Gr this is caused by low working pressure. More over the micro crack and pores are observed on the sample with low pressure which is depicted on the Fig 4.36 (v, w, x) reinforced by 30 wt% Al2O3 and 1.5 wt% Gr. The sample number 5 Figure 4.37 (a at 50 µm, b at 20 µm, c at 5 µm) are reinforced by 10Wt% Al2O3 and 0 Wt% Gr.

The micro structure of the graphite reinforcement is in line with the micro structural analysis of (Z. Mei-juan et al. (2013)).

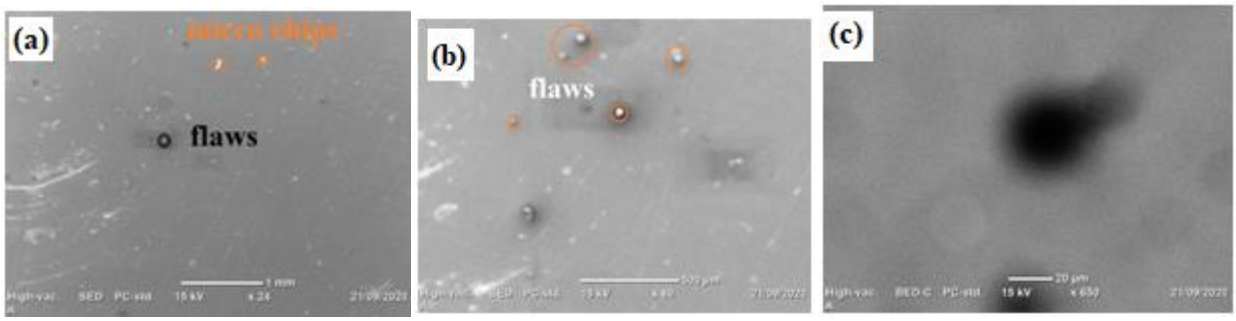


Figure 4.36 The scanning electron microscopic images of samples.figure4.36 (a at 1mm), (b at 500 µm) and (c at 5 µm) has 0 Wt % of $Al_2O_3$ and 0Wt % of Gr.

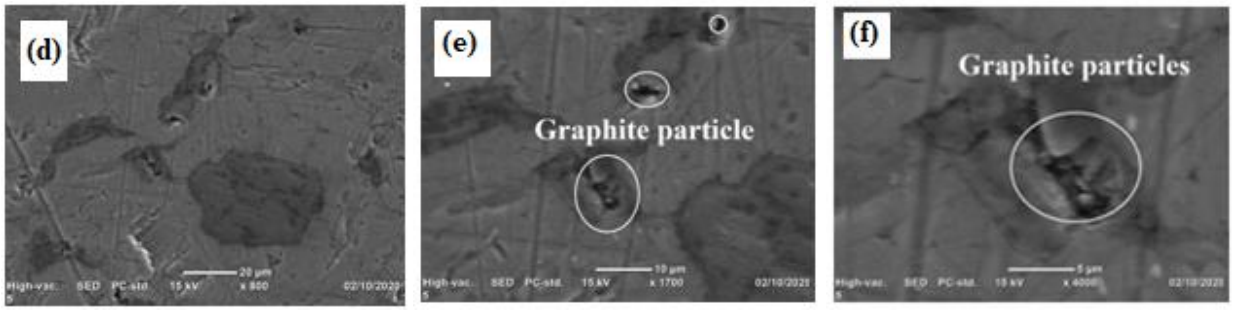


Figure 4.36 (d at 20µm, e at 10 µm, f at 5µm) are the composite with 1.5 Wt% Gr

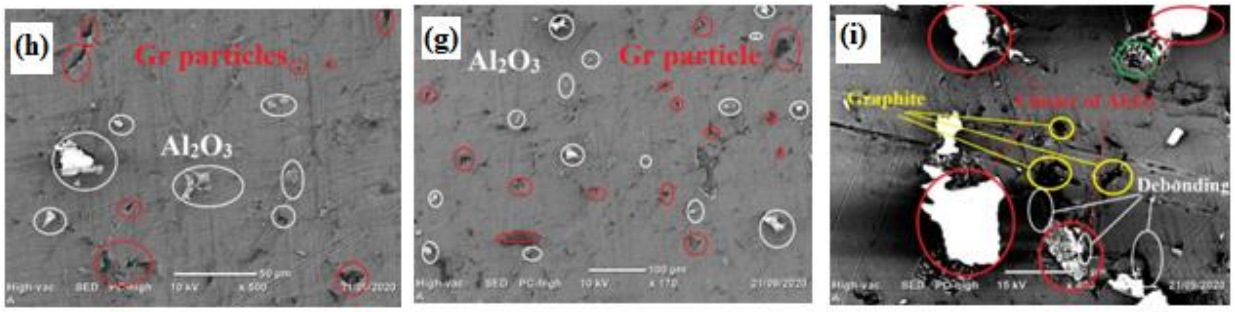


Fig 4.36(h at 50µm, g at 100 µm, i at 10 µm) is reinforced by 10Wt% $Al_2O_3$ and 3Wt% Gr.

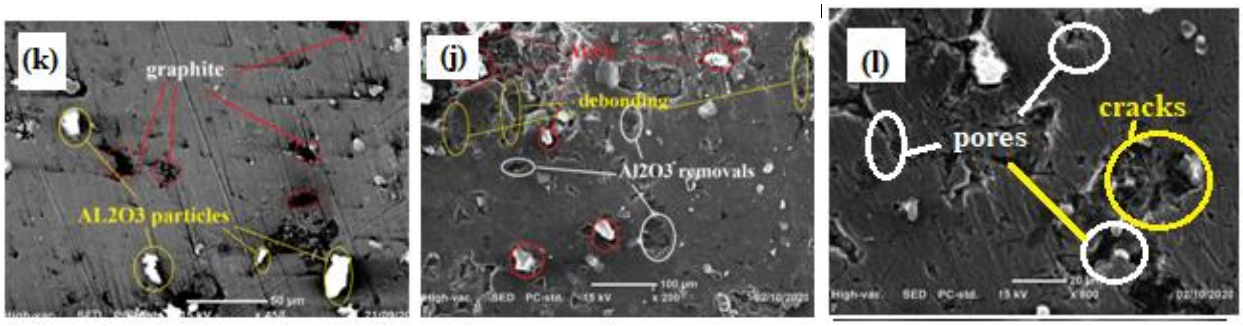


Fig 4.36 (k at 100 µm, j at 50µm,l at 20 µm) is reinforced by 10% $Al_2O_3$ Wt% of $Al_2O_3$ and 3Wt% Gr. Fig

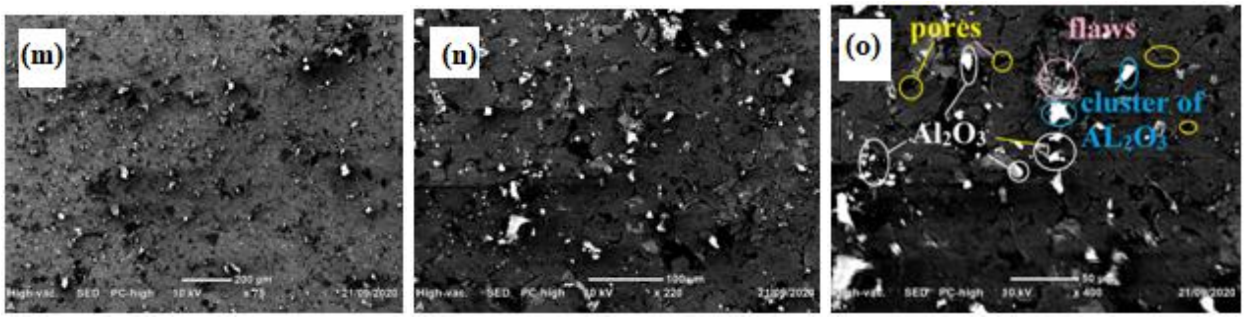


Fig 4.36 (m at 200 µm, n at 100 µm, o at 50 µm) contain 20Wt% $Al_2O_3$ and 4.5 wt% Gr

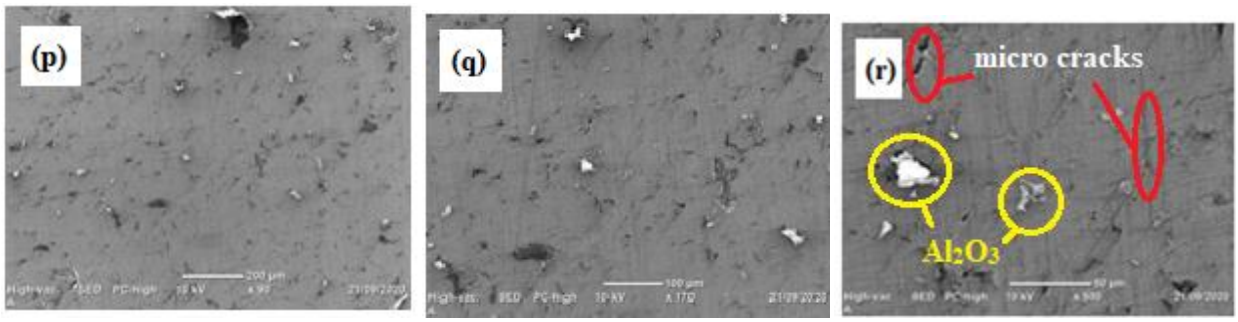


Fig 4.36 (p at 200 µm,q at 100 µm ,r at 50 µm) is reinforced by 10% $Al_2O_3$ Wt% of $Al_2O_3$ and 0 Wt% Gr

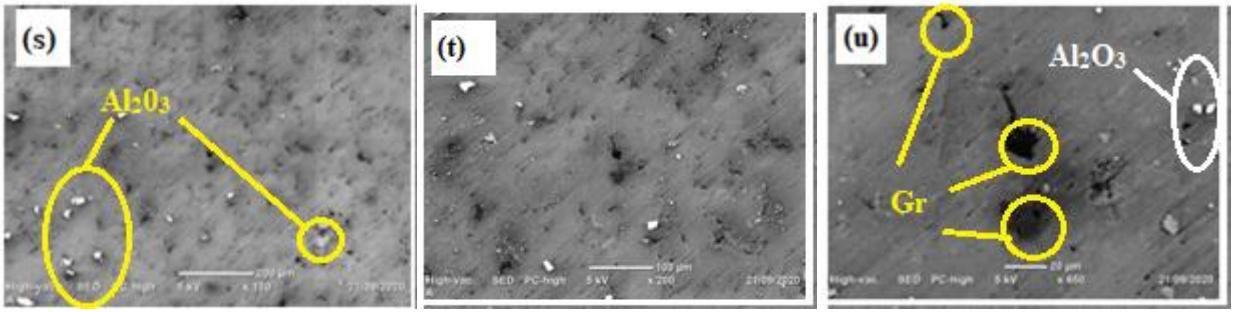


Fig 4.36 (s at 200 µm, t 100 µm, u at 20 µm) are reinforced by 10Wt% Al2O3 and 1.5 Wt% Gr.

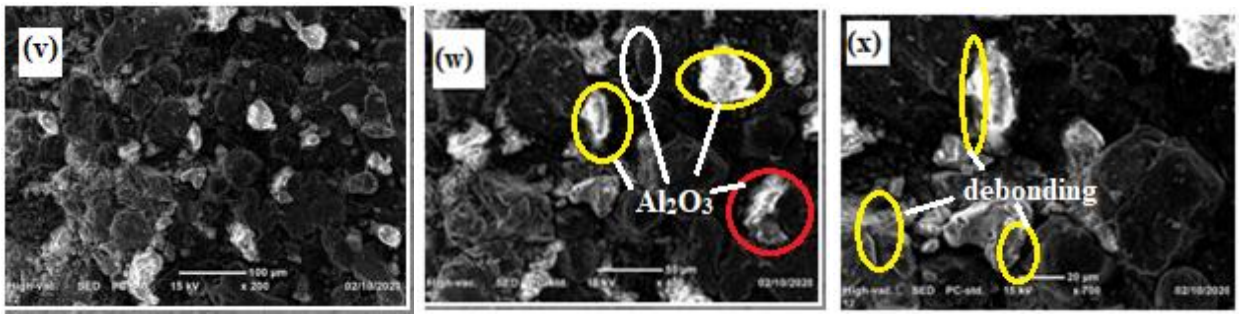


Fig 4.36 (v at 100 µm,w at 50 µm, x at 20 µm) reinforced by 30 wt% Al2O3 and 1.5 wt% Gr

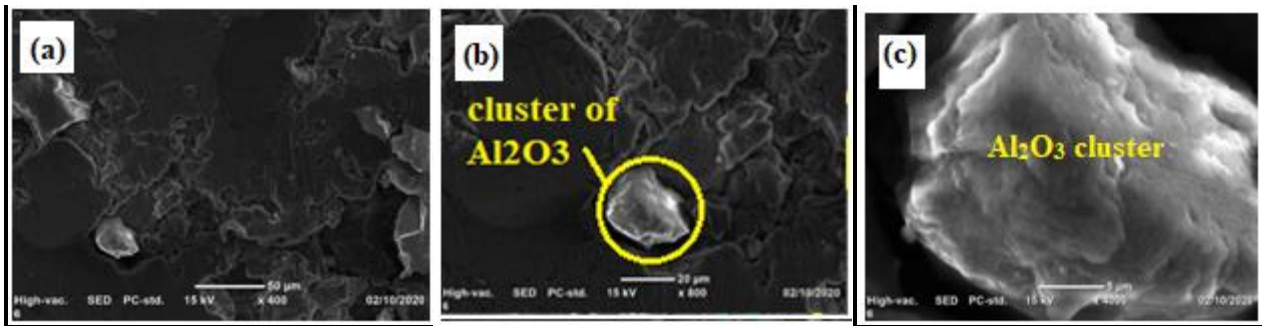


Figure 4.37 (a at 50 µm, b at 20 µm, c at 5 µm) are reinforced by 10Wt% Al2O3 and 0 Wt% Gr.

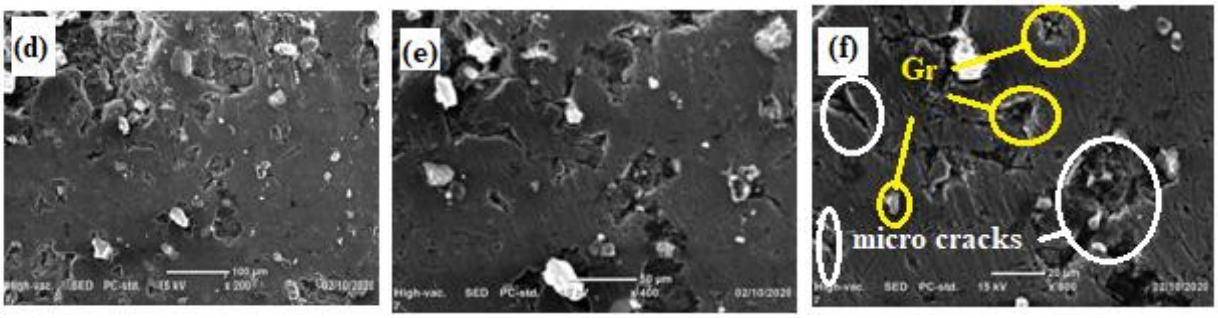


Fig 4.37 (d at 100 µm, e at 50 µm, f at 20 µm) are reinforced by 20 Wt% $Al_2O_3$ and 1.5 Wt% Gr

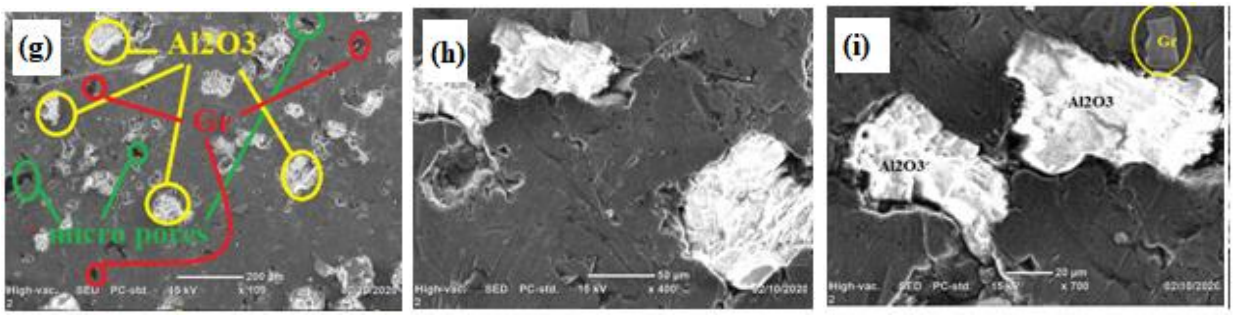


Fig 4.37 (g at 200 µm, h at 50 µm, I at 20 µm) are reinforced by 20%Wt $Al_2O_3$ and 4.5 Wt% Gr.

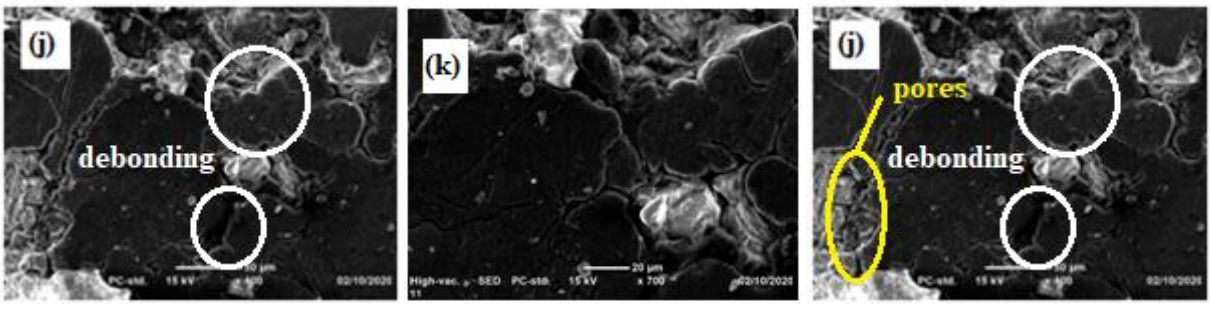


Fig 4.37 (j at 50 µm, k at 20 µm, l at 10 µm) are with 30wt% $Al_2O_3$ and 3 % Gr.

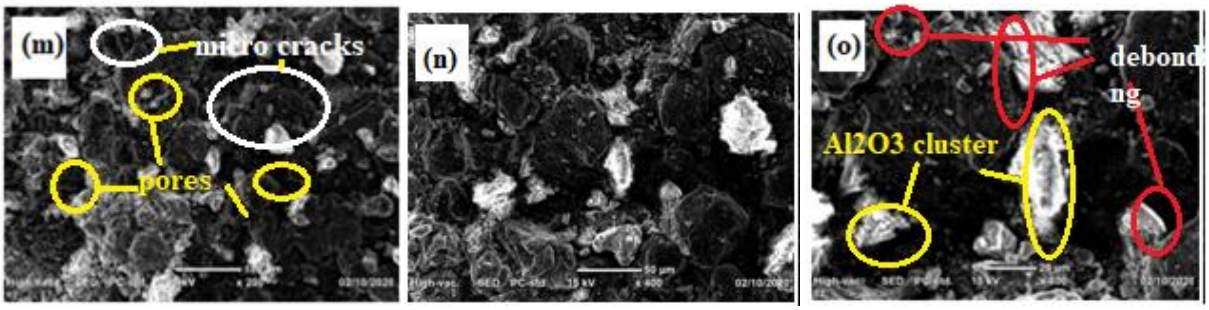


Fig 4.37 (m at 100 µm, n at 50 µm, o at 20 µm) reinforced by 30wt% $Al_2O_3$ and 4.5 % Gr.

As expected, it is found that partial clusters of $Al_2O_3$ bonded to the Al matrix. We also found that the majority of the particles of $Al_2O_3$ were embedded in the matrix, and the spaces between the particles were reduced by increasing the $Al_2O_3$ content. After 30 min of milling, the morphological aspect of the particles is reduced in size, because of the milling time increase of the Al matrix. After 120 min of milling when the powder particles sizes are reduced. This can be attributed to the internal energy developed in the dry ball mill, which facilitates the bonding process by increasing the mass diffusion processes. Thus the particle morphology changes with increasing milling time, $Al_2O_3$ wt%, graphite wt%. These facts are in concordance with specialty literature

## 4.13 Optical Microscopic Analysis

The optical microscope of the composites containing 0-30% by weight of micron Al2O3 and 0-1.5Wt%Gr /Al produced using normal powder metallurgy conditions. Fig 4.38 a) shows the microstructures of the aluminium alloy in which defects and pores are revealed. Whereas the micron $Al_2O_3$ and Gr are distributed throughout the aluminium matrix like islands and the primary aluminium matrix is indicated by the patches of rough matrix with some defect. The fig 4.38 b and e show the composite containing10Wt% $Al_2O_3$ and1.5 Wt% Gr reinforcement .the microstructure show the uniform distribution of both ceramic and solid lubricants additionally lower grain sizes are reported due to high milling time and higher compaction pressure. Figure 4.37c shows 10Wt% $Al_2O_3$ and3 Wt% Gr reinforcement it revealed that micro porosities are present in the inter-grain region. Figure 4.37 d show larger grain sizes due to low compaction time and minimum milling time. Whereas the Figure 4.38(j,I,k) show the sample with 30 Wt% $Al_2O_3$ and3 Wt% Gr due to the higher content of reinforcement and pore nucleation and de-bonding is resulted at the aluminium matrix $Al_2O_3$interfaces (I. Aatthisugan et al. (2017)..

Furthermore, Figure 4.38 (h and i) shows the optical microscope images of MMCs containing 20Wt% $Al_2O_3$ and3 Wt% Gr weights of $Al_2O_3$ and Gr micron particles the image revealed that large grain sizes are observed due to the low compaction pressure and low compaction time. The $Al_2O_3$micro particles are distributed throughout the Al composites containing various weight percentages of graphite particles. The optical micrograph of the$Al_2O_3$ particles in aluminium matrix when the $Al_2O_3$particles content is more than 20% by weight deboning between the grains due to large surface-to volume ratio and poor wettability. These problems induce agglomeration, micro porosities and clustering of Al2O3in the MMNCs. This result is in well agreement with (I. Aatthisugan et al. (2017).

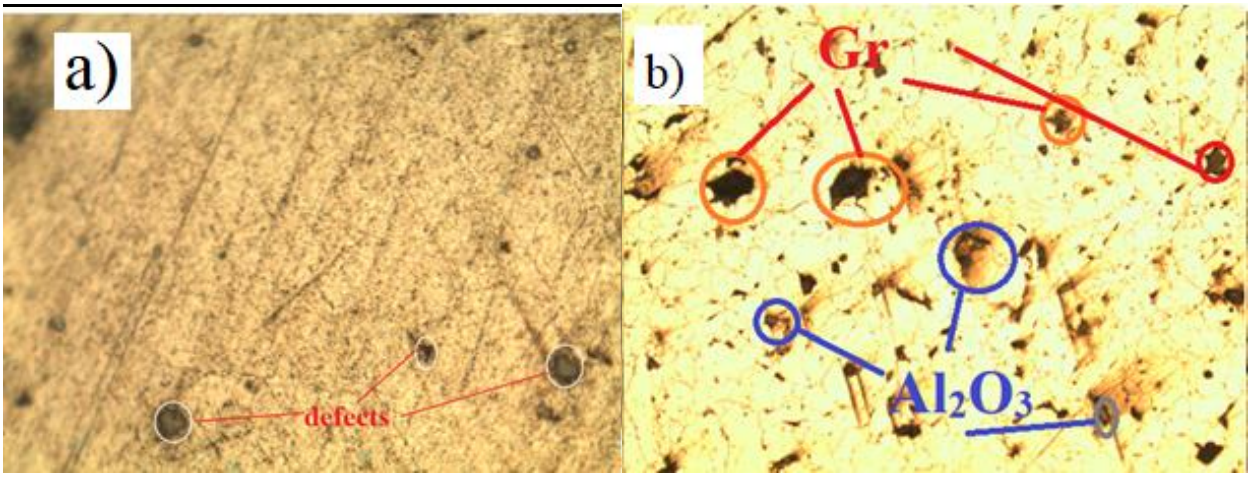


Figure 4.38 a) shows the microstructures of the aluminium alloy figure. (b) Show the composite containing10Wt% $Al_2O_3$ and1.5 Wt% Gr,

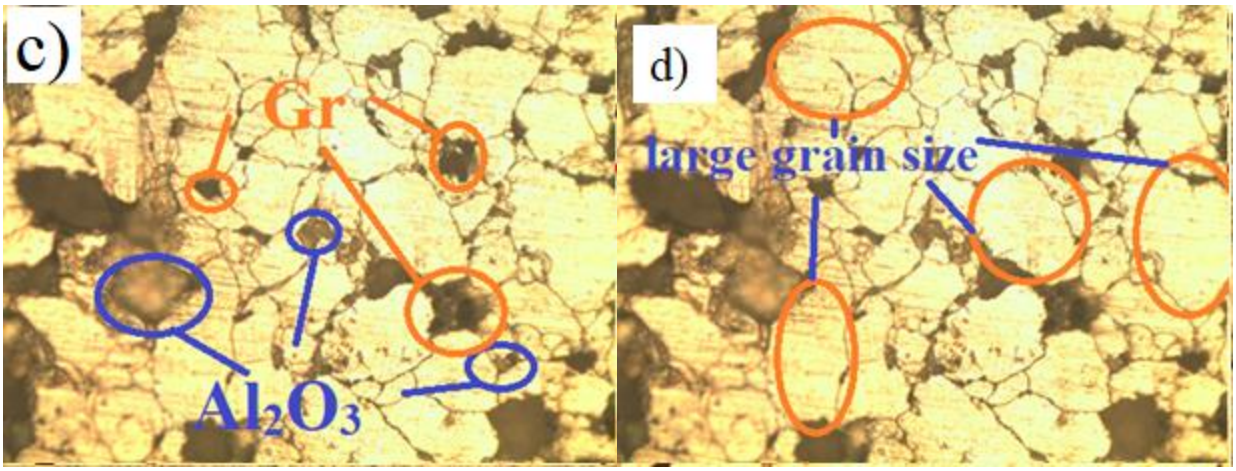


Figure 4.38 c show 10Wt% $Al_2O_3$ and3 Wt% Gr reinforcement.(d) show the grain size of the composite with 10Wt% $Al_2O_3$ and3 Wt% Gr reinforcement

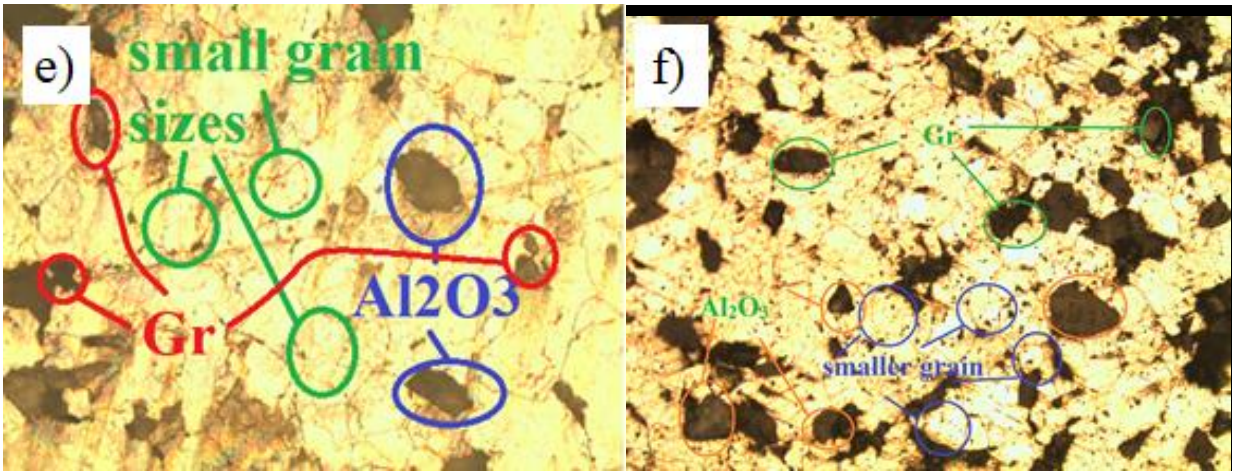


Figure 4.38 (e) show 20Wt% $Al_2O_3$ and3 Wt% Gr reinforcement, (b) show show 10Wt% $Al_2O_3$ and3 Wt% 4.5 Gr reinforcement

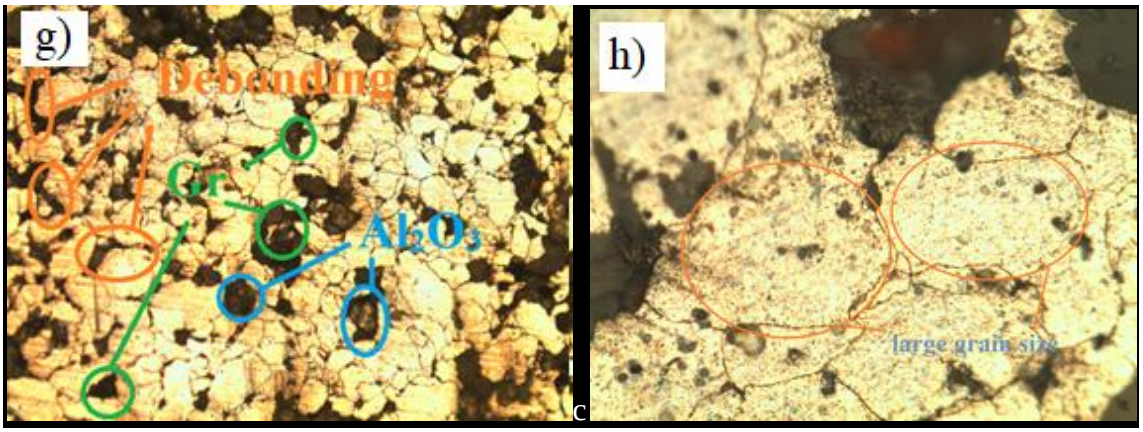


Figure 4.38 (e) show 20Wt% $Al_2O_3$ and1.5 Wt% Gr reinforcement, (h) ) show grain sizes of 20Wt% $Al_2O_3$ and1.5 Wt%

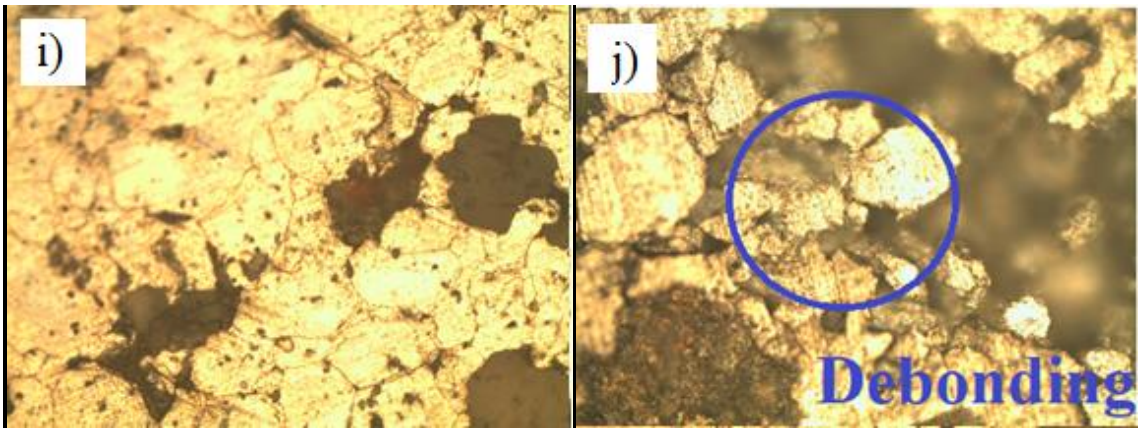


Figure 4.38 (i) show 10 Wt% $Al_2O_3$ and1.5 Wt% Gr reinforcement, (j) show 30 Wt% $Al_2O_3$ and3 Wt% 4.5 Gr reinforcement.

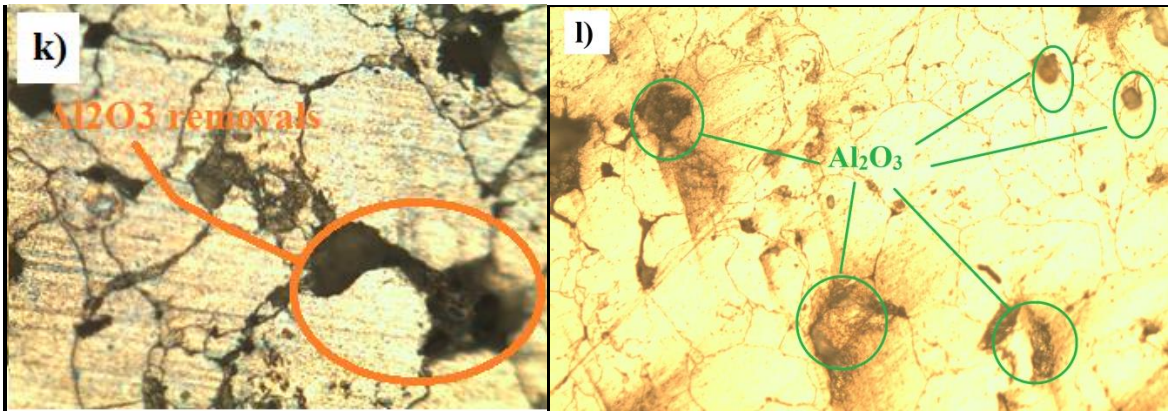


Figure 4.38 (k and i ) show 30Wt% $Al_2O_3$ and 0 Wt% Gr reinforcement

## 4.14 Micro structural conclusion

The microstructure by the scanning microscope shows that the reinforcements are uniformly distributed into the matrix. By using an optical microscope the grain structure is also analyzed. From the microstructure, the following conclusions can be made.

- The composite with high milling time has a lower particular size and uniform distribution; hence it has better service property.
- The composite with above 30 weight percentage of reinforcement show de-bonding and granular dis-integration due to incompatible working pressure. Due to this, the composite with a 30 weight percentage of alumina reinforcement have poor service property.
- With an increase in compaction pressure, the grain size reduction is achieved. It is proved that a sample with reduced grain size has better service property.
- Composite with low milling time and low compaction pressure show agglomeration of alumina and graphite particles. This implies that the sample with low milling time and low compaction strength show poor service property.

# CHAPTER 5

## CONCLUSION AND RECOMMENDATION

### 5.1 Summary

The powders are obtained from Yeshadam Chemical Trading P.L.C Addis Abeba, Ethiopia. Milling process was performed at Chemical Engineering laboratory of Adama Science and Technology University using process controlling agent. The purpose of this process is to ensure size reduction. Compaction process was performed at ceramic lab of Material Science Engineering laboratory. The intention of this process is to change the powder into solid sample. Consequently the sintering process under argon gas atmosphere was executed at Chemical Engineering laboratory with cooperation of Manufacturing Engineering Department laboratory and Chemical Engineering laboratory of ASTU after sintering process the hardness, density, porosity and optical microscopy experimental determination is done at material science metal laboratory whereas the compressive strength is measured at design and manufacturing laboratory. Finally the wear testing was executed at Mechanical Engineering Department laboratory, North Eastern Regional Institute of Science And Technology, Itanagar,India.

### 5.2 Conclusion

The experimental investigation of the aluminum matrix composite reinforced by aluminum oxide and graphite particle was successfully fabricated by powder metallurgy process. From this experimental investigation, the following conclusions are made.

- With an increase in aluminum oxide weight percentage, the hardness, compressive strength, density, and porosity increase.
- The graphite reinforcement induces a decrement in the wear loss and coefficient of friction. Nevertheless, it also caused a decrement in the hardness and compressive strength.
- Mechanical milling of Al/Al2O3/ Gr powder induces sufficient favorable structural modifications that improved the micro-hardness and rate of wear of the sintered hybrid composites.
- The reinforcement of the composite with Al2O3 and graphite causes an increment in the hardness and compressive strength of the composite. Nevertheless, reinforcement by the

graphite particle-induced decrement on both hardness and compressive strength of the hybrid composite.

- The highest hardness is achieved at S9 (20Wt% Al2O3 and 0 Wt% Gr) i.e. (320HV). The condition corresponding to the optimum condition was 20% Al2O3, 1.5% Gr, compaction pressure of 60 Mpa, 60 minutes of compaction time, and 120 minutes of milling time whereas the highest compressive strength was achieved for S9 (20Wt% Al2O3 and 0 Wt% Gr) i.e. 261.56 Mpa and the condition corresponding to the optimum condition was 20% Al2O3, 1.5%Gr, compaction pressure of 60 Mpa, 2700s minute of compaction time and 1800s of milling time for S9.
- The lowest wear loss was obtained for S6(10Wt% Al2O3 and 1.5 Wt% Gr) i.e. 0.0018mm3/m whereas the condition corresponding to the optimum condition is 10% Al2O3,4.5%Gr,10N load, and 1m/s sliding speed. Relatively the lowest coefficient of friction was achieved for S11 (20Wt% Al2O3 and 3 Wt% Gr) i.e.0.35 whereas the condition corresponding to the optimum condition was 10% Al2O3, 4.5% Gr, 30N load, and 1m/s for S8 (10 Wt% Al2O3 and 4.5 Wt% Gr).
- The optimum condition using grey relational grade for theoretical density, actual density, and porosity was 10% Al2O3, 4.5%Gr, compaction pressure of 60 Mpa, 45 minutes of compaction time, and 30 minutes of milling time. The condition corresponding to the optimum condition is 10% Al2O3,4.5%Gr, compaction pressure of 55 Mpa, 15 minutes of compaction time, and 30 minutes of milling time for S8(10Wt% Al2O3 and 4.5 Wt% Gr).
- The optimum condition for the grey relational analysis of wear loss and coefficient of friction was 20% Al2O3,4.5%Gr,30N load, and 0.8 m/s sliding speed. The condition corresponding to the optimum condition was 20% Al2O3,4.5%Gr,20N load, and 0.4 m/s sliding speed for S12(20Wt% Al2O3 and 4.5 Wt% Gr).
- The optimum condition for the grey relational analysis of hardness and compressive strength was 20% Al2O3, 1.5%Gr, compaction pressure of 60 Mpa and 60 minutes of compaction time, and 120 minutes of milling time. The condition corresponding to the optimum condition was 20% Al2O3, 1.5%Gr, compaction pressure of 60 Mpa, 45 minutes of compaction time, and 30 minutes of milling time.

- Wear resistance improved by 43.93% with increase in weight percentage of graphite from 0% to 4.5% whereas wear resistance increased from 30%, 37% with increase in reinforcement from 10wt% to 20 wt% of aluminum oxide, nevertheless increment by 7% was observed for those samples with aluminum oxide reinforcement being permanent when the hybrid graphite reinforcement increased from 0 to 4.5wt%.

## 5.3 Recommendation

Considering the experimental investigation of aluminum Matrix composite reinforced by aluminum and graphite the following recommendations are analyzed.

- It is recommended that if this experiment is conducted in high compaction pressure it is expected to have improved mechanical property.
- In this experimentation milling process was executed by using process control agents. It is highly recommended to use a vacuum ball machine to control oxidation.
- During the sintering process the argon gas tube is inserted into the muffle furnace by using a copper tube. From this experiment, it can be recommended to use a conventional gas condition furnace.
- The powders sizes of the reinforcements are micron due to the unavailability of the Nanoparticle. To induce better results it is recommended to use Nanoparticles.

## 5.4 Future scope

The following are scope of future work:

- The Nanocomposite is well known for their advanced mechanical property and tribological property more than the micro composite. Therefore, further research work can be explored using Nanomaterials for the experimental investigation.
- Regarding the sintering process, in this research, the sintering process is done by connecting the gas tube into a muffle furnace. The sintering of the compacted samples can be carried out through microwave and laser sintering operation.
- Moreover, the ball milling process is done in the presence of a process control agent for 30-120 minutes. Further, the ball milling can be done using a vacuum milling machine or atmosphere gas controlled milling machine is to prevent oxidation.

# REFERENCE

A. A. Premnath, T. Alwarsamy, T. Rajmohan and R. Prabhu , 2014,The influence of alumina on mechanical and tribological characteristics of graphite particle reinforced hybrid Al-MMC† Journal of Mechanical Science and Technology vol 28, No 11, pp. 4737~4744

S Dharmalingaml, R Subramanian and Metin Ko,2013, Optimization of abrasive wear performance in aluminium hybrid metal matrix composites using Taguchi–grey relational analysis, J Engineering Tribology, Vol 227, No 7, pp. 749–760

M. A Ibrahim, Y. Sahin, A. Y.Gidado , M.T. Said, Mechanical Properties of Aluminium Matrix Composite Including SiC/Al2O3 by Powder Metallurgy-A Review, GSJ: Vol 7, Issue 3, March 2019 ISSN 2320-9186

K. Kanthavel, K. R. Sumesh, P. Saravanakumar, 2016, Study of Tribological properties on Al/Al2O3/MoS2hybrid composite processed by powder metallurgy, Alexandria Engineering Journal Vol 55, pp. 13–17

G. Iacob, V. G. Ghica, M. Buzatu, T. Buzatu, M.I. Petrescu, 2015, Studies on wear rate and microhardness of the Al/Al2O3/Gr hybrid composites produced via powder metallurgy, Composites: Part B Vol 69 ,pp. 603–611

M. O. Bodunrin, K. K. Alaneme, L. H. Chown, 2015, Aluminium matrix hybrid composites: a review of reinforcement philosophies; mechanical, corrosion and tribological characteristics, J materrestechnol; Vol 4, No 4,pp 434–445

A. Baradeswaran and A. E. Perumal, 2014, Study on mechanical and wear properties of Al7075 / Al2O3 /graphite hybrid composites, Composites: Part B Vol 56,pp 464–471

X. Qu, F. Wang, Ch. Shi, N. Zhao, E. Liu, Ch. He, F. He , 2018,In situ synthesis of a gamma-Al2O3 whisker reinforced aluminium matrix composite by cold pressing and sintering, Materials Science & Engineering A, Vol 709, pp 223–231

M. Rahimian, N. Parvin, N. Ehsani, 2010,Investigation of particle size and amount of alumina on microstructure and mechanical properties of Al matrix composite made by powder metallurgy, MaterialsScience and Engineering A 527, 1031–1038

M. Rahimian, N. Parvin, N. Ehsani, 2011, The effect of production parameters on microstructure and wear resistance of powder metallurgy Al–$Al_2O_3$ composite, Materials and Design, Vol 32, pp 1031–1038

N. Radhika and R. Subramaniam, 2013, Wear behavior of aluminum/alumina/graphite hybrid metal matrix composites using Taguchi's techniques, Vol 65, No 3, pp 166–174

A. A. Premnath, T. Alwarsamy, T. Rajmohan, R. Prabhu,2014, The influence of alumina on mechanical and tribological characteristics of graphite particle reinforced hybrid Al-MMC, Journal of Mechanical Science and Technology,Vol 28 No 11 ,pp 4737-4744

M. Kumar, A. M. Murugan, 2017, Tribological characterization of Al6061 /alumina /graphite /redmud hybrid composite for brake rotor application, Particulate Science and Technology

V. N. Gaitonde, S. R. Karnik, M. S. Jayaprakash, 2012,Some Studies on Wear and Corrosion Properties of Al5083/Al2O3/Graphite Hybrid Composites, Journal of Minerals and Materials Characterization and Engineering, Vol 11, pp 695-703

M. T. Hayajneh, A. l M. Hassan, A. T. Mayyas, Artificial neural network modeling of the drilling process of self-lubricated aluminum/alumina/graphite hybrid composites synthesized by powder metallurgy technique, Journal of Alloys and Compounds, Vol 478, pp 559–565

D. K. Koli, G. Agnihotri, R. Purohit, Properties and Characterization of Al-Al2O3 Composites Processed by Casting and Powder Metallurgy Routes (Review), International Journal of Latest Trends in Engineering and Technology (IJLTET) , Vol. 2 Issue 4 July 2013

A. Baradeswaran, S.C. Vettivel, A. E.Perumal, N. Selvakumar, R. F. Issac Experimental investigation on mechanical behavior, modeling and optimization of wear parameters of B4C and graphite reinforced aluminium hybrid composites, Materials and Design, Vol 63, pp 620–632

G. Straffelin, 1997, Influence of matrix hardness on the dry sliding behavior of 20 vol.%Al2O3-particulate-reinforced 6061 A1 metal matrix composite; Wear Vol 211, pp 192-197

Himanshu Kala, K.K.S Mer, Sandeep Kumar.(2014) A Review on Mechanical and Tribological Behaviors of Stir Cast Aluminum Matrix Composites; Procedia Materials Science Vol 6, 1951 – 1960

K. K. Alaneme and K. O. Sanusi (2015**)** Microstructural characteristics, mechanical and wear behavior of aluminium matrix hybrid composites reinforced with alumina, rice husk ash and graphite; Engineering Science and Technology, an International Journal,Vol 18,pp 416-422

G. B. V. Kumar, C. S. P. Rao, N. Selvaraj, 2011, Mechanical and Tribological Behavior of Particulate Reinforced Aluminum Metal Matrix Composites – a review Journal of Minerals & Materials Characterization & Engineering, Vol. 10, No.1, pp.59-91,

S.Velicˇkovic´, B. Stojanovic, M. Babic and I. Bobic, 2017, Optimization of tribological properties of aluminum hybrid composites using Taguchi design ´2Journal of Composite Materials, Vol. 51,No 17,pp 2505–2515

P. YuJiang (2005) Structure, thermal and mechanical properties of in situ Al-based metal matrix composite reinforced with Al2O3 and TiC submicron particles; Materials Chemistry and Physics, Vol 93,pp 109–116

S. A. Sajjadi, H. R. Ezatpour, M. T. Parizi**,** 2012, Comparison of microstructure and mechanical properties of A356 aluminum alloy/Al2O3 composites fabricated by stir and compo-casting processes; Materials and Design, Vol 34,pp 106–111

O. Yılmaza and S. Buytozb ,2001, Abrasive wear of Al2O3-reinforced aluminum based MMCs ;Composites Science and Technology, Vol 61, pp 2381–2392

A. Forn∗, M. T. Baile, E. Rupérez**,** 2003**,** Spinel effect on the mechanical properties of metal matrix composite AA6061/Al2O3 p; Journal of Materials Processing Technology ,Vol 143, No 144, pp 58–61

Z. Mei-juan, Y. Xiao-hong, L. Yong-bing**,** CAO Zhan-yi, CHENG Li-ren, PEI Ya-li,(2013) Effect of graphite content on wear property of graphite/Al2O3/Mg-9Al-1Zn-0.8Ce composites, Trans. Nonferrous Met. Soc. China, Vol 20, pp 207-211

A. Devaraju and A. Kumar, 2013,Influence of addition of Gr p/Al2O3p with SiCp on wear properties of aluminum alloy 6061-T6 hybrid composites via friction stir processing; Trans. Nonferrous Met. Soc. China,Vol 23, pp 1275-1280

K. Kanthavel, K. R. Sumesh, P. Saravanakumar (2016) Study of tribological properties on Al/Al2O3/MoS2 hybrid composite processed by powder metallurgy Alexandria; Engineering Journal, Vol 55, pp 13–17

A. Baradeswaran and A. Elayaperumal, 2013 ,Mechanical And Tribological Behavior Of Graphite reinforced Aluminium Matrix Composites, Journal of the Balkan Tribological Association Vol. 19, No 3,pp 354–364

R' S. Bhatia and Kudlipsingh, An Experimental Analysis of Aluminium Metal Matrix Composite using (Al2O3/B4C/Gr Particles );International Journal of Advanced Research in Computer Science Vol. 109, No 3,pp 954–964

Kapil Kumar, Dhirendra Verma, Sudhir Kumar,2014, Processing and Tensile Testing of 2024 Al Matrix Composite Reinforced with Al2O3 Nano-Particles; 5th International & 26th All India Manufacturing Technology, Design and Research Conference (AIMTDR 2014) December 12th– 14th, 2014

M. Nagaral, V. Auradi, Ravishankar ,M K ,2013, Mechanical behavior of aluminum 6061 alloy reinforced with al2o3 & graphite particulate hybrid metal matrix composites; International Journal of Research in Engineering & Technology (IJRET) Vol. 1, Issue 2, July, pp 193-198

A. Manna1, H. S. Bains and P. B. Mahapatra (2011) Experimental study on fabrication of Al–Al2O3/Grp metal matrix composites journal of Composite Materials. Vol 45, No 19,pp 2003–2010

M. Vykuntarao, 2015, Review Influence of reinforced particles on the Mechanical properties of Aluminium Based Metal Matrix Composite; A Chemical Science Review and Letters ISSN 2278-6783

N. Radhika, M. Praveen, S. Mukherjee, 2017, Influence of Process Parameters On Three Body Abrasive Wear Behavior Of Functionally Graded Aluminium Alloy Reinforced With Alumina Journal Of Engineering Science And Technology, Vol. 12, No. 11,pp 2866 - 2879

D. K. Koli, G. Agnihotri, R. Purohit, 2013, Properties and Characterization of Al-Al2O3 Composites Processed by Casting and Powder Metallurgy Routes (Review),International Journal of Latest Trends in Engineering and Technology (IJLTET) ,Vol. 2 Issue 4, 486 ISSN: 2278-621X

J.S.S. Babu, C.G. Kang, H.H. Kim, 2011,Dry sliding wear behavior of aluminum based hybrid composites with graphite nanofiber–alumina fiber, Materials and Design, Vol 32,pp 3920–3925

M. Uthayakumar , S. Aravindan , K. Rajkumar,2013,Technical Report Wear performance of Al–SiC–B4C hybrid composites under dry sliding conditions, Materials and Design, Vol 47,pp 456–464

X. Qu, F. Wang, Ch. Shi, N. Zhao, E. Liu, Ch. He, F. He, 2018, In situ synthesis of a gamma-Al2O3 whisker reinforced aluminium matrix composite by cold pressing and sintering, Materials Science & Engineering A,Vol 709 pp 223–231

M. T. Hayajneh, A. M. Hassan, A. T. Mayyas , 2009,Artificial neural network modeling of the drilling process of self-lubricated aluminum/alumina/graphite hybrid composites synthesized by powder metallurgy technique, Journal of Alloys and Compounds Vol 478 , pp 559–565

V. Mohanavela, K. Rajanb, P. V. Senthilc, S. Aruld, 2017,Mechanical behaviour of hybrid composite (AA6351+Al2O3+Gr) fabricated by stir casting method, Materials Today: Proceedings Vol 4, pp 3093–3101

S. Wakeel and A. A. Khan, 2017, A Review on the Mechanical Properties of Aluminium Based Metal Matrix Composite Via Powder Metallurgy, International Journal of Innovation Sciences and Research,Vol.6, No, 11, pp. 1096-1100,

Z.W. Zhang, Z.Y. Liu, B.L. Xiao, D.R. Ni, Z.Y. Ma, High efficiency dispersal and strengthening of graphene reinforced aluminum alloy composites fabricated by powder metallurgy combined with friction stir processing,Carbon Vol 135, pp 215-223

Sh. P. Dwivedi, A. Kumar Development of graphite and alumina reinforced aluminium based composite material, Materials Today: Proceedings xxx (2020) xxx

V. Umasankar,M. A. Xavior, S. Karthikeyan,2014,Experimental evaluation of the influence of processing parameters on the mechanical properties of SiC particle reinforced AA6061 aluminium alloy matrix composite by powder processing. Journal of Alloys and Compounds Vol 582,pp 380–386

Karthick Ea, Joel Mathaib**,** Michael Tony Jc, Senthil Kumar Marikkannana,Processing, Microstructure and Mechanical Properties of Al2O3 and SiC Reinforced Magnesium Metal Matrix Hybrid Composites, Materials Today: Proceedings,Vol 4,pp. 6750–6756

S. Das, Sh. Das , S.S. Gautam, C.R. Gautam,2020,Optimization of wear coefficient and coefficient of friction of borosilicate glass ceramics using Taguchi coupled grey fuzzy logic technique Materials Today: Proceedings xxx xxx

S. Rajesh, S. Rajakarunakaran, R. S. Pandian, 2012,Modeling and Optimization Of Sliding Specific Wear and Coefficient of Friction of Aluminum Based Red Mud Metal Matrix Composite Using Taguchi Method and Response Surface MethodologyMaterials Physics and Mechanics, Vol 15, pp 150-166

R. Arunachalam, S. Piya, P. k. Krishnan, M. Rajaraman, 2019,Optimization of stir–squeeze casting parameters for production of metal matrix composites using a hybrid analytical hierarchy process–Taguchi-Grey approach

Fei, N. Chin, N. M. Mehat, and Sh. Kamaruddin, 2013, Practical Applications of Taguchi Method for Optimization of Processing Parameters for Plastic Injection Moulding: A Retrospective Review." ISRN Industrial Engineering: pp 1–11. doi: 10. 1155 / 462174.

Ahmad, Naseer, Sh. Kamal, Z. A. Raza, T. Hussain, and F. Anwar, 2016, Multi-Response Optimization in the Development of Oleo-Hydrophobic Cotton Fabric Using Taguchi Based Grey Relational Analysis." Applied Surface Science Vol 367: PP370–381. doi: 10. 1016 /j.apsusc. 2016.01.165.

M. D. Selvam and N. M. Sivaram, Optimal Parameter Design by Taguchi Method for Mechanical Properties of Al6061 Hybrid Composite Reinforced With Fly Ash/Graphite/Copper, International Journal of ChemTech Research CODEN (USA): IJCRGG, ISSN: 0974-4290, ISSN(Online):2455-9555 Vol.10 No.13, pp 128-137, 2017

S. Rajesh, S. Rajakarunakaran, R. S. Pandian, 2012,Modeling and Optimization of Sliding Specific Wear and Coefficient of Friction of Aluminum Based Red Mud Metal Matrix Composite Using Taguchi Method And Response Surface Methodology Materials Physics and Mechanics ,Vol 15, pp 150-166

S.Velic˘kovic´1, B. Stojanovic´1, M. Babic´1 and I. Bobic. Optimization of tribological properties of aluminum hybrid composites using Taguchi design Journal of Composite Materials 2017, Vol. 51, No 17, 2505–2515

Sh. P. Dwivedi, A. Kumar ,2020, Development of graphite and alumina reinforced aluminium based composite material, Materials Today: Proceedings xxx (xxxx) xxx

Karthick Ea, J. Mathaib**,** M. Tony Jc, S. K. Marikkannan,2017,Processing, Microstructure and Mechanical Properties of Al2O3 and SiC Reinforced Magnesium Metal Matrix Hybrid Composites, Materials Today: Proceedings Vol 4 , pp 6750–6756

S. N. Alam , L. Kumar, 2016, Mechanical properties of aluminium based metal matrix composites reinforced with graphite nanoplatelets, Materials Science & Engineering A, Vol 667 pp 16–32

M. Uthayakumar, S. Aravindan , and K. Rajkumar,2013, Technical Report Wear performance of Al–SiC–B4C hybrid composites under dry sliding conditions, Materials and Design Vol 47 pp 456–464

A. Manna1, H.S. Bains and P. B. Mahapatra, 2019,Experimental study on fabrication of Al–Al2O3/Grp metal matrix composites Journal of Composite Materials Vol 45, No 19, pp 2003–2010

S.A. Sajjadi, H.R. Ezatpour, M. T. Pariz, 2012,Comparison of microstructure and mechanical properties of A356 aluminum alloy/Al2O3 composites fabricated by stir and compo-casting processes, Materials and Design ,Vol 34, pp 106–111

R. Harichandran, N. Selvakumar, 2016, Effect of nano/micro B4C particles on the mechanical properties of aluminium metal matrix composites fabricated by ultrasonic cavitation-assisted solidification process, Archives of civil and mechanical engineering 16 (2016) 147-158

I. Aatthisugan, A. R. Rose, D. S. Jebadurai,2017,Mechanical and wear behavior of AZ91D magnesium matrix hybrid composite reinforced with boron carbide and graphite Journal of Magnesium and AlloysVol 5, pp 20–25

M. Merola, Mater. Sci. Eng. (1996),

Nadika et al, 2013, Wear behavior of aluminium/alumina/graphite hybrid metal matrix composites using Taguchi's techniqueswww.researchgate.net/publication/319482665N.

Radhika, M. Praveen, S. Mukherjee, 2017, Influence ofProcess Parameters on Three Body Abrasive Wear Behavior of Functionally Graded Aluminium Alloy Reinforced with Alumina Journal of Engineering Science and Technology Vol. 12, No. 11,pp 2866 – 2879

**APPENDICIES**

Letter Of Acceptance Of The Research On ICMPC-2020 IIT Indore India,Material Today, Elseiver 2020

Dear Author

Thanks for submitting your work to ICMPC@IIT Indore. You paper is now accepted for presentation and publication at 11 ICMPC@IIT Indore. Before we change the status of paper to ACCEPT in EES, kindly register your paper. Details of IIT Indore account is given on website www.icmpc.com.

Once you register, send the proof (amount transferred and the filled registration form) to icmpc@iiti.ac.in. Once these documents are received, we will immediately change the status to ACCEPT and may be after 15 to 20 days, your article will appear online. Kindly note that it will appear in volume only after the conference. Usually we insist the authors to attend the conference in person but if the present problem continues, we will have skype presentation. **So as soon as the paper is accepted, we are not holding the article and pushing it for publication on sciencedirect without delay. The status of paper in EES will be changed to "ACEPT" as soon as registration is done (after acceptance by reviewers).**

Thanks and regards

Conveners and Editorss

# APPENDIX

| S. No. | MATPR Ref | Authors | Title | Affiliation | Registered/Sent To Elsevier For |
|---|---|---|---|---|---|
| 166 | MATPR-D-20-07970R1 | S. K. Chourasiya , G. Gautam<br>A. Kumar | Spray Forming Technique for Aluminium Matrix Materials: A Review | Department of Mechanical Engineering, THDC Institute of Hydropower Engineering and Technology Bhagirathipuram, Tehri-249124,UK, India | Registered |
| 167 | MATPR-D-20-08575 | Rachit Poddar , Ashish Kumar Sahu , Sunil Jha | Experimental Investigation of Nano<br>Second Fiber Laser Micro Grooving<br>on Cylindrical Surface | Research Scholar, Department of Mechanical Engineering, Thapar Institute of Engineering and Technology, Patiala, 147004, India. | UnRegistered |
| 168 | MATPR-D-20-08235 | Arun Kumar Parashar, Ankur<br>Gupta | Investigation of the effect of bagasse ash, hooked steel fibers and<br>glass fibers on the mechanical properties of concrete | Assistant Professor, Department of<br>Civil Engineering, GLA University, Mathura, India | Registered |
| 169 | MATPR-D-20-08230R1 | Ram Sajeevan, Avanish Kumar Dubey | Parametric Study of Die-Sinking Electric Discharge Machining on Aluminium Based Metal Matrix Composite | Mechanical Engineering Department, Motilal Nehru National Institute of Technology,<br>Allahabad (Prayagraj)-211004, India | Registered |
| 170 | MATPR-D-20-08432 | **Robale Dinsa Daba ,**<br>Devendra Kumar Sinha ,<br>Habtamu Beri , Satyam Shivam Gautam*<br>Gulam Mohammed Sayeed Ahmed ,<br>Ram Sewak Singh | Mathematical modelling and optimization of parameters for Al SiFe aluminum alloy reinforced by<br>$Al_2O_3$ and graphite particles using Taguchi method | Program of Mechanical Design and Manufacturing, Engineering, School of Mechanical, Chemical and Materials Engineering, (SoMCME), **ASTU, ADAMA,** Ethiopia | Registered |

# APPENDIX


**PAPER ID: MATPR-D-20-08432R1**

**PAPER TITLE:** Mathematical modeling and optimization of parameters for Al-Si-Fe aluminum alloy reinforced by $Al_2O_3$ and graphite particles using Taguchi Method

**Full Name:** **Dr. Satyam Shivam Gautam**

**Designation:** **Associate Professor**

**Organization & Address:** **Department of Mechanical Engineering, NERIST, Itanagar, Arunachal Pradesh, India 791 109**

**Mobile:** 9436252336 **Phone (o):**

**E-mail:** satyam.gautam@gmail.com

**Category:**

| Faculty/ Research Scholars | Delegates from Industry | Foreign delegates | Student |
|---|---|---|---|
| ☑ | ☐ | ☐ | ☐ |

**IIM Member:**

☐ Yes ☑ No

**Amount paid: Rs 8500** (Faculty/ Research Scholars / Students)

**Name of the Bank:** State Bank of India, NERIST Nirjuli

**Name of the account holder:** Satyam Shivam Gautam

**Date of the transaction:** 01.11.2020

**Online Transaction number:** **IMPS00139359670**

01.11.2020

**Signature with Date**

**Correspondence Address:**
**ICMPC-2020**

E-mail: icmpc-hyd@griet.ac.in, icmpc@iiti.ac.in

Materials

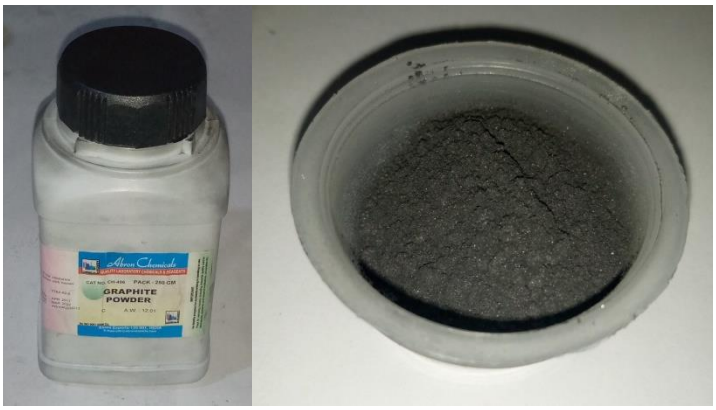


Figure D1  Graphite micro powder (from abron,india) traded by yeshadam trading ethiopia


Figure D2 Aluminium oxide powder from (trust chemicals) traded by yeshadam trading plc Addisabeba, Ethiopia

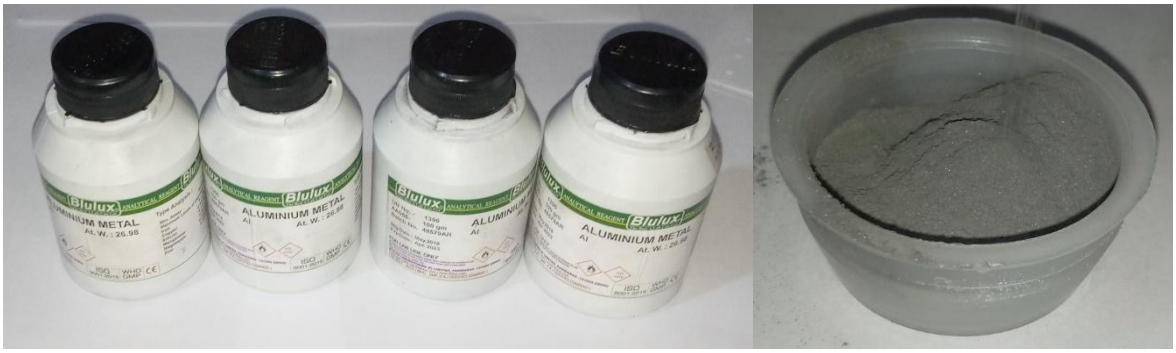

Figure D-3 Aluminium alloy powder from (blulux india) traded by yeshadam trading Addisabeba, Ethiopia.

a) b) c)


Figure D-4 a) stainless steel jar for milling process with steel balls weighing 50g.figure D4 b) toluene which is used as a process controlling agent. Fig c) ball milling machine (Fristsch Pulverisette Germany)

a) b)

Figure D-6 a) The powder re stored inn to plastic jar after milling process. fig b) Shaker (armfield CEN-MVII-00A) utilized for sewing purpose.


Figure D-7 a) the sintering arrangement with gas cylinder fig b)furnace at 600ºC on sintering process.

a) b)

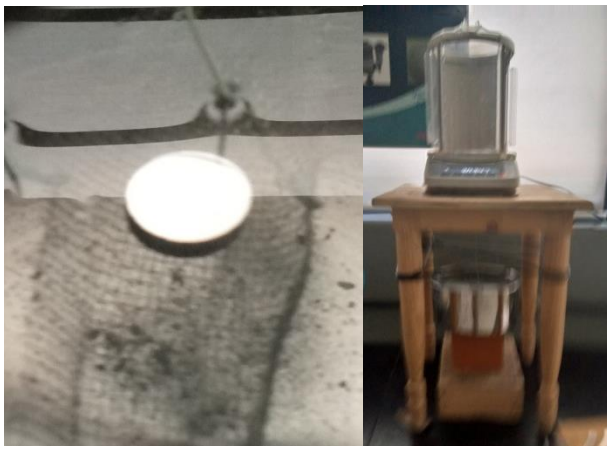

Figure D-8 a) Sample being submerged in water and weighed.Fig b) Arrangement for weight measurement in water.

## APPENDIX-E

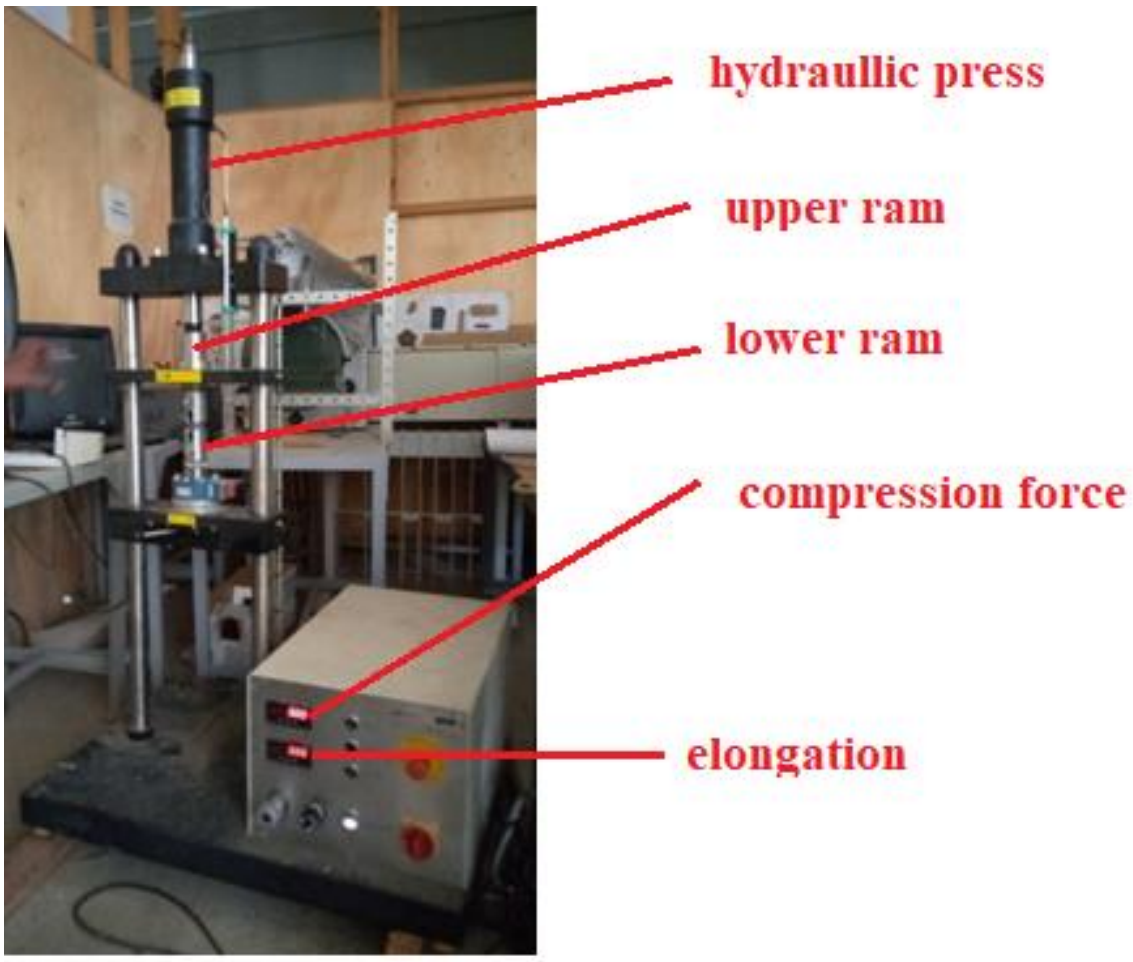


Figure E-1 universal testing machine with its component.